

Final Year Project Dissertation

Structural Stability of Offshore Platforms

Prepared by:

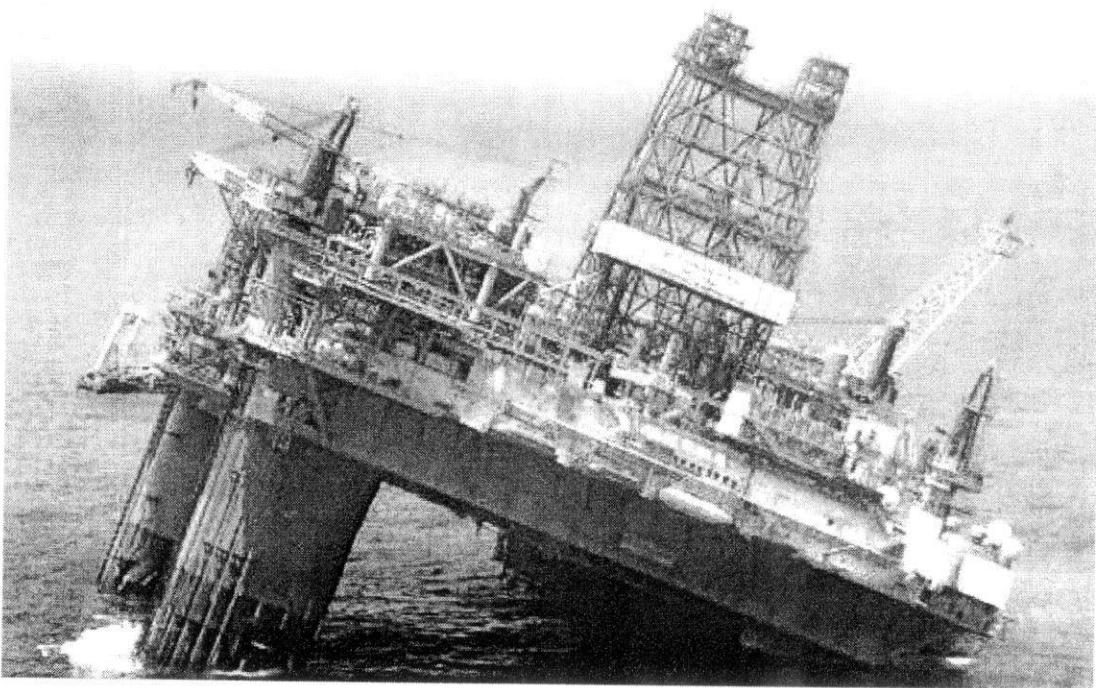
Mohammad Reza Saiedi

ID: 6211, Civil Engineering

Supervisor:

Assoc. Prof. Dr. Nasir Shafiq

June 2007



APPROVAL

Structural Stability of Offshore Platforms
by
Mohammad Reza Saiedi

A project report submitted to the
Civil Engineering Department,
Petronas University of Technology
in partial fulfilment of the
Bachelor of Engineering (Hons) (Civil)

June 2007

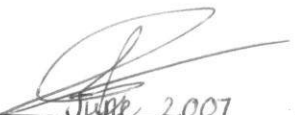
Approved by,



(Assoc. Prof. Dr. Nasir Shafiq)

ORIGINALITY

This is to certify that I am responsible for the work submitted in this project, that the work is my own except as specified in the references, and has not been done by unspecified sources or persons.



June 2007
Mohammad Reza Saiedi

ACKNOWLEDGEMENTS

First and foremost, I would like to thank **Assoc. Prof. Dr. Saied Saiedi** who found time in a very busy schedule to assign tasks to me, monitor my progress and answer my questions. In particular, I am grateful to him for breaking down what seemed like a formidable research project into small manageable tasks, for helping me locate relevant literature and information sources, for assisting me in developing the software application SAOP and interpreting its results, and for guiding me in constructing the scale model of the case study platform. I have also very much benefited from his background in physical modelling, particularly as manager of the recent Pergau Pond Project conducted in UTP. Finally, thanks to his many years of experience in research and paper publication, I was able to structure my thesis in a sound and professional manner.

Second, I would like to express my gratitude to my supervisor, **Assoc. Prof. Dr. Nasir Shafiq**, for his general guidance, support, attention and time.

Finally, I would like to thank **Assoc. Prof. Dr. John Kurian**, the internal examiner during my final presentation, for his careful attention to this report and his encouraging remarks regarding my work in this project.

ABSTRACT

Given the hostile nature of offshore environments, ensuring the structural stability of offshore structures is vital to their design. A computer program was developed for the preliminary stability analysis of offshore platforms under major environmental loads. The program output was interpreted for a minimum facility platform under extreme storm conditions. Also, a thorough framework was set for experimental studies of the platform's stability using a scaled physical model.

Literature review started with gathering general background information on offshore platforms. This included identifying their various types, their numbers worldwide and their construction. Next, structural stability of offshore platforms was studied in terms of the various loads exerted on offshore rigs and methods for their structural analysis. Finally, a recently installed Minimum Facility Platform was examined as an introduction to the case study structure.

The platform chosen as case study for the project was a hypothetical Braced Caisson structure located at 36^m of water in the North Sea. Its conceptual design and reliability assessment under extreme storm conditions were reviewed.

A computer program was developed to calculate total base shear resulting from winds, waves and currents. The program was run for the case study platform under extreme storm conditions and results were interpreted. The breakdown of base shear by environmental loads and structural members was studied. Valuable insights were gained into the sensitivity of platform stability to various design parameters.

The framework was defined for scale model experiments of the case study platform to assess its structural stability. Conducting the experiments by others would then be possible. The author built a model of the case study platform scaled down at 1:110. A hydraulic flume would then replicate storm conditions at the platform site. Experimental setup and procedures were thoroughly specified. Procedures for measurement using a strain gauge were identified. Finally, steps to correlate results with platform stability were established.

CONTENTS

1. INTRODUCTION.....	1
2. OFFSHORE PLATFORMS.....	4
2.1 INTRODUCTION.....	4
2.2 CLASSIFICATIONS.....	6
2.3 STATISTICS.....	17
2.4 CONSTRUCTION.....	18
3. STRUCTURAL STABILITY.....	24
3.1 ENVIRONMENTAL LOADS.....	24
3.2 OTHER LOADS.....	36
3.3 ANALYSIS PROCEDURES.....	45
4. A RECENT MINIMUM FACILITY PLATFORM.....	66
5. CASE STUDY.....	71
5.1 SELECTED PLATFORM.....	71
5.2 JOINT INDUSTRIAL PROJECT (JIP).....	72
5.3 CONCEPTUAL DESIGN.....	75
5.4 RELIABILITY UNDER EXTREME STORM.....	80
6. COMPUTER SIMULATIONS.....	86
6.1 DEVELOPED SOFTWARE (SAOP).....	86
6.2 BREAKDOWN OF BASE SHEAR.....	90
6.3 SENSITIVITY ANALYSIS OF BASE SHEAR.....	95
6.4 DRAG / INERTIA RATIO.....	106
7. SCALE MODEL EXPERIMENTS.....	108
7.1 INTRODUCTION.....	109
7.2 SETUP.....	113
7.3 BUILT MODEL.....	115
7.4 HYDRAULIC LAB FLUME.....	119
7.5 PROCEDURES.....	123
7.6 STRAIN GAUGE MEASUREMENTS.....	127
REFERENCES.....	135
APPENDICES.....	137
A. OFFSHORE PLATFORMS GLOSSARY.....	137
B. SAOP OUTPUT.....	139

1. INTRODUCTION

This report presents the details of the writer's Final Year Project as an undergraduate civil engineering student at UTP. As background for your reading of this report, this chapter includes: (1) the background of the study, (2) the project's objective, (3) the scope of study, (4) the project's feasibility, and (5) an overview of the report format.

Background of Study

Offshore platforms are exposed not only to the extreme conditions of the environment such as wave slam, ice impact, and fatigue, but also to accidental events such as boat impact and objects dropped off the platform. The list of such accidental events that have occurred over the past several decades is myriad. It includes ramming by a supply boat that went full ahead rather than full astern, impact from the reinforced corner of a cargo barge, and impact by a derrick barge whose mooring lines had parted. The dropped-objects category includes a number of pedestal cranes pulled off their supports when they attempted to follow the movements of a supply boat and thus exceeded their allowable radii, also drill collars, casing, a mud pump, and pile hammer.

In the environmental category, horizontal bracings near the waterline have been excited by vortex action and subjected to vertical cycling beyond that for which they were designed, with consequent failure by fatigue. Defective welds and heat-affected zones have led to crack development, and its subsequent propagation has been accelerated by corrosion in the crack. A platform may also be damaged by operational failure, which leads to flooding or overloads. Scour may undermine the legs and lead to excessive lateral response. Finally, corrosion may occur which weakens the structure beyond allowable limits.

Thus, given the dangerous and hostile nature of offshore environments, ensuring the structural stability of offshore platforms is a vital part of their design.

Project Objectives

The objectives of this project were to:

1. Develop a computer program for the preliminary stability analysis of offshore platforms under major environmental loads.
2. Compare the sensitivity of platform stability to various design parameters.
3. Define a thorough framework for experimental studies of a platform's stability using a scaled physical model.

Significance

- The project revealed the sensitivity of platform stability to various design parameters.
- The study provided useful insights into scale modelling, the theories behind offshore platform design, and computer modelling and simulation.
- By deeply familiarizing the writer with many aspects of offshore platforms, the research work gave him a head-start in his future career potentially as a civil engineer in the oil and gas industry.

Scope of Study

Due to constraints in time and resources, the study was confined in scope as follows:

1. Only one simple case study was considered. See *Chapter 5: Case Study* for details.
2. The geometric scale of the physical model was no greater than 1:110. See *Section 7.2: Setup > Geometric Scale* for details.
3. Only extreme storm conditions were studied. Fatigue conditions were not studied. See *Section 7.5: Procedures > Loads > Fatigue* for details.
4. Only simple formulae and phenomena were considered in the developed computer program. See *6.1: See Developed Software: SAOP: Limitations* for details.
5. The following considerations were specifically excluded from the study:
 - a. Failure of the foundation
 - b. Ship Collision
 - c. Damage to conductors/risers
 - d. Wave impingement on the deck
 - e. Wave breaking
 - f. Fire and blast effects

The above factors are very important, and in practice may actually govern the system reliability of the concepts studied. For this reason, the results and conclusions from this study should be used with caution.

6. The various analyses carried out in the project were based on the North Sea environmental and geotechnical conditions, and standard North Sea design, fabrication, installation, and operation procedures will be assumed. Although some effort will be made to generalise the reliability results to other environmental conditions, care should be exercised in extrapolating the results to other geographical locations with wholly different environmental and geotechnical conditions, and design, fabrication, installation, operation and maintenance practices.

Feasibility

Resources

Technical resources were available through companies involved with offshore platforms, the internet, and the writer's supervisor.

Time Frame

The project was completed on time as sufficient time had been considered for every stage.

Report Format

This report includes six main chapters:

- Offshore Platforms
- Structural Stability
- A Recent Minimum Facility Platform
- Case Study
- Computer Simulations
- Scale Model Experiments

Offshore Platforms, Structural Stability, and A Recent Minimum Facility Platform constitute the literature review. *Case Study, Computer Simulations* and *Scale Model Experiments* make up the methodology of this project. Results and discussions are included at the end of each methodology chapter.

2. OFFSHORE PLATFORMS

The literature review carried out for this project is summarized in this chapter and the next. This chapter contains general background information on offshore platforms.

2.1 INTRODUCTION

The structure shown in Figure 2.1 is instantly recognizable as an offshore rig. This type of structure, more correctly described as a fixed steel offshore installation or platform forms the backbone of the offshore industry and there are in excess of 7,000 such structures dotted about the oceans of the world.

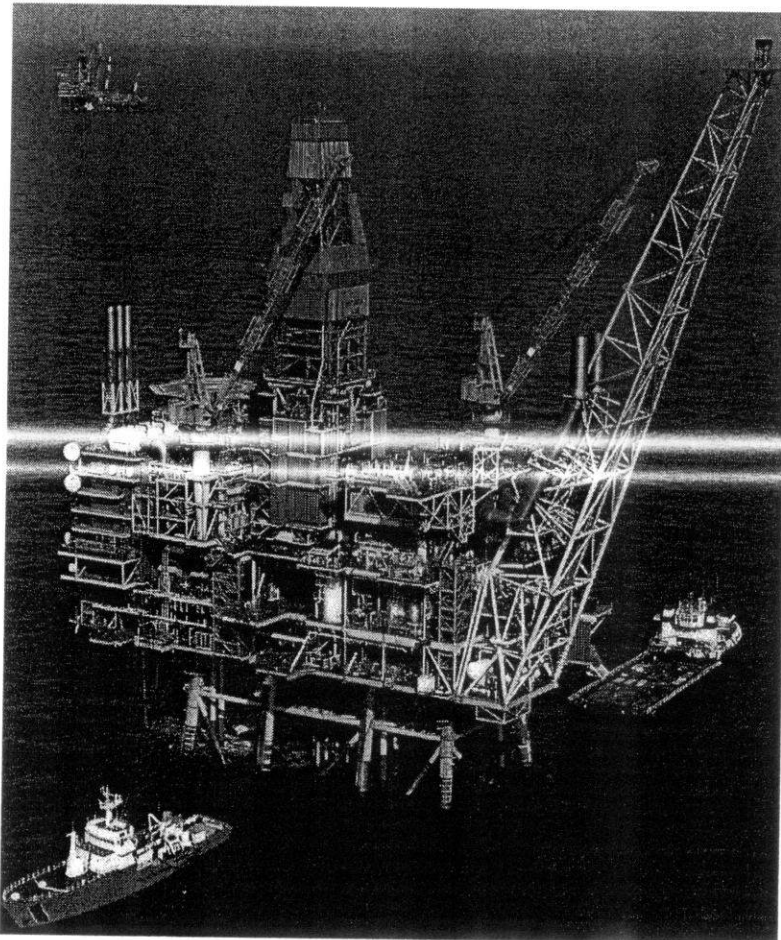


Figure 2.1: An offshore platform

The typical offshore drilling and production platform does not exist for its own sake but rather is thought of as a necessary but expensive support for the primary functions which are the reason for the project. These functions are to drill wells, produce oil and gas, process it as necessary, and discharge it to pipelines to shore or a loading terminal.

From the platform, conductors are installed. On the deck, derrick and drilling modules are installed, so that the wells can be drilled. Processing modules are installed on the deck, and all the necessary support modules for accommodations, power and water generation, sewage disposal, communication, and heliport. Cranes are installed to handle drill collars and casing, and all consumables from barges or supply boats to the deck. On the deck are stored drilling mud, cement, fresh water, and diesel oil. Other functions, such as re-injection of water or gas, may also be performed from the platform. An emergency flare stack is provided in order to flare excess gas. While diesel oil is used initially to fuel operations, produced gas may be used after production and processing are established.

Depending on the circumstances, the platform may be attached to the ocean floor, consist of an artificial island, or be floating. Generally, oil platforms are located on the continental shelf, though as technology improves, drilling and production in deeper waters becomes both feasible and profitable.

Operations

The writer chose Petroleum Engineering as his specialization in the final year of his Civil Engineering undergraduate program. The courses offered in this specialization have familiarized the writer with operations associated with offshore platforms in the oil and gas industry. They have opened his eyes to the vital role offshore platforms play in the recovery of petroleum and how they help meet the ever-increasing demands of the global market.

The Petroleum Engineering courses are introductory but comprehensive in nature and have been designed so that graduates are technically prepared for, and have an essential knowledge of the petroleum industry into which they will be recruited. The courses include:

- Reservoir Engineering
- Petroleum Exploration
- Drilling and Production Technology
- Facilities Engineering, Transportation and Storage

2.2 CLASSIFICATIONS

In this section the various types of offshore platforms are introduced. There are two basic categories of offshore platforms: those that can be moved from place to place, allowing for drilling in multiple locations, and those rigs that are permanently placed.

Moveable Offshore Platforms

Moveable rigs are often used for exploratory purposes because they are much cheaper to use than permanent platforms. Once large deposits of hydrocarbons have been found, a permanent platform is built to allow their extraction. The sections below describe a number of different types of moveable offshore platforms.

Drilling Barges

Drilling barges (Figure 2.2) are used mostly for inland, shallow water drilling. This typically takes place in lakes, swamps, rivers, and canals. Drilling barges are large, floating platforms, which must be towed by tugboat from location to location. Suitable for still, shallow waters, drilling barges are not able to withstand the water movement experienced in large open water situations.

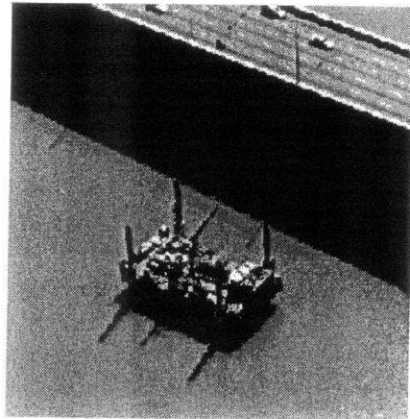


Figure 2.2: A drilling barge

Jack-Up Rigs

Jack-up rigs (Figure 2.3) are similar to drilling barges, with one difference. Once a jack-up rig is towed to the drilling site, three or four 'legs' are lowered until they rest on the sea bottom (Figure 2.4). This allows the working platform to rest above the surface of the water, as opposed to a floating barge. However, jack-up rigs are suitable for shallower waters, as extending these legs down too deeply would be impractical. These rigs are typically safer to operate than drilling barges, as their working platform is elevated above the water level.

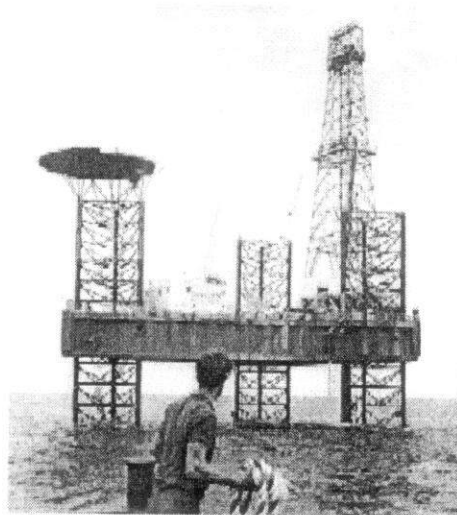


Figure 2.3: A jackup rig

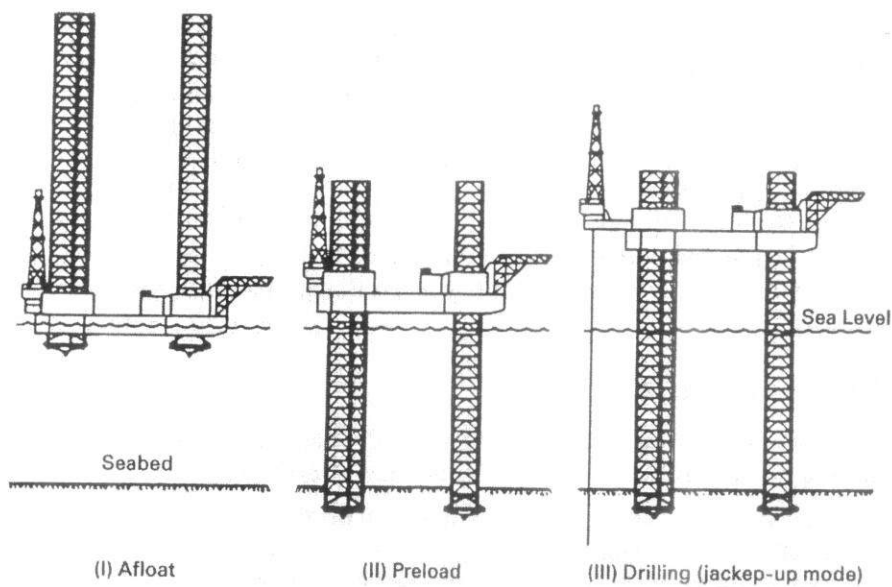


Figure 2.4: Installation of jakup rigs

Drillships

Drillships (Figure 2.5) are exactly as they sound: ships designed to carry out drilling operations. These boats are specially designed to carry drilling platforms out to deep-sea locations. A typical drillship will have, in addition to all of the equipment normally found on a large ocean ship, a drilling platform and derrick located on the middle of its deck. In addition, drillships contain a hole (or 'moonpool'), extending right through the ship down through the hull, which allow for the drill string to extend through the boat, down into the water. Drillships are often used to drill in very deep water, which can often be quite turbulent. Drillships use what is known as 'dynamic positioning' systems. Drillships are equipped with electric motors on the underside of the ships hull, capable of propelling the ship in any direction. These motors are integrated into the ships computer system, which uses satellite positioning technology, in conjunction with sensors located on the drilling template, to ensure that the ship is directly above the drill site at all times.

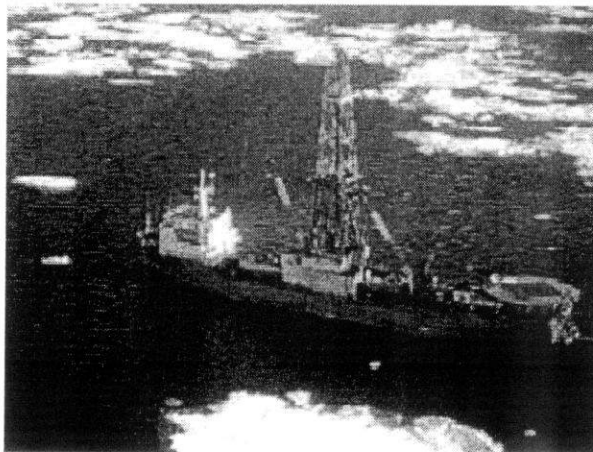


Figure 2.5: A Drillship in the Beaufort Sea

Submersible Rigs

Submersible rigs, also suitable for shallow water, are like jack-up rigs in that they come in contact with the ocean or lake floor. These rigs consist of platforms with two hulls positioned on top of one another. The upper hull contains the living quarters for the crew, as well as the actual drilling platform. The lower hull works much like the outer hull in a submarine - when the platform is being moved from one place to another, the lower hull is filled with air - making the entire rig buoyant. When the rig is positioned over the drill site, the air is let out of the lower hull, and the rig submerges to the sea or lake floor. This type of rig has the advantage of mobility in the water, however once again its use is limited to shallow water areas.

Semi-Submersible Rigs

Semi-submersible rigs (Figure 2.6) are the most common type of offshore drilling rigs, combining the advantages of submersible rigs with the ability to drill in deep water. Semi-submersible rigs work on the same principle as submersible rigs; through the 'inflating' and 'deflating' of its lower hull. The main difference with a semi-submersible rig, however, is that when the air is let out of the lower hull, the rig does not submerge to the sea floor. Instead, the rig is partially submerged, but still floats above the drill site. When drilling, the lower hull, filled with water, provides stability to the rig. Semi-submersible rigs are held in place by huge anchors, each weighing upwards of ten tons. These anchors, combined with the submerged portion of the rig, ensure that the platform is stable and safe enough to be used in turbulent offshore waters. Semi-submersible rigs can be used to drill in much deeper water than the rigs mentioned above.

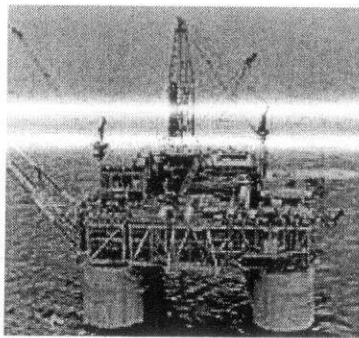


Figure 2.6: A semi-submersible rig

Permanent Offshore Platforms

As mentioned, moveable rigs are commonly used to drill exploratory wells. In some instances, when exploratory wells find commercially viable natural gas or petroleum deposits, it is economical to build a permanent platform from which well completion, extraction, and production can occur. These large, permanent platforms are extremely expensive, however, and generally require large expected hydrocarbon deposits to be economical to construct. Some of the largest offshore platforms are located in the North Sea, where because of almost constant inclement weather, structures able to withstand high winds and large waves are necessary. A typical permanent platform in the North Sea must be able to withstand wind speeds of over 90 knots, and waves over 60 feet high. Correspondingly, these platforms are among the largest structures built by man. See Figure 2.7.

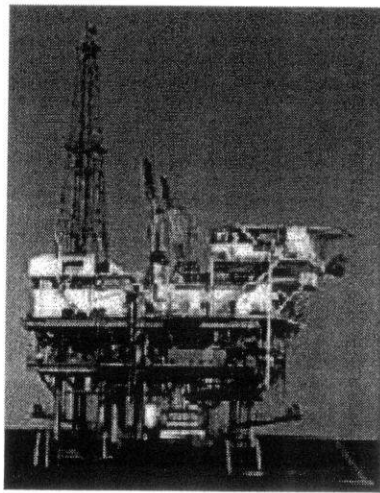


Figure 2.7: An Offshore Platform

There are a number of different types of permanent offshore platforms, each useful for a particular depth range. See Figure 2.8. For reference, the fixed platform (the shallowest shown) is usually in no more than 1,500 feet of water - whereas the height of the Hoover Dam, from top to bottom, is less than half that, at just under 730 feet. Figure 2.9 gives another overview of various offshore platforms and their feasible depth ranges.

Because of their size, most permanent offshore rigs are constructed near land, in pieces. As the components of the rig are completed, they are taken out to the drilling location. Sometimes construction or assembly can even take place as the rig is being transported to its intended destination.

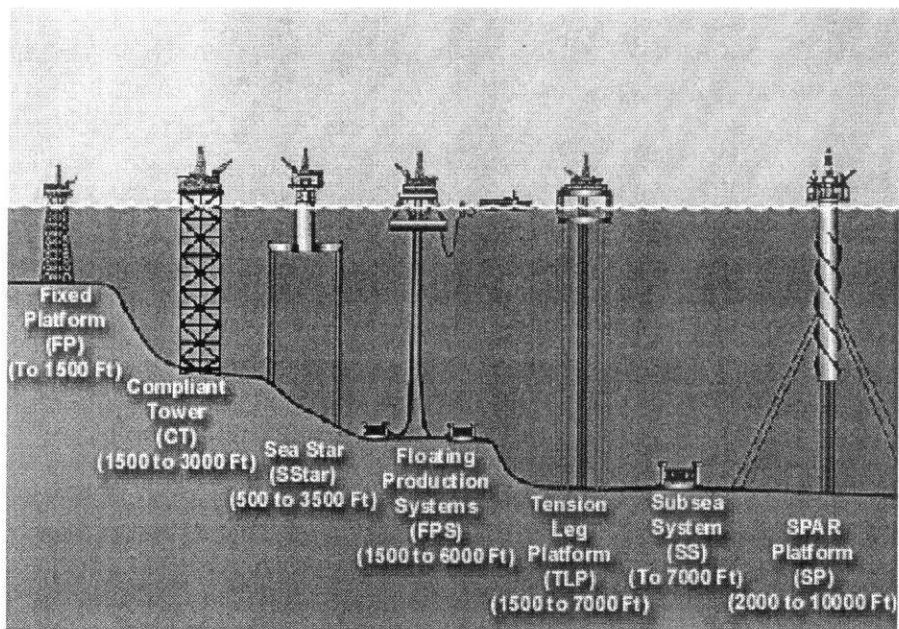


Figure 2.8: Offshore Drilling Platforms and typical depth ranges

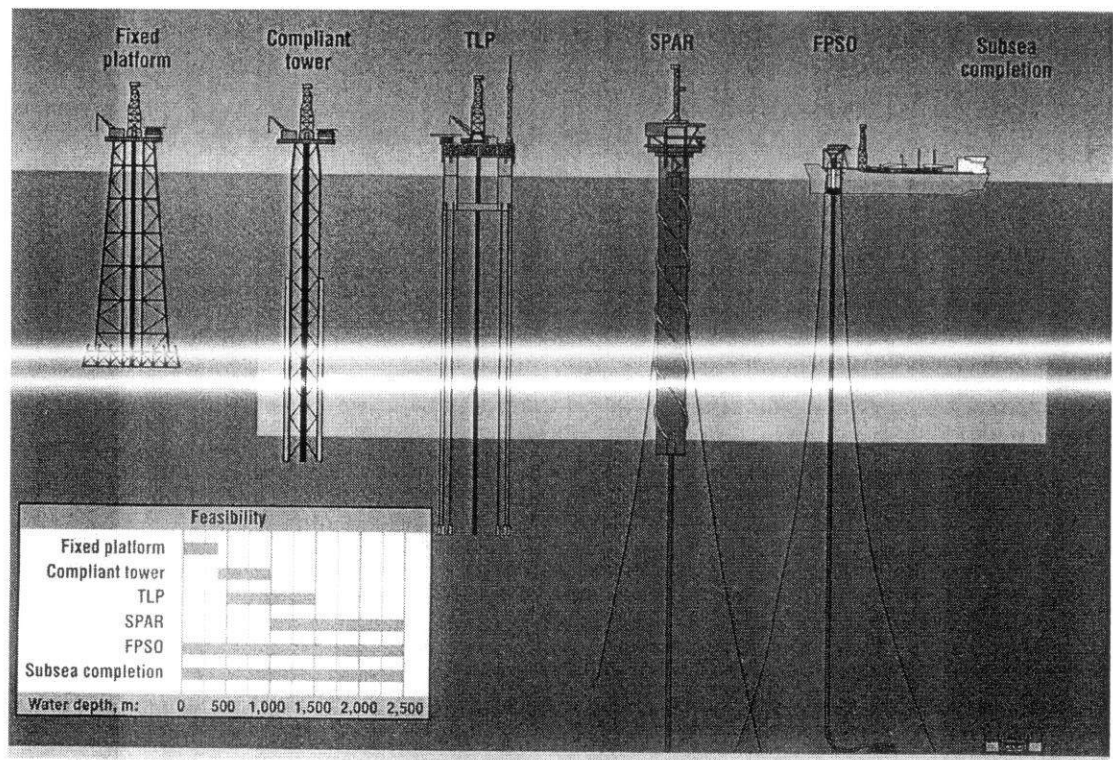


Figure 2.9: Various Offshore Platforms and feasible depth ranges

Fixed Platforms

In certain instances, in shallower water, it is possible to physically attach a platform to the sea floor. This is what is shown above as a fixed platform rig. The 'legs' are constructed with concrete or steel, extending down from the platform, and fixed to the seafloor with piles. With some concrete structures, the weight of the legs and seafloor platform is so great, that they do not have to be physically attached to the seafloor, but instead simply rest on their own mass. There are many possible designs for these fixed, permanent platforms. The main advantages of these types of platforms are their stability, as they are attached to the sea floor there is limited exposure to movement due to wind and water forces. However, these platforms cannot be used in extremely deep water, it simply is not economical to build legs that long. Figure 2.10 shows a typical fixed steel platform and its components.

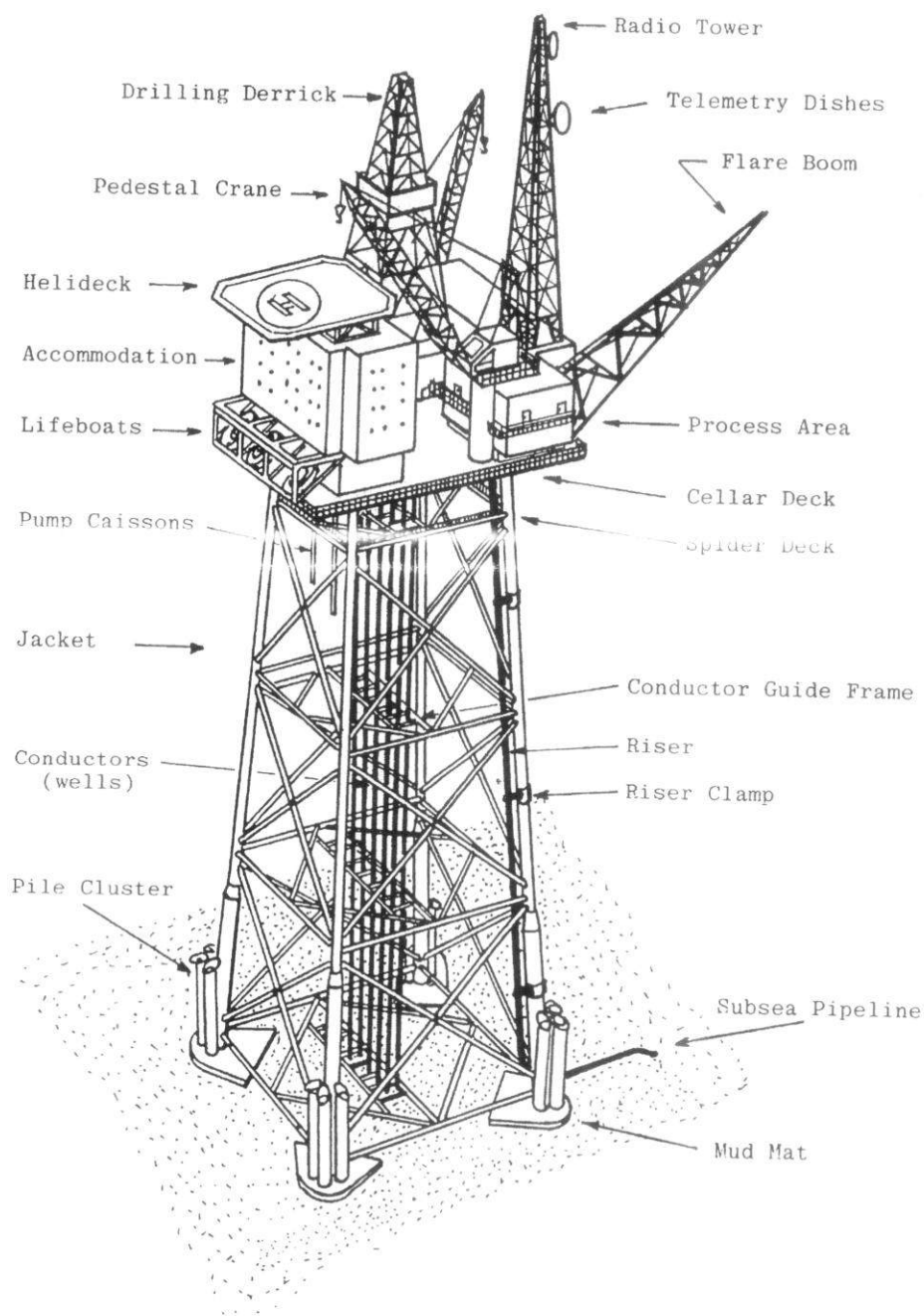


Figure 2.10: A typical fixed steel platform and its components

Compliant Towers

Compliant towers are much like fixed platforms. They consist of a narrow tower, attached to a foundation on the seafloor and extending up to the platform. This tower is flexible, as opposed to the relatively rigid legs of a fixed platform. This flexibility allows it to operate in much deeper water, as it can 'absorb' much of the pressure exerted on it by the wind and sea. Despite its flexibility, the compliant tower system is strong enough to withstand hurricane conditions.

Seastar Platforms

Seastar platforms (Figure 2.11) are like miniature tension leg platforms. The platform consists of a floating rig, much like the semi-submersible type discussed above. A lower hull is filled with water when drilling, which increases the stability of the platform against wind and water movement. In addition to this semi-submersible rig, however, Seastar platforms also incorporate the tension leg system employed in larger platforms. Tension legs are long, hollow tendons that extend from the seafloor to the floating platform. These legs are kept under constant tension, and do not allow for any up or down movement of the platform. However, their flexibility does allow for side-to-side motion, which allows the platform to withstand the force of the ocean and wind without breaking the legs off. Seastar platforms are typically used for smaller deep-water reservoirs, when it is not economical to build a larger platform. They can operate in water depths of up to 3,500 feet.

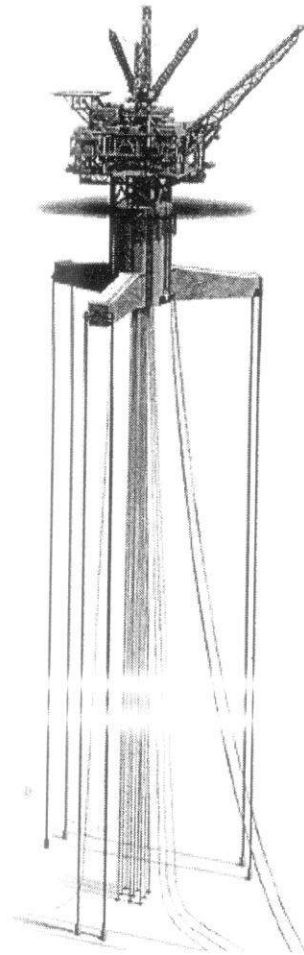


Figure 2.11: A Seastar platform

Spar Platforms

SPAR platforms are among the largest offshore platforms in use. These huge platforms consist of a large cylinder supporting a typical fixed rig platform. The cylinder however does not extend all the way to the seafloor, but instead is tethered to the bottom by a series of cables and lines. The large cylinder serves to stabilize the platform in the water, and allows for movement to absorb the force of potential hurricanes. The first SPAR platform in the Gulf of Mexico was installed in September of 1996. It's cylinder measured 770 feet long, and was 70 feet in diameter, and the platform operated in 1,930 feet of water. Figure 2.12 illustrates the configuration of a typical SPAR platform.

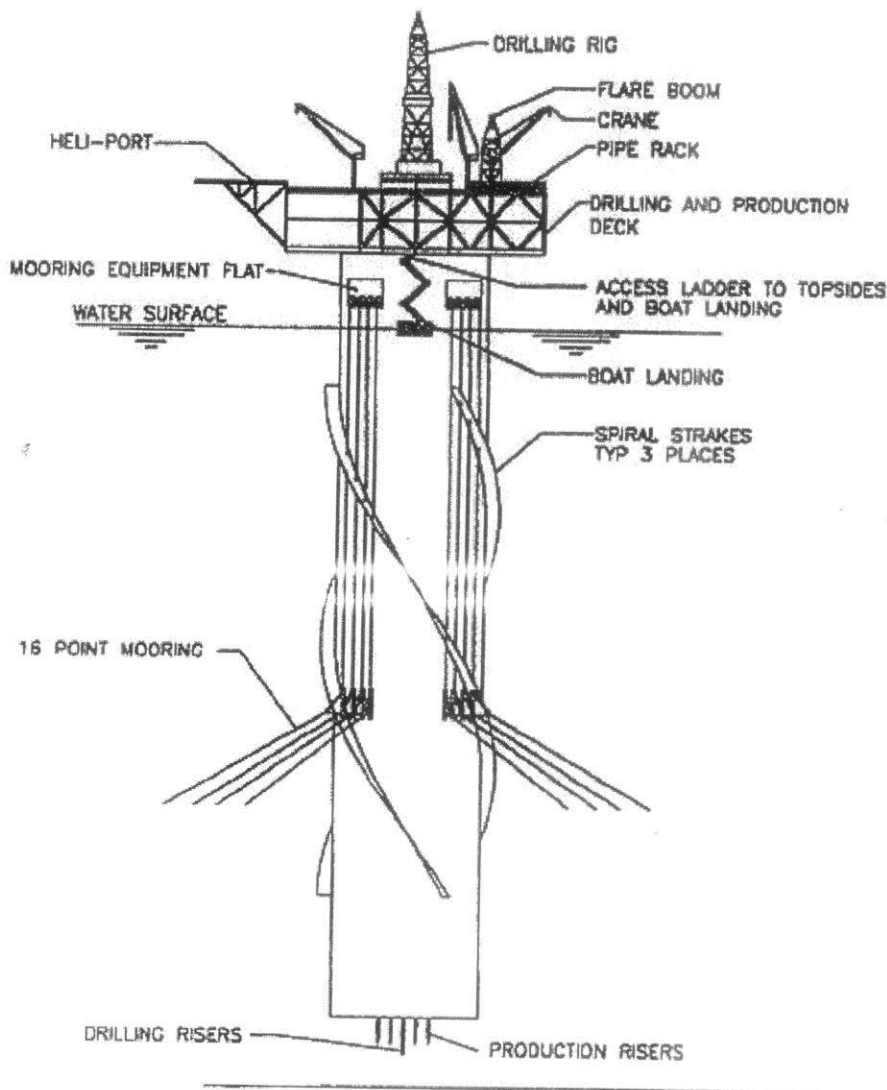


Figure 2.12: Configuration of a typical SPAR platform

Floating Production Systems

Floating Production Systems (Figure 2.13) are essentially semi-submersible drilling rigs, as discussed above, except that they contain petroleum production equipment, as well as drilling equipment. Ships can also be used as floating production systems. The platforms can be kept in place through large, heavy anchors, or through the dynamic positioning system used by drill-ships. With a floating production system, once the drilling has been completed, the wellhead is actually attached to the seafloor, instead of up on the platform. The extracted petroleum is transported via risers from this wellhead to the production facilities on the semi-submersible platform. These production systems can operate in water depths of up to 6,000 feet.

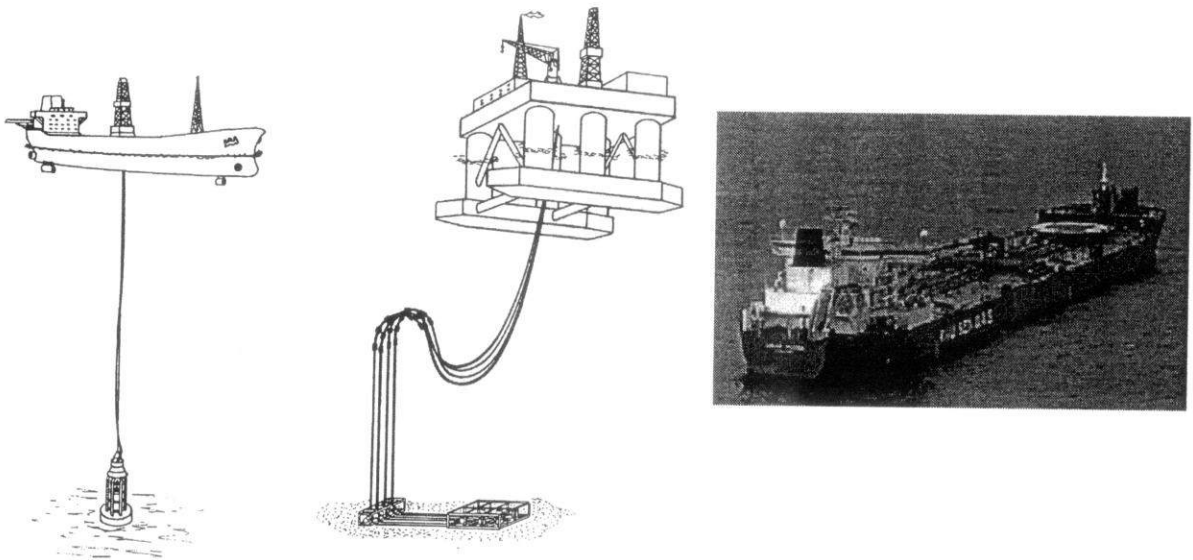


Figure 2.13: Floating Production Systems

Subsea System

Subsea production systems are wells located on the sea floor, as opposed to at the surface. Like in a floating production system, the petroleum is extracted at the seafloor, and then can be 'tied-back' to an already existing production platform. The well can be drilled by a moveable rig, and instead of building a production platform for that well, the extracted oil and natural gas can be transported by riser or even undersea pipeline to a nearby production platform. This allows one strategically placed production platform to service many wells over a reasonably large area. Subsea systems are typically in use at depths of 7,000 feet or more, and do not have the ability to drill, only to extract and transport.

Tension Leg Platforms

Tension leg platforms (Figure 2.14) are larger versions of the Seastar platform. The long, flexible legs are attached to the seafloor, and run up to the platform itself. As with the Seastar platform, these legs allow for significant side to side movement (up to 20 feet), with little vertical movement. Tension leg platforms can operate as deep as 7,000 feet. Figure 2.15 shows the typical components of Tension Leg Platforms.

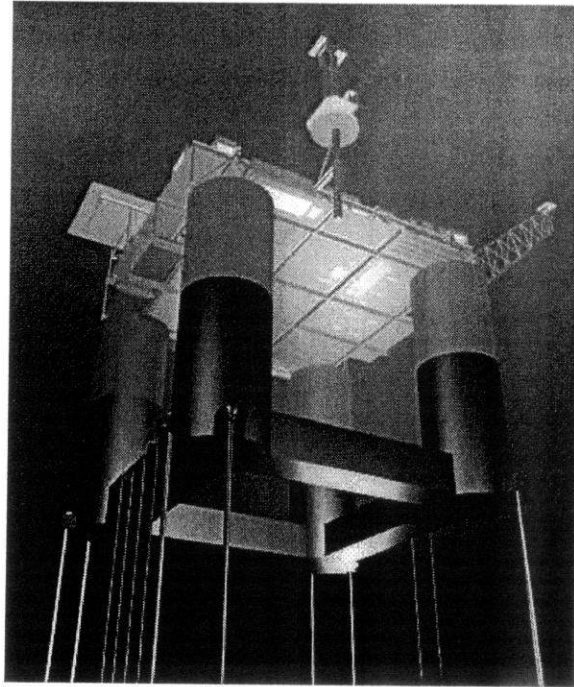


Figure 2.14: A Tension Leg Platform

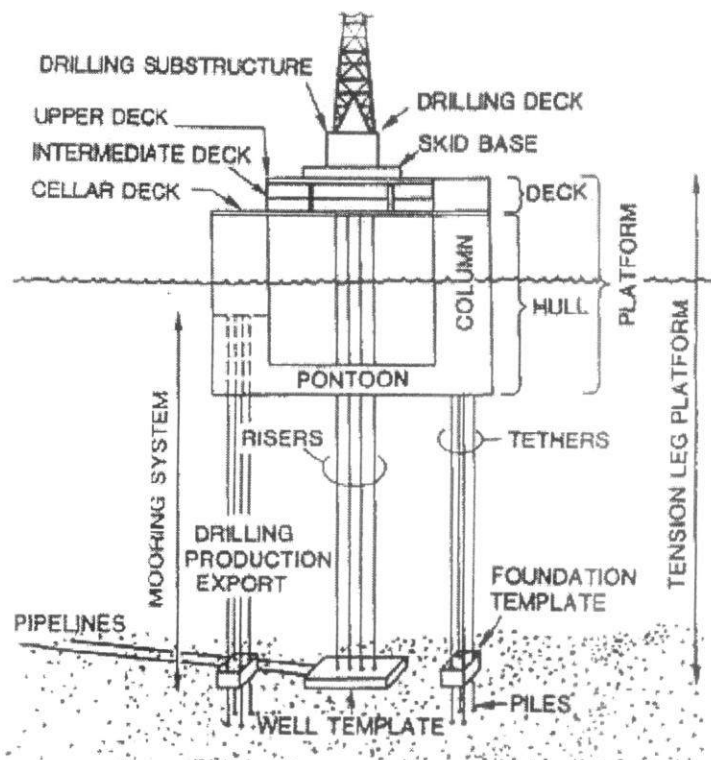


Figure 2.15: Tension Leg Platform components

A Broad Classification of Platforms

Table 2.1 classifies platforms in terms of their functions.

Table 2.1: Classification of platforms by functions

Category	Type of unit – description
Drilling	Drilling platforms whose sole purpose is to drill
Production	Traditional (manned) production platforms, steel jackets or GBSs. Included are also platforms with drilling, production, and accommodation facilities (i.e. large integrated platforms)
Wellhead	Wellhead platforms (normally unmanned) with no processing facilities, serving as “well support”. Often linked to the main production platforms.
Compression	Gas compression platforms
Pumping	Pumping platforms
Injection/riser	Water or gas injection and riser platforms
Accommodation	Accommodation platforms

2.3 STATISTICS

Today there are more than 6,500 offshore oil and gas production installations world wide, located on the continental shelves of some 53 countries. Over 4,000 are situated in the US Gulf of Mexico, some 900 in Asia, some 700 in the Middle East and around 1000 in the North Sea and North East Atlantic.

The first offshore fields of oil and gas in the North Sea were discovered in the late 1960s. The UK, Norway, Denmark, The Netherlands, and to a lesser extent Germany, have all benefited from the discoveries made.

There are more than 500 offshore oil and gas installations in operation in the UK Continental Shelf (UKCS) today. These include sub-sea equipment fixed to the ocean floor as well as platforms ranging from the smaller structures in the Southern and Central North Sea to the enormous installations in the northern North Sea built to withstand very harsh weather conditions in deep waters. Many of the structures were built in the 1970s and were hailed as technological feats when they were installed.

Table 2.2 shows the number of international offshore rigs by geographic region in mid-2006.

Table 2.2: International offshore rigs

August 2006	US Gulf of Mexico		Europe/Mediterranean		Worldwide	
	Mobile	Platform	Mobile	Platform*	Mobile	Platform*
Total rigs in fleet	147	55	99	109	651	288
year ago	154	61	101	109	642	293
Contracted rigs	124	28	96	107	597	230
year ago	132	28	95	108	571	228
Rig utilization, %	84.4	50.9	97.0	98.2	91.7	79.9
year ago	85.7	45.9	94.1	99.1	88.9	77.8

Source: ODS-Petrodata Weekly Mobile Offshore Rig Count

*Updated quarterly

2.4 CONSTRUCTION

By taking the subject “Construction of Marine and Offshore Structures” taught by Dr. Nasir Shafiq, the writer familiarized himself with the construction, transportation and installation of offshore platforms. What follows is a summary of the course syllabus based on the chapters of the textbook.

Introduction

The oceans are the dominant features of Earth, comprising more than two thirds of its surface, stabilizing its temperature so that life as we know it can exist, providing the water vapour which later falls as rain on the continental “islands,” the original source of life and the ultimate collector or sink of all superficial matter, including waste. Oceans have been both a barrier and a conduit over which people and goods have moved with relative ease, spreading culture while garnering Earth’s remote resources.

Yet the ocean is fiercely inhospitable, making us dependent on land bases for support. Storm waves have destroyed even the largest vessels, as well as the puny attempts of humans to protect the coastline from the oceans’ attack. The northernmost ocean, the Arctic, is almost completely covered with perpetual sea ice, while the southern, the Antarctic, carries with it huge tabular icebergs that stretch beyond the horizon.

Opportunity and challenge, safety and terror, wealth and destruction: these are the paradoxes of the seas.

Physical Environmental Aspects of Marine and Offshore Construction

The oceans present a unique set of environmental conditions which dominate the methods, equipment, support, and procedures to be employed in construction offshore. This same unique environment also, of course, dominates the design. Many books have addressed the extreme environmental events and adverse exposures as they affect design. Unfortunately, relatively little attention has been given in published texts to the environment’s influence on construction. Since the design of offshore structures is based to a substantial degree upon the ability to construct, there is an obvious need to understand and adapt to environmental aspects as they affect construction. These considerations are even more dominant in many coastal projects where breaking waves and high surf make normal construction practices impossible. To a lesser extent, they have an important role in harbour and river construction.

In this chapter, the principal environmental factors are examined individually. As will be repeatedly emphasized elsewhere in this book, a typical construction project will be subjected to many of these concurrently, and it will be necessary to consider their interaction with each other and with the construction activity.

Geotechnical Aspects: Seafloor and Marine Soils

There are certain specific problem conditions which have caused many constructional problems. Throughout this chapter, reference will frequently be made to the difficulties which geotechnical engineers have in obtaining proper samples and data in critical seafloor soils. While great progress continues to be made in improving sampling methods and in applying new techniques such as electrical resistivity, shear velocity, and geophysical methods, many types of seafloor soils continue to give difficulty. In many of these cases, the in-place strength will be greater than indicated by conventional sampling methods. With low-technology and crude sampling methods, critical constituents may not be recovered or identified. Construction engineers need to recognize these problems, so that they may adequately interpret the geotechnical reports and logs of borings and make appropriate decisions regarding their construction methods, equipment, and procedures. Failure to recognize these potential problem areas has led to a substantial number of cases of serious cost overruns and delays.

Most structures in the ocean extend over substantial areas. There may be significant variations in soil properties over this extent. Because of the cost and time required, it may not be possible to obtain a sufficient number of borings to show the true situation with its variations. There is a tendency to place undue emphasis on the few borings that may be available. Geophysical methods such as “sparker surveys” and a study of the site geology may help to alert the constructor to the range of soil properties that may be encountered.

Materials and Fabrication for Offshore Structures

The principal materials for offshore structures are steel and concrete. The fabrication and/or construction contractor is generally responsible for their procurement and quality control, although in some cases, especially pipeline steel, the basic material may be separately purchased by the client (operator) and made available to the constructor.

These materials must perform in a harsh environment, subject to the many corrosive and erosive actions of the sea, under dynamic cyclic and impact conditions over a wide range of temperatures. Thus, special criteria and requirements are imposed on the material qualities and their control.

Fabrication is especially critical for both steel and concrete in order to assure that the structure will perform properly under both service and extreme loads. The cyclic nature of the loading combined with the corrosive environment tends to propagate cracks; hence improper fabrication details and procedures may grow into serious problems. Fabrication is also rendered more difficult because of the large sizes of offshore structures. Spatial dimensions are difficult to measure and maintain, and thermal strains cause significant temporary distortions. Details of fabrication become highly important.

Marine & Offshore Construction Equipment

The demands of the marine working environment, coupled with the demand for large-scale structures, have led to the development of a great many types of specialized and advanced construction equipment. Indeed, the response of equipment manufacturers and constructors has been rapid and effective. The availability of construction equipment of greater capabilities has in turn played a major role in altering construction methods and in making technically feasible and economically justifiable complex structures in extremely demanding environments. These developments will continue as industrial development, principally the offshore petroleum industry, military requirements, and maritime commerce, continue their current rate of growth.

The major construction equipment has been designed to work in and under the sea and hence has drawn heavily on naval architecture to ensure serviceability and stability as well as limited and predictable motion response under the prevailing marine and offshore conditions. This extension from conventional barges and ships, directed primarily for transport, to construction, drilling, and dredging operations has in turn forced the naval architectural profession to develop a methodology adaptable to a wide variety of configurations and dynamic forces. While transport hurricanes and icebreakers follow open leads in the pack ice, fixed structures must survive the full brunt of such environmental extremes.

Life safety must be paramount in offshore operations. The nature of the work is inherently demanding and dangerous. The equipment must be designed not only for serviceability but also for safe operations.

Marine and especially offshore equipment is very expensive: each hour has a high value in ownership or rental, plus high operating costs. Therefore, the equipment must be designed with reliability and redundancy. As a general rule, it should be capable of efficient operations in 70% or more of the days in the working season. Construction engineers must understand the capabilities and limitations of the equipment they use. They must be alert to detect early signs of problems before they develop to catastrophic proportions. Thus a full understanding of equipment performance is essential. In subsequent subsections of this chapter, principal generic types of marine and offshore construction equipment will be discussed.

The marine construction industry has been subject to dramatic cyclic variations, from over-demand to recession. In times such as those in which this chapter is being written (1998), when the demand for large specialized equipment exceeds the supply, two responses have developed. One is the placement of orders with shipyards and crane manufacturers for new construction of the standard offshore equipment, upgraded to allow its use in deeper water and in exposed environments. The other, very interesting development has been that in which existing equipment is being modified and new procedures are being developed in order to perform tasks which hitherto were only possible with large conventional equipment.

These latter are making extensive use of the newly developed hydraulic jacks, with long strokes, high capacity, and the ability to accommodate transverse relative motion by means of rollers and low-friction materials such as Teflon. For inshore marine operations, such as bridges and locks and dams, these same two contrary approaches

are being employed. This is especially true where physical constructions limit maneuverability and draft limits access.

There are a number of basic considerations applicable to all offshore construction equipment. These are motion response, buoyancy, draft, freeboard, stability, and damage control.

Marine Operations

In this chapter, relevant marine and offshore operations are described. These include towing, mooring, ballasting, handling heavy loads at sea, personnel transfer, surveying, and diving.

Installation of Piles in Marine and Offshore Structures

Piling for marine and offshore structures must be installed to develop the required capacities in bearing, uplift, and lateral resistance. For offshore bridge piers, control and minimization of settlements may also be criteria. Stiffness under lateral loads, as well as strength, and the ability to accept overloads in a ductile mode are also important characteristics.

Deep water, long, unsupported column lengths, large cyclic bending forces, and large lateral and axial forces all combine to make offshore piles large in diameter and long in length. Piles in most offshore practice are steel pipe piles ranging from 1 m up to 2 m (and even 4 m) in diameter and in lengths from 40 to 300 m. Pile capacities have design ultimate values of up to 10,000 tons, far above those of conventional onshore piles. Similarly, marine piles for harbours are generally much larger and more heavily reinforced than piles for land foundations.

Offshore Platforms: Steel Jackets and Pin Piles

This chapter addresses the typical offshore platform, originated in the Gulf of Mexico and now spread worldwide. Its range extends from water depths of 12 m to over 400 m and from relatively benign climates in Southeast Asia to those of the North Sea and North Atlantic. Over 4000 such platforms have been constructed. Jackets, the main component of the system, range in weight from a few hundred tons to over 40,000 tons.

The principal structural components of the offshore platform are the jacket, the piles, and the deck. The concept is very simple: the jacket is prefabricated on shore as a space frame, then it is transported to the site and seated on the seafloor. The piles are then driven through sleeves in the jacket, and connected to the sleeves. The deck is now set.

Jackets are also employed for offshore terminal construction, especially for the loading platform and breasting dolphins.

The typical offshore drilling and production platform does not exist for its own sake but rather is thought of as a necessary but expensive support for the primary functions which are the reason for the project. These functions are to drill wells, produce oil and gas, process it as necessary, and discharge it to pipelines to shore or a loading terminal.

From the platform, conductors are installed, held by conductor guides bracketed out from the jacket. On the deck, derrick and drilling modules are installed, so that the wells can be drilled. Processing modules are installed on the deck, and all the necessary support modules for accommodations, power and water generation, sewage disposal, communication, and heliport. Cranes are installed to handle drill collars and casing, and all consumables from barges or supply boats to the deck. On the deck are stored drilling mud, cement, fresh water, and diesel oil. Other functions, such as re-injection of water or gas, may also be performed from the platform. An emergency flare stack is provided in order to flare excess gas. While diesel oil is used initially to fuel operations, produced gas may be used after production and processing are established.

The construction phase of a jacket for an offshore platform include fabrication, load-out, transport, launching, upending and seating, piling, deck installation, and module erection.

Concrete Offshore Platforms: Gravity-Base Structures

Offshore platforms of the gravity-base category are designed to be founded at or just below the seafloor, transferring their loads to the soil by means of shallow footings. Such gravity-base platforms have usually been constructed of reinforced and prestressed concrete but a few have been built of steel or a hybrid of concrete and steel.

These platforms are almost always constructed in their vertical (final) attitude, enabling much or all of the deck girders and equipment to be installed at an inshore site and transported with the substructure to the installation site. These structures are usually self-floating, although, when necessary, additional lift forces may be developed by temporary buoyancy tanks or special lifting vessels.

To minimize soil-bearing loads, these structures have a large base "footprint." To provide buoyancy, they have large enclosed volumes. They thus generate much greater inertial forces under waves and earthquake, 50,000 to 100,000 tons of lateral force being typical, with special structures developing even more. Thus sliding tends to become the dominant mode of failure, at least for water depths up to 150 to 200 m. To transfer this lateral load into the soil and thus prevent sliding, steel skirts and steel dowels are employed, designed to penetrate and thus force the failure surface farther below the seafloor. Such skirts also provide protection against scour and piping. While the skirts are typically fixed to the base of the platform during fabrication, in special cases where shallow water limits draft, skirts or spuds may be installed through sleeves after the structure has been seated on the seafloor.

The construction of a typical concrete gravity-base platform takes place in a well-defined sequence of stages. For each stage, there are several important criteria which must be met:

1. The structure must be watertight and have stability and freeboard at all stages of construction.
2. The loading conditions and combinations acting on the structure are significantly different from one stage to the next. Structural integrity must be assured at each stage.

3. Ballasting and compressed-air systems (if these latter are employed) must be carefully and positively controlled at all stages.

To meet the above criteria, it becomes necessary to control weights and dimensions with great care. These structures are very large and massive, extending 100 to 200 m or more on the three axes.

There are numerous substages in each main stage of constructing gravity-base platforms. Each such stage must be carefully analysed to be sure all criteria are met from the beginning to the end of that stage.

Most errors to date have been due either to overlooking an intermediate stage or to combining two or more stages to save computational effort. Detailed sketches of each substage, along with evaluation of the pertinent hydrostatic, hydrodynamic, and structural loadings, must be prepared to enable visualization by both design and construction engineers.

The internal subdivisions of the structure are subjected to differential pressures, primarily due to the different ballast water heads acting on each side. Compressed air may be used on occasion to pressurize a compartment; the pressures occasioned thereby must be considered.

Accidental conditions must also be considered: the loss of compressed air from under the base skirts on one side, rupture and flooding of one compartment due to collision from a boat, a broken ballast pipe, or a failed penetration. Under these accidents, the structure may be permitted to suffer minor local distress so long as its integrity, stability, and buoyancy are maintained. Progressive collapse — for example, where one compartment floods, overloading the adjoining bulkhead which in turn fails, and so on — cannot be permitted.

A more-detailed description of the special requirements and considerations at each step and stage are presented in this chapter.

Topside Installation

In recent years, almost all topside facilities have been first fabricated into modules and then transported by barge and set on the platform by an offshore derrick barge. The capacity of offshore derrick barges has steadily grown to where 1200-ton modules are commonplace and individual lifts of 4000 to 11,000 tons and more have been made.

The purpose of using larger modules is to enable more of the fit-up and testing to be completed at the shore site. This not only has the advantage of enabling the work to be done under optimal conditions, but disperses the work so that it can be accomplished concurrently with other modules and other structural work.

3. STRUCTURAL STABILITY

This chapter comprises the second chapter of the project's literature review. It starts with a description of the loads imposed on offshore structures. Next, it explains how to conceptually design offshore platforms, structurally analyse them and assess their reliability/stability in difficult conditions.

3.1 ENVIRONMENTAL LOADS

Introduction

Environmental loads are those caused by environmental phenomena such as wind, waves, current, tides, earthquakes, temperature, ice, sea bed movement, and marine growth. Their characteristic parameters, defining design load values, are determined in special studies on the basis of available data.

Whilst the design of buildings onshore is usually influenced mainly by the permanent and operating loads, the design of offshore structures is dominated by environmental loads, especially waves, and the loads arising in the various stages of construction and installation.

More than 10% of all offshore accidents are due to extreme environmental conditions. Figure 3.1, taken from the USCG database, summarises the overall causation data for 71,470 accidents recorded from 1991 to 2001.

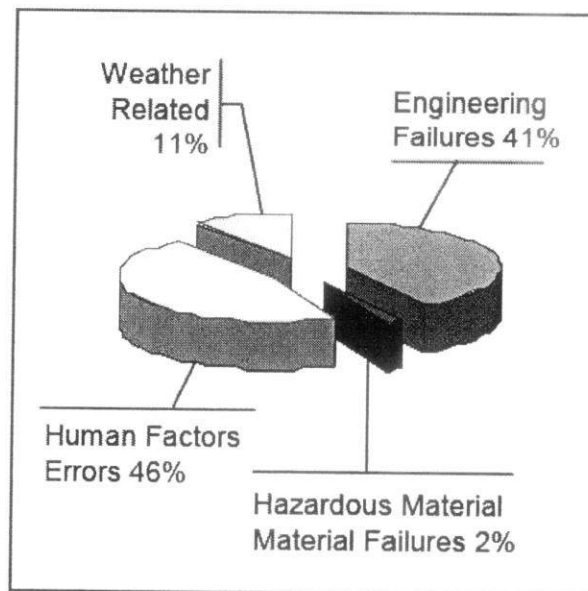


Figure 3.1: Environmental conditions cause over 10% of all offshore accidents.

Wind Loads

Wind loads act on the portion of a platform above the water level, as well as on any equipment, housing, derrick, etc. located on the deck. An important parameter pertaining to wind data is the time interval over which wind speeds are averaged. For averaging intervals less than one minute, wind speeds are classified as gusts. For averaging intervals of one minute or longer they are classified as sustained wind speeds.

The wind velocity profile may be taken from API-RP2A:

$$V_h/V_H = (h/H)^{1/n} \quad (1)$$

V_h is the wind velocity at height h ,

V_H is the wind velocity at reference height H , typically 10m above mean water level, $1/n$ is $1/13$ to $1/7$, depending on the sea state, the distance from land and the averaging time interval. It is approximately equal to $1/13$ for gusts and $1/8$ for sustained winds in the open ocean.

From the design wind velocity $V(\text{m/s})$, the static wind force $F_w(\text{N})$ acting perpendicular to an exposed area $A(\text{m}^2)$ can be computed as follows:

$$F_w = (1/2) \rho V^2 C_s A \quad (2)$$

ρ is the wind density ($\rho \approx 1.225 \text{ Kg/m}^3$)

C_s is the shape coefficient ($C_s = 1.5$ for beams and sides of buildings, $C_s = 0.5$ for cylindrical sections and $C_s = 1.0$ for total projected area of platform).

Shielding and solidity effects can be accounted for in the judgement of the designer, using appropriate coefficients.

For combination with wave loads, the DNV and DOE-OG rules recommend the more unfavourable of the following two loadings:

- a. 1-minute sustained wind speeds combined with extreme waves.
- b. 3-second gusts.

Wave Loads

The wave loading of an offshore structure is usually the most important of all environmental loadings for which the structure must be designed. The forces on the structure are caused by the motion of the water due to the waves which are generated by the action of the wind on the surface of the sea. Determination of these forces requires the solution of two separate, though interrelated problems. The first is the sea state computed using an idealisation of the wave surface profile and the wave kinematics given by an appropriate wave theory. The second is the computation of the wave forces on individual members and on the total structure, from the fluid motion.

Two different analysis concepts are used:

- The design wave concept, where a regular wave of given height and period is defined and the forces due to this wave are calculated using a high-order wave theory. Usually the 100-year wave, i.e. the maximum wave with a return period of 100 years, is chosen. No dynamic behaviour of the structure is considered. This static analysis is appropriate when the dominant wave periods are well above the period of the structure. This is the case of extreme storm waves acting on shallow water structures.
- Statistical analysis on the basis of a wave scatter diagram for the location of the structure. Appropriate wave spectra are defined to perform the analysis in the frequency domain and to generate random waves, if dynamic analyses for extreme wave loadings are required for deepwater structures. With statistical methods, the most probable maximum force during the lifetime of the structure is calculated using linear wave theory. The statistical approach has to be chosen to analyse the fatigue strength and the dynamic behaviour of the structure.

Wave theories

Wave theories describe the kinematics of waves of water on the basis of potential theory. In particular, they serve to calculate the particle velocities and accelerations and the dynamic pressure as functions of the surface elevation of the waves. The waves are assumed to be long-crested, i.e. they can be described by a two-dimensional flow field, and are characterized by the parameters: wave height (H), period (T) and water depth (d) as shown in Figure 3.2.

Different wave theories of varying complexity, developed on the basis of simplifying assumptions, are appropriate for different ranges of the wave parameters. Among the most common theories are: the linear Airy theory, the Stokes fifth-order theory, the solitary wave theory, the cnoidal theory, Dean's stream function theory and the numerical theory by Chappellear.

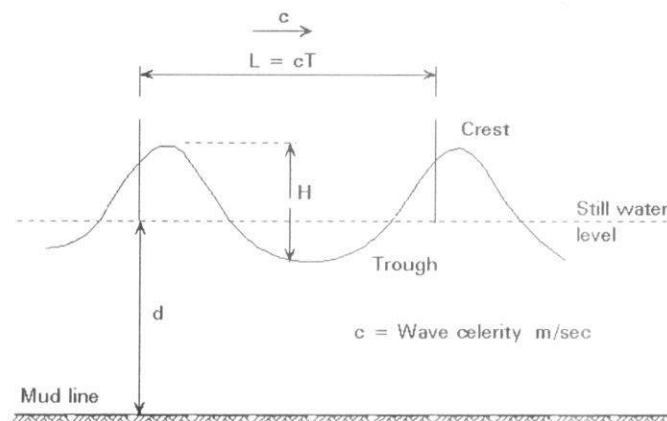


Figure 3.2: Wave Symbols

Wave Statistics

In reality waves do not occur as regular waves, but as irregular sea states. The irregular appearance results from the linear superposition of an infinite number of regular waves with varying frequency. The best means to describe a random sea state is using the wave energy density spectrum $S(f)$, usually called the wave spectrum for simplicity. It is formulated as a function of the wave frequency f using the parameters: significant wave height H_s (i.e. the mean of the highest third of all waves present in a wave train) and mean wave period (zero-upcrossing period) T_0 . As an additional parameter the spectral width can be taken into account.

Wave directionality can be introduced by means of a directional spreading function $D(f, \sigma)$, where σ is the angle of the wave approach direction. A directional wave spectrum $S(f, \sigma)$ can then be defined as:

$$S(f, \sigma) = S(f) \cdot D(f, \sigma) \quad (3)$$

The response of the structure, i.e. forces, motions, is calculated by multiplication of the wave energy spectrum with the square of a linear transfer function. From the resulting response spectrum the significant and the maximum expected response in a given time interval can be easily deduced.

Wave forces on structural members

Structures exposed to waves experience substantial forces much higher than wind loadings. The forces result from the dynamic pressure and the water particle motions. Two different cases can be distinguished:

- Large volume bodies, termed hydrodynamic compact structures, influence the wave field by diffraction and reflection. The forces on these bodies have to be determined by costly numerical calculations based on diffraction theory.
- Slender, hydrodynamically transparent structures have no significant influence on the wave field. The forces can be calculated in a straight-forward manner with Morison's equation. As a rule, Morison's equation may be applied when $D/L \leq 0.2$, where D is the member diameter and L is the wave length.

The steel jackets of offshore structures can usually be regarded as hydrodynamically transparent. The wave forces on the submerged members can therefore be calculated by Morison's equation, which expresses the wave force as the sum of an inertia force proportional to the particle acceleration and a non-linear drag force proportional to the square of the particle velocity:

$$F = C_M \frac{\rho \pi D^2}{4} \dot{v} + C_D \frac{\rho D}{2} v |v| \quad (4)$$

where

F is the wave force per unit length on a circular cylinder (N)

v , $|v|$ are water particle velocity normal to the cylinder, calculated with the selected wave theory at the cylinder axis (m/s)

\dot{v} is water particle acceleration normal to the cylinder, calculated with the selected wave theory at the cylinder axis (m/s^2)

ρ is the water density (kg/m^3)

D is the member diameter, including marine growth (m)

C_D , C_M are drag and inertia coefficients, respectively.

In this form the equation is valid for fixed tubular cylinders. For the analysis of the motion response of a structure it has to be modified to account for the motion of the cylinder. The values of C_D and C_M depend on the wave theory used, surface roughness and the flow parameters. According to API-RP2A, $C_D \approx 0.6$ to 1.2 and $C_M \approx 1.3$ to 2.0 . Additional information can be found in the DNV rules.

The total wave force on each member is obtained by numerical integration over the length of the member. The fluid velocities and accelerations at the integration points are found by direct application of the selected wave theory.

In addition to the forces given by Morison's equation, the lift forces F_L and the slamming forces F_S , typically neglected in global response computations, can be important for local member design. For a member section of unit length, these forces can be estimated as follows:

$$F_L = (1/2) \rho C_L D v^2 \quad (5)$$

$$F_S = (1/2) \rho C_s D v^2 \quad (6)$$

where C_L , C_s are the lift and slamming coefficients respectively, and the rest of the symbols are as defined in Morison's equation. Lift forces are perpendicular to the member axis and the fluid velocity v and are related to the vortex shedding frequency. Slamming forces acting on the underside of horizontal members near the mean water level are impulsive and nearly vertical. Lift forces can be estimated by taking $C_L \approx 1.3 C_D$. For tubular members $C_s \approx \pi$.

Basic Wave Parameters

In the above equations to include compute the drag and inertia forces, one needs to calculate the maximum particle velocities and accelerations. Table 3.1 contains the basic equations of wave mechanics.

Table 3.1: Basic Equations Describing Wave Mechanics

Relative Depth	Shallow Water $\frac{d}{L} < \frac{1}{20}$ $kd < \frac{\pi}{10}$	Transitional Water $\frac{1}{20} < \frac{d}{L} < \frac{1}{2}$ $\frac{\pi}{10} < kd < \frac{\pi}{2}$	Deep Water $\frac{d}{L} > \frac{1}{2}$ $kd > \frac{\pi}{2}$
1. Wave profile	Same As >	$\eta = \frac{H}{2} \cos \left[\frac{2\pi x}{L} - \frac{2\pi t}{T} \right] = \frac{H}{2} \cos \theta$	< Same As
2. Wave celerity	$C = \frac{L}{T} = \sqrt{gd}$	$C = \frac{L}{T} = \frac{gT}{2\pi} \tanh \left(\frac{2\pi d}{L} \right)$	$C = C_0 = \frac{L}{T} = \frac{gT}{2\pi}$
3. Wavelength	$L = T\sqrt{gd} = CT$	$L = \frac{gT^2}{2\pi} \tanh \left(\frac{2\pi d}{L} \right)$	$L = L_0 = \frac{gT^2}{2\pi} = C_0 T$
4. Group velocity	$C_g = C = \sqrt{gd}$	$C_g = nC = \frac{1}{2} \left[1 + \frac{4\pi d/L}{\sinh(4\pi d/L)} \right] C$	$C_g = \frac{1}{2} C = \frac{gT}{4\pi}$
5. Water particle velocity			
(a) Horizontal	$u = \frac{H}{2} \sqrt{\frac{g}{d}} \cos \theta$	$u = \frac{H}{2} \frac{gT}{L} \frac{\cosh[2\pi(z+d)/L]}{\cosh(2\pi d/L)} \cos \theta$	$u = \frac{\pi H}{T} e^{\left(\frac{2\pi z}{L}\right)} \cos \theta$
(b) Vertical	$w = \frac{H\pi}{T} \left(1 + \frac{z}{d} \right) \sin \theta$	$w = \frac{H}{2} \frac{gT}{L} \frac{\sinh[2\pi(z+d)/L]}{\cosh(2\pi d/L)} \sin \theta$	$w = \frac{\pi H}{T} e^{\left(\frac{2\pi z}{L}\right)} \sin \theta$
6. Water particle accelerations			
(a) Horizontal	$a_x = \frac{H\pi}{T} \sqrt{\frac{g}{d}} \sin \theta$	$a_x = \frac{g\pi H}{L} \frac{\cosh[2\pi(z+d)/L]}{\cosh(2\pi d/L)} \sin \theta$	$a_x = 2H \left(\frac{\pi}{T} \right)^2 e^{\left(\frac{2\pi z}{L}\right)} \sin \theta$
(b) Vertical	$a_z = -2H \left(\frac{\pi}{T} \right)^2 \left(1 + \frac{z}{d} \right) \cos \theta$	$a_z = -\frac{g\pi H}{L} \frac{\sinh[2\pi(z+d)/L]}{\cosh(2\pi d/L)} \cos \theta$	$a_z = -2H \left(\frac{\pi}{T} \right)^2 e^{\left(\frac{2\pi z}{L}\right)} \cos \theta$
7. Water particle displacements			
(a) Horizontal	$\xi = -\frac{HT}{4\pi} \sqrt{\frac{g}{d}} \sin \theta$	$\xi = -\frac{H}{2} \frac{\cosh[2\pi(z+d)/L]}{\sinh(2\pi d/L)} \sin \theta$	$\xi = -\frac{H}{2} e^{\left(\frac{2\pi z}{L}\right)} \sin \theta$
(b) Vertical	$\zeta = \frac{H}{2} \left(1 + \frac{z}{d} \right) \cos \theta$	$\zeta = \frac{H}{2} \frac{\sinh[2\pi(z+d)/L]}{\sinh(2\pi d/L)} \cos \theta$	$\zeta = \frac{H}{2} e^{\left(\frac{2\pi z}{L}\right)} \cos \theta$
8. Subsurface pressure	$p = \rho g(\eta - z)$	$p = \rho g \eta \frac{\cosh[2\pi(z+d)/L]}{\cosh(2\pi d/L)} - \rho g z$	$p = \rho g \eta e^{\left(\frac{2\pi z}{L}\right)} - \rho g z$

Current Loads

There are tidal, circulations and storm generated currents. Figure 3.3 shows a wind and tidal current profile typical of the Gulf of Mexico. When insufficient field measurements are available, current velocities may be obtained from various sources, e.g. Appendix A of DNV. In platform design, the effects of current superimposed on waves are taken into account by adding the corresponding fluid velocities in vector terms. Since the drag force varies with the square of the velocity, this addition can greatly increase the forces on a platform. For slender members, cyclic loads induced by vortex shedding may also be important and should be examined.

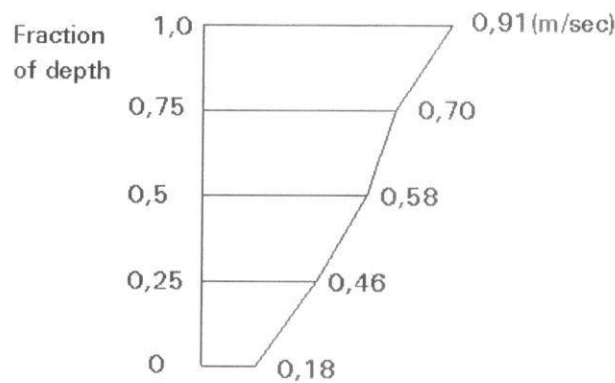


Figure 3.3: Typical wind and tidal current profile in the Gulf of Mexico

The drag force by the current on all members is computed using the basic drag force. The drag coefficient is estimated from empirical curves such as those shown in Figure 3.4 considering the effect of marine growth as roughness.

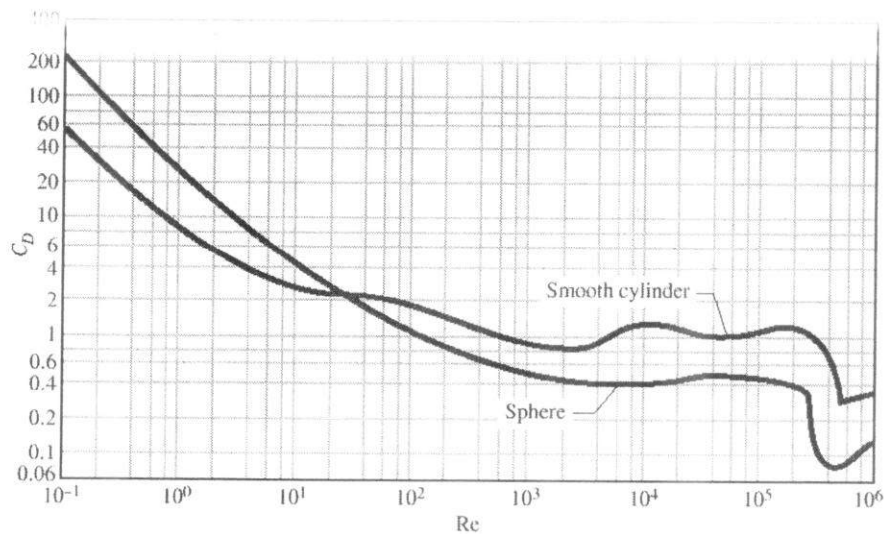


Figure 3.4: Drag Coefficient as function of Re and surface roughness

Real-Life Design Values

Figure 3.5 summarizes the values of major environmental parameters in extreme storm conditions for the Ringhorne Platform designed, constructed and installed by Heerema for ExxonMobil from 2000 to 2002. Maximum wind speed, wave height and tidal current speed are assumed to occur simultaneously in one big storm. These contribute to the maximum stress in members that should not exceed their capacities.

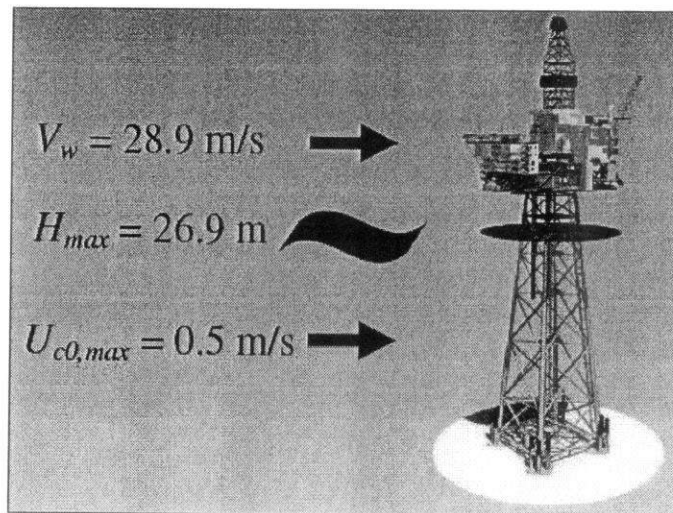


Figure 3.5: Typical Design Values of Major Environmental Factors

Earthquake Loads

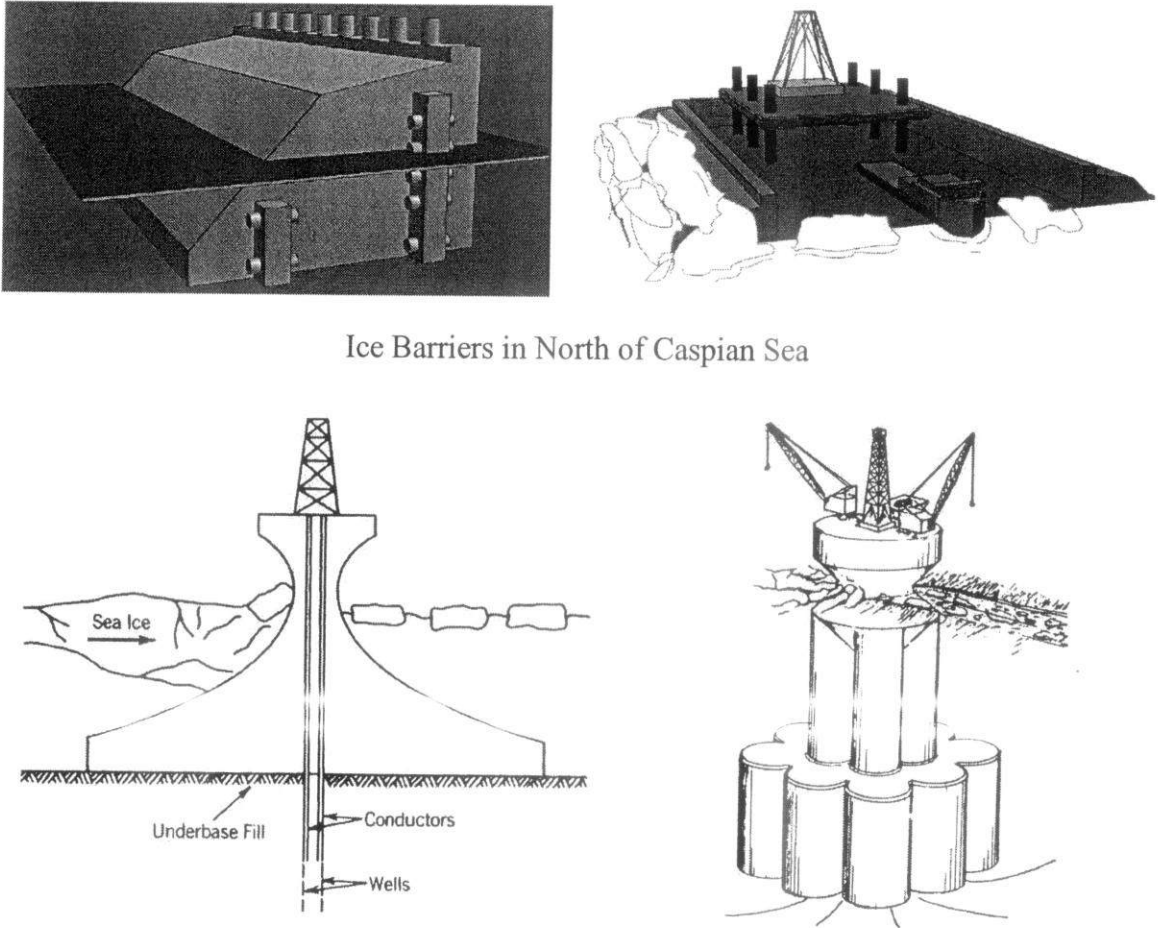
Offshore structures in seismic regions are typically designed for two levels of earthquake intensity: the strength level and the ductility level earthquake. For the strength level earthquake, defined as having a "reasonable likelihood of not being exceeded during the platform's life" (mean recurrence interval $\sim 200 - 500$ years), the structure is designed to respond elastically. For the ductility level earthquake, defined as close to the "maximum credible earthquake" at the site, the structure is designed for inelastic response and to have adequate reserve strength to avoid collapse.

For strength level design, the seismic loading may be specified either by sets of accelerograms or by means of design response spectra. Use of design spectra has a number of advantages over time history solutions (base acceleration input). For this reason design response spectra are the preferable approach for strength level designs.

Designs for ductility level earthquakes will normally require inelastic analyses for which the seismic input must be specified by sets of 3-component accelerograms, real or artificial, representative of the extreme ground motions that could shake the platform site. The characteristics of such motions, however, may still be prescribed by means of design spectra, which are usually the result of a site specific seismotectonic study.

Ice and Snow Loads

Ice is a primary problem for marine structures in the arctic and sub-arctic zones. Ice formation and expansion can generate large pressures that give rise to horizontal as well as vertical forces. In addition, large blocks of ice driven by current, winds and waves with speeds that can approach 0.5 to 1.0 m/s, may hit the structure and produce impact loads. Figure 3.6 shows some measures adopted to overcome the force exerted by ice.



Ice Barriers in North of Caspian Sea

Figure 3.6: Methods to overcome the force exerted by ice on offshore platforms

As a first approximation, statically applied, horizontal ice forces may be estimated as follows:

$$F_i = C_i f_c A \quad (7)$$

where:

A is the exposed area of structure,
 f_c is the compressive strength of ice,
 C_i is the coefficient accounting for shape, rate of load application and other factors,
 with usual values between 0.3 and 0.7.

Generally, detailed studies based on field measurements, laboratory tests and analytical work are required to develop reliable design ice forces for a given geographical location. In addition to these forces, ice formation and snow accumulations increase gravity and wind loads, the latter by increasing areas exposed to the action of wind.

Loads due to Temperature Variations

Offshore structures can be subjected to temperature gradients which produce thermal stresses. To take account of such stresses, extreme values of sea and air temperatures which are likely to occur during the life of the structure must be estimated. Relevant data for the North Sea are given in BS6235. In addition to the environmental sources, human factors can also generate thermal loads, e.g. through accidental release of cryogenic material, which must be taken into account in design as accidental loads. The temperature of the oil and gas produced must also be considered.

Sea Floor Movements

Movement of the sea floor can occur as a result of active geologic processes, storm wave pressures, earthquakes, pressure reduction in the producing reservoir, etc. The loads generated by such movements affect, not only the design of the piles, but the jacket as well. Such forces are determined by special geotechnical studies and investigations.

Marine Growth

Marine growth (Figure 3.7) is accumulated on submerged members. Its main effect is to increase the wave forces on the members by increasing not only exposed areas and volumes, but also the drag coefficient due to higher surface roughness. In addition, it increases the unit mass of the member, resulting in higher gravity loads and in lower member frequencies. Depending upon geographic location, the thickness of marine growth can reach 0.3m or more. It is accounted for in design through appropriate increases in the diameters and masses of the submerged members.

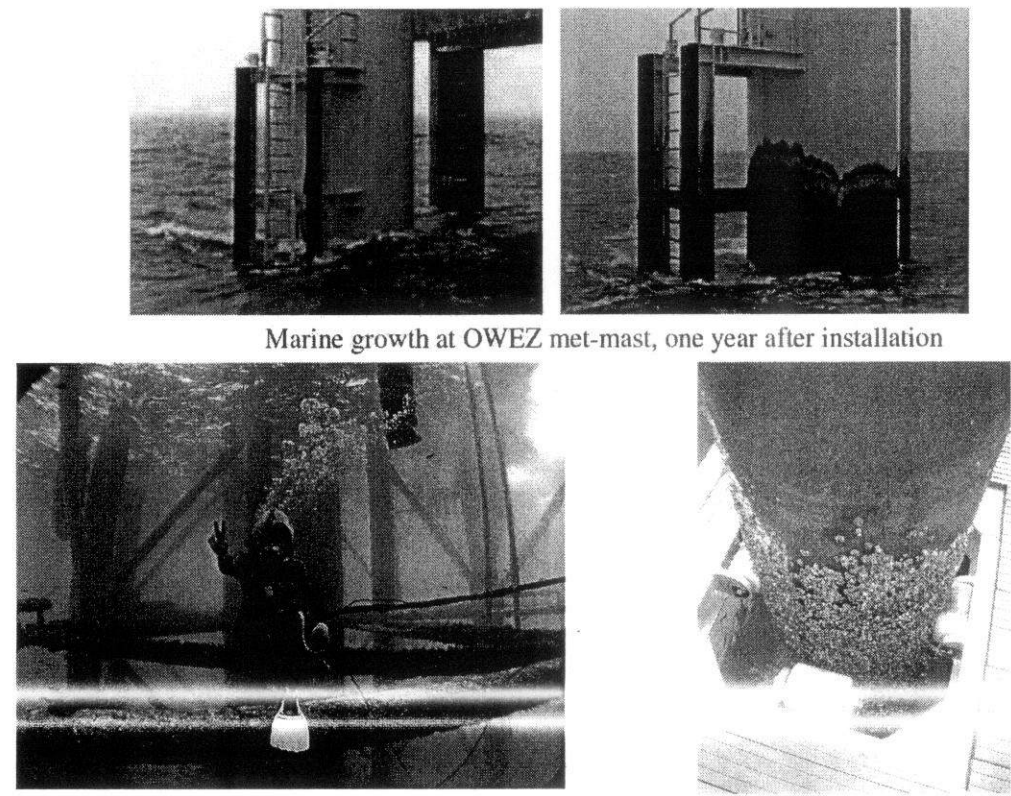


Figure 3.7: Marine growth on submerged and exposed members

According to N-003, NORSOK standard, belonging to Norway practiced for the North Sea, in the absence of more accurate data and if regular cleaning is not planned, marine growth thickness can be taken from Table 3.8. This thickness may be assumed to increase linearly up to the given values over 2 year period after the structure has been placed in the sea. Roughness height may be taken as 20 mm below +2 m. Roughness should be considered when determining the coefficients in Morison’s equation. The weight of marine growth is classified as a variable function. In the absence of more accurate data, the specific weight of the marine growth in air may be taken to be 13 kN/m³.

Table 3.8: Norwegian standard for marine growth on members

Water depth, m	56-59° N	59-72° N
Above + 2	0	0
+2 to - 40	100 mm	60 mm
Under - 40	50 mm	30 mm

Tides

Tides affect the wave and current loads indirectly, i.e. through the variation of the level of the sea surface. The tides are classified as: (a) astronomical tides - caused essentially from the gravitational pull of the moon and the sun and (b) storm surges - caused by the combined action of wind and barometric pressure differentials during a storm. The combined effect of the two types of tide is called the storm tide. Tide dependent water levels and the associated definitions, as used in platform design, are shown in Figure 3.3. The astronomical tide range depends on the geographic location and the phase of the moon. Its maximum, the spring tide, occurs at new moon. The range varies from centimetres to several metres and may be obtained from special maps. Storm surges depend upon the return period considered and their range is on the order of 1.0 to 3.0m. When designing a platform, extreme storm waves are superimposed on the still water level (see Figure 3.9), while for design considerations such as levels for boat landing places, barge fenders, upper limits of marine growth, etc., the daily variations of the astronomical tide are used.

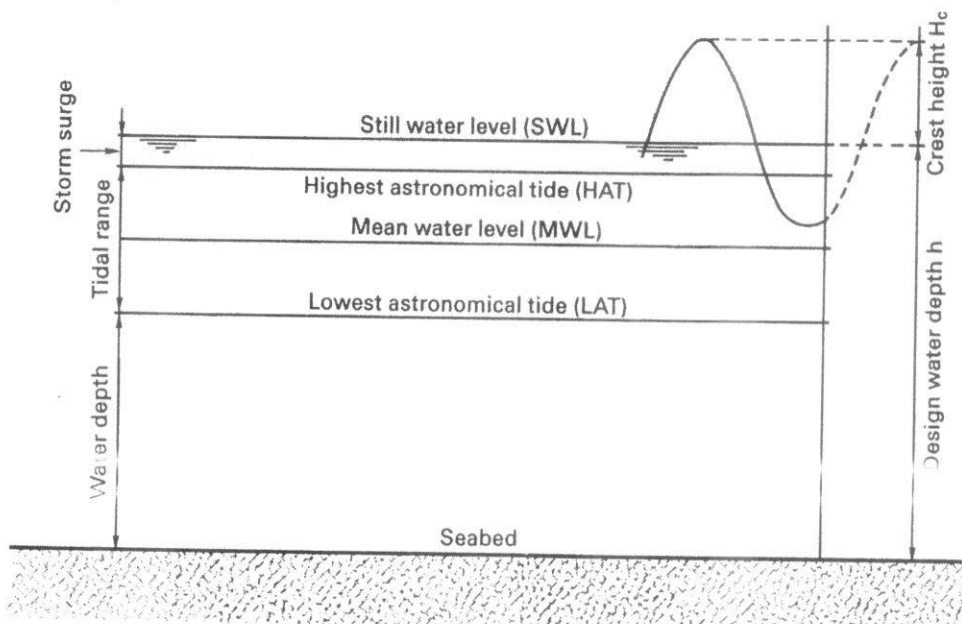


Figure 3.9: Tide-related definitions of sea surface level

Concluding Summary

- Environmental loads form a major category of loads which control many aspects of platform design.
- The main environmental loads are due to wind, waves, current, earthquakes, ice and snow, temperature variations, marine growth, tides and seafloor movements.
- Widely accepted rules of practice provide guideline values for most environmental loads.
- For major structures, specification of environmental design loads requires specific studies.
- Some environmental loads can be highly uncertain.
- The definition of certain environmental loads depends upon the type of analysis used in the design.

3.2 OTHER LOADS

Introduction

In this section, the various categories of loads, except environmental, for which a pile-supported steel offshore platform must be designed are presented. These categories include permanent (dead) loads, operating (live) loads, loads generated during fabrication and installation (due to lifts, loadout, transportation, launching and upending) and accidental loads. In addition, the different load combinations for all types of loads, including environmental, as required (or suggested) by applicable regulations (or codes of practice) are given.

The categories of loads described herein are the following:

1. Permanent (dead) loads
2. Operating (live) loads
3. Fabrication and installation loads
4. Accidental loads

1. Permanent (Dead) Loads

Permanent loads include the following:

- a) Weight of the structure in air, including the weight of grout and ballast, if necessary.
- b) Weights of equipment, attachments or associated structures which are permanently mounted on the platform.
- c) Hydrostatic forces on the various members below the waterline. These forces include buoyancy and hydrostatic pressures.

Sealed tubular members must be designed for the worst condition when flooded or non-flooded.

2. Operating (Live) Loads

Operating loads arise from the operations on the platform and include the weight of all non-permanent equipment or material, as well as forces generated during operation of equipment. More specifically, operating loads include the following:

- a) The weight of all non-permanent equipment (e.g. drilling, production), facilities (e.g. living quarters, furniture, life support systems, heliport, etc), consumable supplies, liquids, etc.
- b) Forces generated during operations, e.g. drilling, vessel mooring, helicopter landing, crane operations, etc.

The necessary data for computation of all operating loads are provided by the operator and the equipment manufacturers. The data need to be critically evaluated by the designer. The following values are recommended in BS6235:

- a. crew quarters and passageways: 3.2 KN/m^2
- b. working areas: 8.5 KN/m^2
- c. storage areas: $\gamma H \text{ KN/m}^2$

where:

γ is the specific weight of stored materials, not to be taken less than 6.87 KN/m^3
 H is the storage height (m).

Forces generated during operations are often dynamic or impulsive in nature and must be treated as such. For example, according to the BS6235 rules, two types of helicopter landing should be considered, heavy and emergency landing. The impact load in the first case is to be taken as 1.5 times the maximum take-off weight, while in the second case this factor becomes 2.5. In addition, a horizontal load applied at the points of impact and taken equal to half the maximum take-off weight must be considered. Loads from rotating machinery, drilling equipment, etc. may normally be treated as harmonic forces. For vessel mooring, design forces are computed for the largest ship likely to approach at operational speeds. According to BS6235, the minimum impact to be considered is of a vessel of 2500 tonnes at 0.5 m/s.

3. Fabrication and Installation Loads

These loads are temporary and arise during fabrication and installation of the platform or its components. During fabrication, erection lifts of various structural components generate lifting forces, while in the installation phase forces are generated during platform loadout, transportation to the site, launching and upending, as well as during lifts related to installation.

According to the DNV rules, the return period for computing design environmental conditions for installation as well as fabrication should normally be three times the duration of the corresponding phase. API-RP2A, on the other hand, leaves this design return period up to the owner, while the BS6235 rules recommend a minimum recurrence interval of 10 years for the design environmental loads associated with transportation of the structure to the offshore site.

3.1 Lifting Forces

Lifting forces are functions of the weight of the structural component being lifted, the number and location of lifting eyes used for the lift, the angle between each sling and the vertical axis and the conditions under which the lift is performed (Figure 3.10). All members and connections of a lifted component must be designed for the forces resulting from static equilibrium of the lifted weight and the sling tensions. Moreover, API-RP2A recommends that in order to compensate for any side movements, lifting eyes and the connections to the supporting structural members should be designed for the combined action of the static sling load and a horizontal force equal to 5% this load, applied perpendicular to the padeye at the centre of the pin hole. All these design forces are applied as static loads if the lifts are performed in the fabrication yard. If, however, the lifting derrick or the structure to be lifted is on a floating vessel, then dynamic load factors should be applied to the static lifting forces. In particular, for

lifts made offshore API-RP2A recommends two minimum values of dynamic load factors: 2.0 and 1.35. The first is for designing the padeyes as well as all members and their end connections framing the joint where the padeye is attached, while the second is for all other members transmitting lifting forces. For loadout at sheltered locations, the corresponding minimum load factors for the two groups of structural components become, according to API-RP2A, 1.5 and 1.15, respectively.

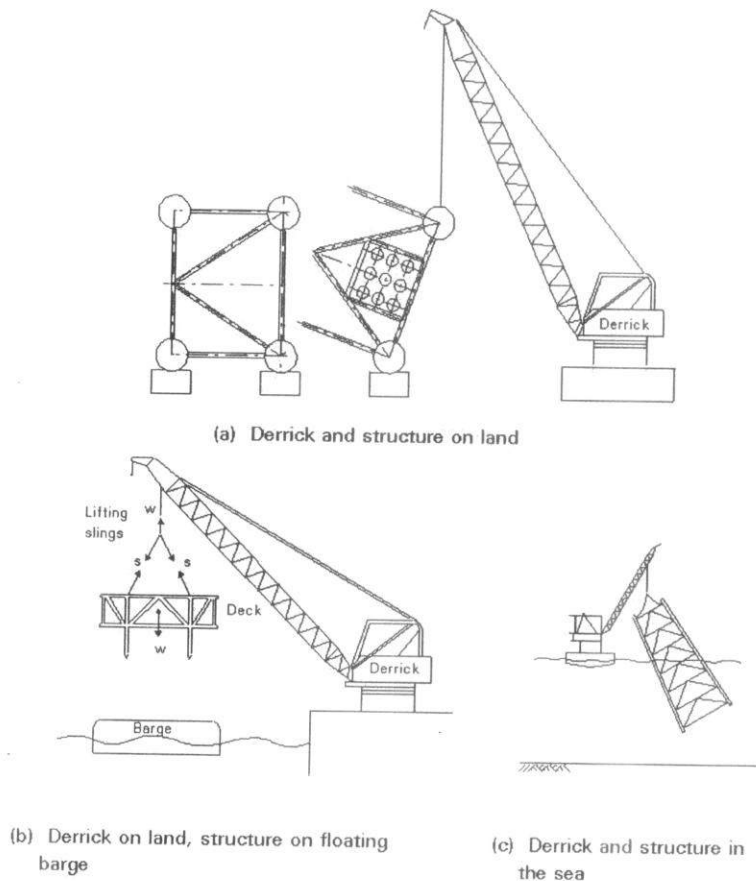


Figure 3.10: Lifts under various conditions

3.2 Loadout Forces

These are forces generated when the jacket is loaded from the fabrication yard onto the barge. If the loadout is carried out by direct lift, then, unless the lifting arrangement is different from that to be used for installation, lifting forces need not be computed, because lifting in the open sea creates a more severe loading condition which requires higher dynamic load factors. If loadout is done by skidding the structure onto the barge, a number of static loading conditions must be considered, with the jacket supported on its side. Such loading conditions arise from the different positions of the jacket during the loadout phases, from movement of the barge due to tidal fluctuations, marine traffic or change of draft, and from possible support settlements. Since movement of the jacket is slow, all loading conditions can be taken as static.

3.3 Transportation Forces

These forces are generated when platform components (jacket, deck) are transported offshore on barges or self-floating. They depend upon the weight, geometry and support conditions of the structure (by barge or by buoyancy) and also on the environmental conditions (waves, winds and currents) that are encountered during transportation. The types of motion that a floating structure may experience are shown schematically in Figure 3.11.

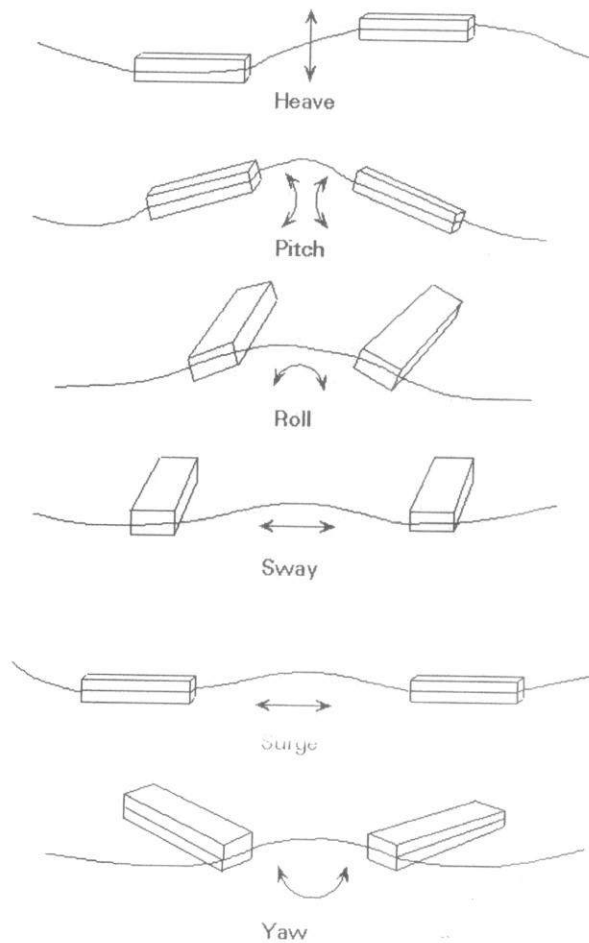


Figure 3.11: Types of motion of a floating object

In order to minimize the associated risks and secure safe transport from the fabrication yard to the platform site, it is important to plan the operation carefully by considering, according to API-RP2A, the following:

1. Previous experience along the tow route
2. Exposure time and reliability of predicted "weather windows"
3. Accessibility of safe havens
4. Seasonal weather system
5. Appropriate return period for determining design wind, wave and current conditions, taking into account characteristics of the tow such as size, structure, sensitivity and cost.

Transportation forces are generated by the motion of the tow, i.e. the structure and supporting barge. They are determined from the design winds, waves and currents. If the structure is self-floating, the loads can be calculated directly. According to API-RP2A, towing analyses must be based on the results of model basin tests or appropriate analytical methods and must consider wind and wave directions parallel, perpendicular and at 45° to the tow axis. Inertial loads may be computed from a rigid body analysis of the tow by combining roll and pitch with heave motions, when the size of the tow, magnitude of the sea state and experience make such assumptions reasonable. For open sea conditions, the following may be considered as typical design values:

Single - amplitude roll: 20°

Single - amplitude pitch: 10°

Period of roll or pitch: 10 second

Heave acceleration: 0.2 g

When transporting a large jacket by barge, stability against capsizing is a primary design consideration because of the high centre of gravity of the jacket. Moreover, the relative stiffness of jacket and barge may need to be taken into account together with the wave slamming forces that could result during a heavy roll motion of the tow when structural analyses are carried out for designing the tie-down braces and the jacket members affected by the induced loads. Special computer programs are available to compute the transportation loads in the structure-barge system and the resulting stresses for any specified environmental condition.

3.4 Launching and Upending Forces

Figure 3.12 shows the stages to be considered in the assessment of loads for the design of offshore platforms.

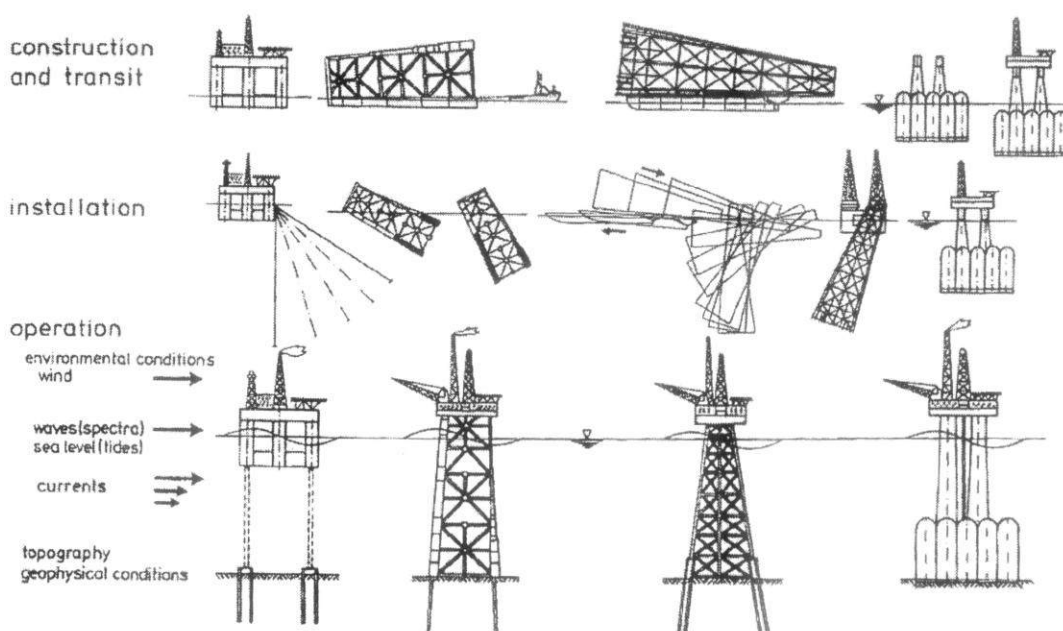


Figure 3.12: Stages of the life of an offshore platform

Various forces are generated during the launch of a jacket from the barge into the sea and during the subsequent upending into its proper vertical position to rest on the seabed. A schematic view of these operations can be seen in Figure 3.13.

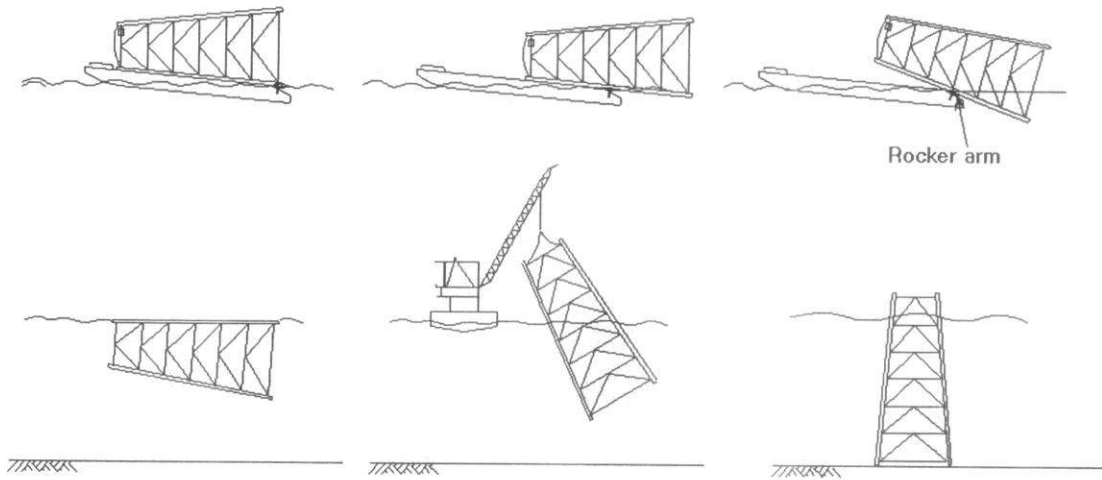


Figure 3.13: Launching and upending sequences of a platform jacket

There are five stages in a launch-upending operation:

- a. Jacket slides along the skid beams
- b. Jacket rotates on the rocker arms
- c. Jacket rotates and slides simultaneously
- d. Jacket detaches completely and comes to its floating equilibrium position
- e. Jacket is upended by a combination of controlled flooding and simultaneous lifting by a derrick barge.

The loads, static as well as dynamic, induced during each of these stages and the force required to set the jacket into motion can be evaluated by appropriate analyses, which also consider the action of wind, waves and currents expected during the operation.

To start the launch, the barge must be ballasted to an appropriate draft and trim angle and subsequently the jacket must be pulled towards the stern by a winch. Sliding of the jacket starts as soon as the downward force (gravity component and winch pull) exceeds the friction force. As the jacket slides, its weight is supported on the two legs that are part of the launch trusses. The support length keeps decreasing and reaches a minimum, equal to the length of the rocker beams, when rotation starts. It is generally at this instant that the most severe launching forces develop as reactions to the weight of the jacket. During stages (d) and (e), variable hydrostatic forces arise which have to be considered at all members affected. Buoyancy calculations are required for every stage of the operation to ensure fully controlled, stable motion. Computer programs are available to perform the stress analyses required for launching and upending and also to portray the whole operation graphically.

4. Accidental Loads

According to the DNV rules, accidental loads are loads, ill-defined with respect to intensity and frequency, which may occur as a result of accident or exceptional circumstances. Accidental loads are also specified as a separate category in the NPD regulations, but not in API-RP2A, BS6235 or the DOE-OG rules. Examples of accidental loads are loads due to collision with vessels, fire or explosion, dropped objects, and unintended flooding of buoyancy tanks. Special measures are normally taken to reduce the risk from accidental loads. For example, protection of wellheads or other critical equipment from a dropped object can be provided by specially designed, impact resistant covers. According to the NPD regulations, an accidental load can be disregarded if its annual probability of occurrence is less than 10^{-4} . This number is meant as an order of magnitude estimate and is extremely difficult to compute. Earthquakes are treated as an environmental load in offshore structure design.

5. Load Combinations

The load combinations used for designing fixed offshore structures depend upon the design method used, i.e. whether limit state or allowable stress design is employed. The load combinations recommended for use with allowable stress procedures are:

- a) Dead loads plus operating environmental loads plus maximum live loads, appropriate to normal operations of the platform.
- b) Dead loads plus operating environmental loads plus minimum live loads, appropriate to normal operations of the platform.
- c) Dead loads plus extreme (design) environmental loads plus maximum live loads, appropriate for combining with extreme conditions.
- d) Dead loads plus extreme (design) environmental loads plus minimum live loads, appropriate for combining with extreme conditions.

Moreover, environmental loads, with the exception of earthquake loads, should be combined in a manner consistent with their joint probability of occurrence during the loading condition considered. Earthquake loads, if applicable, are to be imposed as a separate environmental load, i.e., not to be combined with waves, wind, etc. Operating environmental conditions are defined as representative of severe but not necessarily limiting conditions that, if exceeded, would require cessation of platform operations.

The DNV rules permit allowable stress design but recommend the semi-probabilistic limit state design method, which the NPD rules also require. BS6235 permits both methods but the design equations it gives are for the allowable stress method. API-RP2A is very specific in recommending not applying limit state methods. According to the DNV and the NPD rules for limit state design, four limit states must be checked:

1. Ultimate limit state

For this limit state the following two loading combinations must be used:

Ordinary: $1.3 P + 1.3 L + 1.0 D + 0.7 E$, and
Extreme : $1.0 P + 1.0 L + 1.0 D + 1.3 E$

where P, L, D and E stand for Permanent (dead), Operating (live), Deformation (e.g., temperature, differential settlement) and Environmental loads respectively. For well controlled dead and live loads during fabrication and installation, the load factor 1.3 may be reduced to 1.2. Furthermore, for structures that are unmanned during storm conditions and which are not used for storage of oil and gas, the 1.3 load factor for environmental loads - except earthquakes - may be reduced to 1.15.

2. Fatigue limit state

All load factors are to be taken as 1.0.

3. Progressive Collapse limit state

All load factors are to be taken as 1.0.

4. Serviceability limit state

All load factors are to be taken as 1.0.

6. Concluding Summary

- In addition to environmental loads, an offshore structure must be designed for dead and live loads, fabrication and installation loads as well as accidental loads.
- Widely accepted rules of practice are usually followed for specifying such loads.
- The type and magnitude of fabrication, transportation and installation loads depend upon the methods and sequences used for the corresponding phases.
- Dynamic and impact effects are normally taken into account by means of appropriate dynamic load factors.
- Accidental loads are not well defined with respect to intensity and probability of occurrence. They will typically require special protective measures.
- Load combinations and load factors depend upon the design method to be used. API-RP2A is based on allowable stress design and recommends against limit state design, BSI favours allowable stress design, while DNV and NPD recommend limit state design.

3.3 ANALYSIS PROCEDURES

In this section analytical models used in offshore engineering are briefly described. Acceptance criteria for the verification of offshore structures are presented.

Simple rules for preliminary member sizing are given and procedures for static in-place and dynamic analysis are described.

Methods of fatigue analysis are described including the fatigue model (structural, hydrodynamic loading, and joint stress models) and the methods of fatigue damage assessment.

Abnormal and accidental conditions are considered relating to earthquake, impact and progressive collapse.

Analyses required for load-out and transportation and for installation are outlined. Local analyses for specific parts of the structure which are better treated by dedicated models outside of the global analysis are identified.

1. INTRODUCTION

The analysis of an offshore structure is an extensive task, embracing consideration of the different stages, i.e. execution, installation, and in-service stages, during its life. Many disciplines, e.g. structural, geotechnical, naval architecture, metallurgy are involved.

This document is purposely limited to presenting an overview of available analysis procedures and providing benchmarks for the reader to appreciate the validity of his assumptions and results. They primarily address jackets, which are more unusual structures compared to decks and modules, and which more closely resemble onshore petrochemical plants.

2. ANALYTICAL MODEL

The analytical models used in offshore engineering are in some respects similar to those adopted for other types of steel structures. Only the salient features of offshore models are presented here.

The same model is used throughout the analysis process with only minor adjustments being made to suit the specific conditions, e.g. at supports in particular, relating to each analysis.

2.1 Stick Models

Stick models (beam elements assembled in frames) are used extensively for tubular structures (jackets, bridges, flare booms) and lattice trusses (modules, decks).

2.1.1 Joints

Each member is normally rigidly fixed at its ends to other elements in the model. If more accuracy is required, particularly for the assessment of natural vibration modes, local flexibility of the connections may be represented by a joint stiffness matrix.

2.1.2 Members

In addition to its geometrical and material properties, each member is characterised by hydrodynamic coefficients, e.g. relating to drag, inertia, and marine growth, to allow wave forces to be automatically generated.

2.2 Plate Models

Integrated decks and hulls of floating platforms involving large bulkheads are described by plate elements. The characteristics assumed for the plate elements depend on the principal state of stress which they are subjected to. Membrane stresses are taken when the element is subjected merely to axial load and shear. Plate stresses are adopted when bending and lateral pressure are to be taken into account.

3. ACCEPTANCE CRITERIA

3.1 Code Checks

The verification of an element consists of comparing its characteristic resistance(s) to a design force or stress. It includes:

- a strength check, where the characteristic resistance is related to the yield strength of the element,
- a stability check for elements in compression where the characteristic resistance relates to the buckling limit of the element.

An element (member or plate) is checked at typical sections (at least both ends and midspan) against resistance and buckling. This verification also includes the effect of water pressure for deepwater structures.

Tubular joints are checked against punching under various load patterns. These checks may indicate the need for local reinforcement of the chord using over-thickness or internal ring-stiffeners.

Elements should also be verified against fatigue, corrosion, temperature or durability wherever relevant.

3.2 Allowable Stress Method

This method is presently specified by American codes (API, AISC).

The loads remain unfactored and a unique coefficient is applied to the characteristic resistance to obtain an allowable stress as shown in Table 3.2.

Table 3.2: Load factor

Condition	Axial	Strong axis bending	Weak axis bending
Normal	0.60	0.66	0.75
Extreme	0.80	0.88	1.00

"Normal" and "Extreme" respectively represent the most severe conditions:

- under which the plant is to operate without shut-down.
- the platform is to endure over its lifetime.

3.3 Limit State Method

This method is enforced by European and Norwegian Authorities and has now been adopted by API as it offers a more uniform reliability.

Partial factors are applied to the loads and to the characteristic resistance of the element, reflecting the amount of confidence placed in the design value of each parameter and the degree of risk accepted under a limit state, i.e:

- Ultimate Limit State (ULS): corresponds to an ultimate event considering the structural resistance with appropriate reserve.
- Fatigue Limit State (FLS): relates to the possibility of failure under cyclic loading.
- Progressive Collapse Limit State (PLS): reflects the ability of the structure to resist collapse under accidental or abnormal conditions.
- Service Limit State (SLS): corresponds to criteria for normal use or durability (often specified by the plant operator).

3.3.1 Load factors

Norwegian Authorities specify the sets of load factors presented in Table 3.3:

Table 3.3: Load factor

Limit State	Load Categories				
	P	L	D	E	A
ULS (normal)	1.3	1.3	1.0	0.7	0.0
ULS (extreme)	1.0	1.0	1.0	1.3	0.0
FLS	0.0	0.0	0.0	1.0	0.0
PLS (accidental)	1.0	1.0	1.0	1.0	1.0
PLS (post-damage)	1.0	1.0	1.0	1.0	0.0
SLS	1.0	1.0	1.0	1.0	0.0

where the respective load categories are:

P are permanent loads (structural weight, dry equipments, ballast, hydrostatic pressure).

L are live loads (storage, personnel, liquids).

D are deformations (out-of-level supports, subsidence).

E are environmental loads (wave, current, wind, earthquake).

A are accidental loads (dropped object, ship impact, blast, fire).

3.3.2 Material factors

The material partial factors for steel is normally taken equal to 1.15 for ULS and 1.00 for PLS and SLS design.

3.3.3 Classification of Design Conditions

Guidance for classifying typical conditions into typical limit states is given in Table 3.4.

Table 3.4: Guide to classification into limit states

Condition	Loadings				Design Criterion
	P/L	E	D	A	
Construction	P				ULS,SLS
Load-Out	P	reduced wind	support disp		ULS
Transport	P	transport wind and wave			ULS
Tow-out (accidental)	P			flooded compart	PLS
Launch	P				ULS
Lifting	P				ULS
In-Place (normal)	P + L	wind, wave & snow	actual		ULS,SLS
In-Place (extreme)	P + L	wind & 100 year wave	actual		ULS SLS
In-Place (exceptional)	P + L	wind & 10000 year wave	actual		PLS
Earthquake	P + L	10^{-2} quake			ULS
Rare Earthquake	P + L	10^{-4} quake			PLS
Explosion	P + L			blast	PLS
Fire	P + L			fire	PLS
Dropped Object	P + L			drill collar	PLS
Boat Collision	P + L			boat impact	PLS
Damaged Structure	P + reduced L	reduced wave & wind			PLS

4. PRELIMINARY MEMBER SIZING

The analysis of a structure is an iterative process which requires progressive adjustment of the member sizes with respect to the forces they transmit, until a safe and economical design is achieved.

It is therefore of the utmost importance to start the main analysis from a model which is close to the final optimized one.

The simple rules given below provide an easy way of selecting realistic sizes for the main elements of offshore structures in moderate water depth (up to 80m) where dynamic effects are negligible.

4.1 Jacket Pile Sizes

- Calculate the vertical resultant (dead weight, live loads, buoyancy), the overall shear and the overturning moment (environmental forces) at the mudline.
- Assuming that the jacket behaves as a rigid body, derive the maximum axial and shear force at the top of the pile.
- Select a pile diameter in accordance with the expected leg diameter and the capacity of pile driving equipment.
- Derive the penetration from the shaft friction and tip bearing diagrams.
- Assuming an equivalent soil subgrade modulus and full fixity at the base of the jacket, calculate the maximum moment in the pile and derive its wall thickness.

4.2 Deck Leg Sizes

- adapt the diameter of the leg to that of the pile.
- determine the effective length from the degree of fixity of the leg into the deck (depending upon the height of the cellar deck).
- calculate the moment caused by wind loads on topsides and derive the appropriate thickness.

4.3 Jacket Bracings

- select the diameter in order to obtain a span/diameter ratio between 30 and 40.
- calculate the axial force in the brace from the overall shear and the local bending caused by the wave assuming partial or total end restraint.
- derive the thickness such that the diameter/thickness ratio lies between 20 and 70 and eliminate any hydrostatic buckle tendency by imposing $D/t < 170\sqrt[3]{H}$ (H is the depth of member below the free surface).

4.4 Deck Framing

- select a spacing between stiffeners (typically 500 to 800mm).
- derive the plate thickness from formulae accounting for local plastification under the wheel footprint of the design forklift truck.
- determine by straight beam formulae the sizes of the main girders under "blanket" live loads and/or the respective weight of the heaviest equipments.

5. STATIC IN-PLACE ANALYSIS

The static in-place analysis is the basic and generally the simplest of all analyses. The structure is modelled as it stands during its operational life, and subjected to pseudo-static loads.

This analysis is always carried at the very early stage of the project, often from a simplified model, to size the main elements of the structure.

5.1 Structural Model

5.1.1 Main Model

The main model should account for eccentricities and local reinforcements at the joints.

Typical models for North Sea jackets may feature over 800 nodes and 4000 members.

5.1.2 Appurtenances

The contribution of appurtenances (risers, J-tubes, caissons, conductors, boat-fenders, etc.) to the overall stiffness of the structure is normally neglected.

They are therefore analysed separately and their reactions applied as loads at the interfaces with the main structure.

5.1.3 Foundation Model

Since their behaviour is non-linear, foundations are often analysed separately from the structural model.

They are represented by an equivalent load-dependent secant stiffness matrix; coefficients are determined by an iterative process where the forces and displacements at the common boundaries of structural and foundation models are equated.

This matrix may need to be adjusted to the mean reaction corresponding to each loading condition.

5.2 Loadings

5.2.1 Gravity Loads

Gravity loads consist of:

- dead weight of structure and equipments, and
- live loads (equipments, fluids, personnel).

Depending on the area of structure under scrutiny, live loads must be positioned to produce the most severe configuration (compression or tension); this may occur for instance when positioning the drilling rig.

5.2.2 Environmental Loads

Environmental loads consist of wave, current and wind loads assumed to act simultaneously in the same direction.

In general eight wave incidences are selected; for each the position of the crest relative to the platform must be established such that the maximum overturning moment and/or shear are produced at the mud-line.

5.3 Loading Combinations

The static in-place analysis is performed under different conditions where the loads are approximated by their pseudo-static equivalent.

The basic loads relevant to a given condition are multiplied by the appropriate load factors and combined to produce the most severe effect in each individual element of the structure.

6. DYNAMIC ANALYSIS

A dynamic analysis is normally mandatory for every offshore structure, but can be restricted to the main modes in the case of stiff structures.

6.1 Dynamic Model

The dynamic model of the structure is derived from the main static model. Some simplifications may however take place:

- local joint reinforcements and eccentricities may be disregarded.
- masses are lumped at the member ends.
- the foundation model may be derived from cyclic soil behaviour.

6.2 Equations of Motion

The governing dynamic equations of multi-degrees-of-freedom systems can be expressed in the matrix form:

$$\mathbf{MX}'' + \mathbf{CX}' + \mathbf{KX} = \mathbf{P}(t)$$

where

\mathbf{M} is the mass matrix

\mathbf{C} is the damping matrix

\mathbf{K} is the stiffness matrix

\mathbf{X} , \mathbf{X}' , \mathbf{X}'' are the displacement, velocity and acceleration vectors (function of time).

$\mathbf{P}(t)$ is the time dependent force vector; in the most general case it may depend on the displacements of the structure also (i.e. relative motion of the structure with respect to the wave velocity in Morison equation).

6.2.1 Mass

The mass matrix represents the distribution of masses over the structure.

Masses include that of the structure itself, the appurtenances, liquids trapped in legs or tanks, the added mass of water (mass of water displaced by the member and determined from potential flow theory) and the mass of marine growth.

Masses are generally lumped at discrete points of the model. The mass matrix consequently becomes diagonal but local modes of vibration of single members are ignored (these modes may be important for certain members subjected to an earthquake). The selection of lumping points may significantly affect the ensuing solution.

As a further simplification to larger models involving considerable degrees-of-freedom, the system can be condensed to a few freedoms while still retaining its basic energy distribution.

6.2.2 Damping

Damping is the most difficult to estimate among all parameters governing the dynamic response of a structure. It may consist of structural and hydrodynamic damping.

- **Structural Damping:** Structural damping is associated with the loss of energy by internal friction in the material. It increases with the order of the mode, being roughly proportional to the strain energy involved in each.
- **Hydrodynamic Damping:** Damping provided by the water surrounding the structure is commonly added to the former, but may alternatively be accounted as part of the forcing function when vibrations are close to resonance (vortex-shedding in particular).

Representation of Damping

Viscous damping represents the most common and simple form of damping. It may have one of the following representations:

- modal damping: a specific damping ratio ζ expressing the percentage to critical associated with each mode (typically $\zeta = 0.5\%$ structural; $\zeta = 1.5\%$ hydrodynamic)
- proportional damping: defined as a linear combination of stiffness and mass matrices.

All other types of non-viscous damping should preferably be expressed as an equivalent viscous damping matrix.

6.2.3 Stiffness

The stiffness matrix is in all aspects similar to the one used in static analyses.

6.3 Free Vibration Mode Shapes and Frequencies

The first step in a dynamic analysis consists of determining the principal natural vibration mode shapes and frequencies of the undamped, multi-degree-of-freedom structure up to a given order (30th to 50th). This consists of solving the eigen-value problem:

$$\mathbf{KX} = \lambda \mathbf{MX}$$

For rigid structures having a fundamental vibration period well below the range of wave periods (typically less than 3 s), the dynamic behaviour is simply accounted for by multiplying the time-dependent loads by a dynamic amplification factor (DAF):

$$\text{DAF} = \frac{1}{\sqrt{(1 - \beta^2)^2 + (2\beta\gamma)^2}}$$

where $\beta = T_N/T$ is the ratio of the period of the structure to the wave period.

6.4 Modal Superposition Method

A convenient technique consists of uncoupling the equations through the normal modes of the system. This method is only applicable if:

- each mass, stiffness and damping matrix is time-independent.
- non-linear forces are linearized beforehand (drag).

The total response is obtained by summing the responses of the individual single-degree-of-freedom oscillators associated to each normal mode of the structure.

This method offers the advantage that the eigen modes provide substantial insight into the problem, and can be re-used for as many subsequent response calculations as needed at later stages.

It may however prove time-consuming when a large number of modes is required to represent the response accurately. Therefore:

- The simple superposition method (mode-displacement) is applied to a truncated number of lowest modes for predicting earthquake response.
- It must be corrected by the static contribution of the higher modes (mode-acceleration method) for wave loadings.

6.4.1 Frequency Domain Analysis

Such analysis is most appropriate for evaluating the steady-state response of a system subjected to cyclic loadings, as the transient part of the response vanishes rapidly under the effect of damping.

The loading function is developed in Fourier series up to an order η :

$$p(t) = \sum_{j=1}^{\eta} p_j e^{i(\omega_j t + \phi_j)}$$

The plot of the amplitudes p_j versus the circular frequencies ω_j is called the amplitude power spectra of the loading. Usually, significant values of p_j only occur within a narrow range of frequencies and the analysis can be restricted to it.

The relationship between response and force vectors is expressed by the transfer matrix H , such as:

$$H = [-M \omega^2 + i C \omega + K]$$

the elements of which represent:

$$H_{j,k} = \frac{X_j}{P_k} = \frac{\text{deflection in freedom } j}{\text{force in freedom } k}$$

The spectral density of response in freedom j versus force is then:

$$S_{X_j} = \sum_{k=1}^{\eta} |H_{jk}|^2 S_{P_k}(f)$$

The fast Fourier transform (FFT) is the most efficient algorithm associated with this kind of analysis.

6.4.2 Time Domain Analysis

The response of the i -th mode may alternatively be determined by resorting to Duhamel's integral:

$$X_j(t) = \int_0^t P_j(\tau) h(t - \tau) d\tau$$

The overall response is then obtained by summing at each time step the individual responses over all significant modes.

6.5 Direct Integration Methods

Direct step-by-step integration of the equations of motion is the most general method and is applicable to:

- non-linear problems involving special forms of damping and response-dependent loadings.
- responses involving many vibration modes to be determined over a short time interval.

The dynamic equilibrium at an instant τ is governed by the same type of equations, where all matrices (mass, damping, stiffness, load) are simultaneously dependent on the time and structural response as well.

All available integration techniques are characterised by their stability (i.e. the tendency for uncontrolled divergence of amplitude to occur with increasing time steps). Unconditionally stable methods are always to be preferred (for instance Newmark-beta with $\beta = 1/4$ or Wilson-theta with $\theta = 1.4$).

7. FATIGUE ANALYSIS

A fatigue analysis is performed for those structures sensitive to the action of cyclic loadings such as:

- wave (jackets, floating structures).
- wind (flare booms, stair towers).
- structures under rotating equipments.

7.1 Fatigue Model

7.1.1 Structural Model

The in-place model is used for the fatigue analysis.

Quasi-static analysis is often chosen; it permits all local stresses to be comprehensively represented. The dynamic effects are accounted for by factoring the loads by the relevant DAF.

Modal analysis may be used instead; it offers computational efficiency, but may also overlook important local response modes, particularly near the waterline where direct wave action causes high out-of-plane bending (see Section 5.2 of this chapter). The mode-acceleration method may overcome this problem.

7.1.2 Hydrodynamic Loading Model

A very large number of computer runs may be necessary to evaluate the stress range at the joints. The wave is repeatedly generated for:

- different blocks of wave heights (typically from 2 to 28m in steps of 2m), each associated with a characteristic wave and zero-upcrossing period.
- different incidences (typically eight).
- different phases to determine the stress range for a given wave at each joint.

7.1.3 Joint Stress Model

Nominal joint stresses are calculated for eight points around the circumference of the brace. The maximum local (hot spot) stress is obtained by multiplying the former by a stress concentration factor (SCF) given by parametric formulae which are functions of the joint geometry and the load pattern (balanced/unbalanced).

7.1.4 Fatigue Damage Model

The fatigue failure of joints in offshore structures primarily depends on the stress ranges and their number of occurrences, formulated by S-N curves:

$$\log N_i = \log \alpha + m \log \Delta \sigma_i$$

The number of cycles to failure N_i corresponds to a stress range. The effect of the constant stresses, mainly welding residual stresses, is implicitly accounted for in this formulation.

The cumulative damage caused by n_i cycles of stress $\Delta \sigma_i$, over the operational life of the platform (30 to 50 years) is obtained by the Palmgren-Miner rule:

$$D = \sum_i \frac{n_i}{N_i}$$

The limit of this ratio depends on the position of the joint with respect to the splash zone (typically ± 4 m on either side of the mean sea level). The ratio should normally not exceed:

- 1.0 above,
- 0.1 within,
- 0.3 below the splash zone.

7.1.5 Closed Form Expression

The damage may alternatively be expressed in closed form:

$$D = \frac{N}{\alpha^m} \frac{\Delta \sigma^m}{[\ln(N)]^{km}} \Gamma(km + 1)$$

where

α , m are coefficients of the selected S-N curve.

$\Delta \sigma$ is the stress range exceeded once in N cycles.

k is a long-term distribution parameter, depending on the position of the joint in the structure.

N is the total number of cycles.

7.2 Deterministic Analysis

This analysis consists of time-domain analysis of the structure. The main advantage of this representation is that non-linear effects (drag, high order wave theories) are handled explicitly.

A minimum of four regular waves described in terms of height and associated period are considered for each heading angle.

7.3 Spectral Analysis

Waves of a given height are not characterised by a unique frequency, but rather by a range of frequencies. If this range corresponds to a peak in the structural response, the fatigue life predicted by the deterministic method can be seriously distorted.

This problem is overcome by using a scatter diagram, in which the joint occurrence of wave height and period is quantified. Wave directionality may also be accounted for. Eventually the most thorough representation of a sea state consists of:

- the frequency spectrum constructed from the significant wave heights and mean zero-crossing periods.
- the directionality function derived from the mean direction and associated spreading function.

This approach requires that the physical process be approximately linear (or properly linearised) and stationary. Transfer functions TF are determined from time-domain analyses involving various wave heights, each with different period and incidence:

$$TF(\omega, \theta) = \frac{\Delta \sigma}{H}$$

The response has normally a narrow-banded spectrum and can be described by a Rayleigh distribution.

The zero-upcrossing frequency of stress cycles is then approximated by:

$$T_z = \frac{2\pi}{\sqrt{\frac{m_0}{m_2}}}$$

where m_n is the n th order moment of the response.

The significant stress range is readily obtained for each sea state as:

$$\sigma_{sig} = 4 \sqrt{\sum_{\omega} \sum_{\theta} [TF(\omega, \theta)]^2 S(\omega, \theta) \Delta \omega \Delta \theta}$$

where $S(\omega, \theta)$ is the directional wave energy spectrum.

7.4 Wind Fatigue

7.4.1 Wind Gusts

The fatigue damage caused by the fluctuating part of wind (gusts) on slender structures like flare booms and bridges is usually predicted by spectral methods.

The main feature of such analysis is the introduction of coherence functions accounting for the spanwise correlation of forces.

7.4.2 Vortex Shedding

Vortex induced failure occurs for tubes subjected to a uniform or oscillating flow of fluid.

Within a specific range of fluid velocities, eddies are shed at a frequency close to the resonant frequency of the member.

This phenomenon involves forced displacements.

8. ABNORMAL AND ACCIDENTAL CONDITIONS

This type of analysis addresses conditions which may considerably affect the integrity of the structure, but only have a limited risk of occurrence.

Typically all events with a probability level less than the 10^{-4} threshold are disregarded.

8.1 Earthquake Analysis

8.1.1 Model

Particular attention shall be paid to:

- foundations: the near field (i.e. the soil mass in the direct vicinity of the structure) shall accurately represent load-deflection behaviour. As a general rule the lateral foundation behaviour is essentially controlled by horizontal ground motions of shallow soil layers.
- modal damping (in general taken as 5% and 7% of critical for ULS and PLS analyses respectively).

8.1.2 Ductility Requirements

The seismic forces in a structure are highly dependent on its dynamic characteristics. Design recommendations are given by API to determine an efficient geometry. The recommendations call for:

- providing sufficient redundancy and symmetry in the structure.
- favouring X-bracings instead of K-bracings.
- avoiding abrupt changes in stiffness.
- improving the post-buckling behaviour of bracings.

8.1.3 Analysis Method

Earthquake analyses can be carried out according to the general methods. However their distinctive feature is that they represent essentially a base motion problem and that the seismic loads are therefore dependent on the dynamic characteristics of the structure.

Modal spectral response analysis is normally used. It consists of a superposition of maximum mode response and forms a response spectrum curve characteristic of the input motion. This spectrum is the result of time-histories of a SDOF system for

different natural periods of vibration and damping. Direct time integration can be used instead for specific accelerograms adapted to the site.

8.2 Impact

The analysis of impact loads on structures is carried out locally using simple plastic models. Should a more sophisticated analysis be required, it can be accomplished using time-domain techniques.

The whole energy must be absorbed within acceptable deformations.

8.2.1 Dropped Object/Boat Impact

When a wellhead protection cover is hit by a drill collar, or a tube (jacket leg, fender) is crushed by a supply boat, two load/deformation mechanisms occur simultaneously:

- local punch-through (cover) or denting (tube).
- global deformation along plastic hinges with possible appearance of membrane forces.

8.2.2 Blast and Fire

Owing to the current lack of definitive guidance regarding explosions and fire, the behaviour of structures in such events has so far been only predicted by simple models based on:

- equivalent static overpressure and plastic deformation of plates for blast analysis.
- the reduction of material strength and elastic modulus under temperature increase.

In the aftermath of recent mishaps however, more accurate analyses may become mandatory, based on a better understanding of the pressure-time histories and the effective resistance and response of structures to explosions and fire.

8.3 Progressive Collapse

Some elements of the structure (legs, bracings, bulkheads) may partially or completely lose their strength as a result of accidental damage.

The purpose of such analysis is to ensure that the spare resistance of the remaining structure is sufficient to allow the loads to redistribute.

Since such a configuration is only temporary (mobilisation period prior to repairs) and that operations will also be restricted around the damaged area, reduced live and environmental loads are generally accepted.

In this analysis, the damaged elements are removed from the model. Their residual strength may be represented by forces applied at the boundary nodes with the intact structure.

9. LOAD OUT & TRANSPORTATION

9.1 Load-Out

The load-out procedure consists of moving the jacket or module from its construction site to the transportation barge by skidding, or by using trailers underneath it.

The barge may be floating and is continuously deballasted as the package progresses onto it, or grounded on the bottom of the harbour.

9.1.1 Skidding

The most severe configuration during skidding occurs when the part of the structure is cantilevering out:

- from the quayside before it touches the barge.
- from the barge just after it has left the quay.

The analysis should also investigate the possibility of high local reactions being the result of settlement of the skidway or errors in the ballasting procedure.

9.1.2 Load-Out by Trailers

As the reaction on each trailer can be kept constant, analysis of load-out by trailers only requires a single step to determine the optimal distribution of trailers.

9.2 Transportation

9.2.1 Naval Architectural Model

The model consists of the rigid-body assembly of the barge and the structure.

Barges are in general characterised by a low length/beam ratio and a high beam/draught ratio, as well as sharp corners which introduce heavy viscous damping.

For jacket transport, particular care shall be taken in the representation of overhanging parts (legs, buoyancy tanks) which contribute significantly to the righting moment.

Dry-transported decks and modules may be simply represented by their mass and moments of inertia.

This analysis shall provide the linear and angular accelerations and displacements of the structure to be entered in the structural model as inertia forces, and also the partition and intensity of buoyancy and slamming forces.

9.2.2 Structural Model

The jacket model is a simplified version of the in-place model, from which eccentricities and local reinforcements may be omitted.

The barge is modelled as a plane grid, with members having the equivalent properties of the longitudinal and transversal bulkheads.

As the barge passes over a wave trough or a crest, a portion only of the barge is supported by buoyancy (long barges may be spanning over a whole trough or be half-cantilevered).

The model therefore represents the jacket and the barge as two structures coupled together by the seafastening members.

10. INSTALLATION

10.1 Launching

10.1.1 Naval Architectural Model

A three dimensional analysis is carried out to evaluate the global forces acting on the jacket at various time steps during the launch sequence.

At each time step, the jacket/barge rigid body system is repositioned to equilibrate the internal and external forces produced by:

- jacket weight, inertia, buoyancy and drag forces.
- barge weight, buoyancy and ballast forces.
- vertical reactions and friction forces between jacket and barge.

The maximum reaction on the rocker arm is normally obtained when the jacket just starts rotating about the rocker hinge.

10.1.2 Structural Model

The structural model is in all aspects identical to the one used for the transportation analysis, with possibly a finer representation of the launch legs.

The rocker arm is also represented as a vertical beam hinged approximately at midspan. Interface loads obtained by the rigid body analysis are input at boundary conditions on the launch legs. All interface members must remain in compression, otherwise they are inactivated and the analysis restarted for that step.

Once the tilting phase has begun, the jacket is analysed at least for each main leg node being at the vertical of the rocker arm pivot.

10.2 Upending

No dedicated structural analysis is required for this phase, which is essentially a naval architecture problem.

A local analysis of the lugs is performed for crane-assisted upendings.

10.3 Docking

Docking of a jacket onto a pre-installed template requires guides to be analysed for local impact. The same requirement applied for bumpers to aid the installation of modules.

10.4 Unpiled Stability

The condition where the jacket may for a while stand unpiled on the seafloor is analysed for the design installation wave.

The stability of the jacket as a whole (overturning tendency) is investigated, together with the resistance of the mudmats against soil pressure.

10.5 Piling

The piles are checked during driving for the dynamic stresses caused by the impact wave of the hammer blow. The maximum cantilevered (stick-up) length of pile must be established for the self-weight of the pile and hammer combined, accounting for first and second order moments arising from the pile batter. Hydrodynamic actions are added for underwater driving.

Elements in the vicinity of the piles (guides, sleeves) shall also be checked, see Section 11.1.

10.6 Lifting

10.6.1 Model

The model used for the lift analysis of a structure consists of the in-place model plus the representation of the rigging arrangement (slings, spreader frames).

For single lifts the slings converge towards the hook joint, which is the sole vertical support in the model and shall be located exactly on the vertical through the centre of gravity (CoG) of the model.

For heavier dual-crane lifts, the CoG shall be contained in the vertical plane defined by the two hook joints.

The mathematical instability of the model with respect to horizontal forces is avoided by using soft horizontal springs at the padeyes. The force and elongation in these springs should always remain small.

10.6.2 Design Factors

Different factors are applied to the basic sling forces to account for specific effects during lifting operations.

10.6.2.1 Skew Load Factor (SKL)

This factor represents the effect of fabrication tolerances and lack-of-fit of the slings on the load repartition in a statically undetermined rigging arrangement (4 slings or more). Skew factors may either be directly computed by applying to a pair of opposite slings a temperature difference such that their elongation/shortening corresponds to the mismatch, or determined arbitrarily (typically 1/3 - 2/3 repartition).

10.6.2.2 Dynamic Amplification Factor (DAF)

This factor accounts for global dynamic effects normally experienced during lifting operations. DnV recommends minimum values as in Table 3.5.

Table 3.5: Load factor

Lifted Weight W (tonnes)	up to 100 t	100 t to 1000t	1000 t to 2500t	more than 2500 t
DAF offshore	1.30	1.20	1.15	1.10
DAF inshore	1.15	1.10	1.05	1.05

10.6.2.3 Tilt Effect Factor (TEF)

This factor accounts for additional sling loading caused by the rotation of the lifted object about a horizontal axis and by the longitudinal deviation of the hooks from their theoretical position in the case of a multi-hook lift. It shall normally be based on 5° and 3° tilt respectively depending on whether cranes are on different vessels or not.

10.6.2.4 Yaw Effect Factor (YEF)

This factor accounts for the rotation of the lifted object about a vertical axis (equal to 1.05 typically).

10.6.3 Consequence Factors

Forces in elements checked under lift conditions are multiplied by a factor reflecting the consequence a failure of that specific element would have on the integrity of the overall structure:

- 1.30 for spreader frames, lifting points (padeyes) and their attachment to the structure.
- 1.15 for all members transferring the load to the lifting points.
- 1.00 for other elements.

11. LOCAL ANALYSES AND DESIGN

Local analyses address specific parts of the structure which are better treated by dedicated models outside the global analysis. The list of analyses below is not exhaustive.

11.1 Pile/Sleeve Connections

Underwater pile/sleeve connection is usually achieved by grouting the annulus between the outside of the pile and the inner sleeve.

The main verifications address:

- the shear stresses in the concrete.
- the fatigue damage in the shear plates and the attachment welds to the main jacket accumulated during pile driving and throughout the life of the platform.

11.2 Members within the Splash Zone

Horizontal members (conductor guide frames in particular) located within the splash zone (± 5 m on either side of the mean-sea-level approximately) shall be analysed for fatigue caused by repeated wave slamming.

A slamming coefficient $C_s = 3.5$ is often selected.

11.3 Straightened Nodes

Typical straightened nodes (ring-stiffened nodes, bottle legs nodes with diaphragms) are analysed by finite-elements models, from which parametric envelope formulae are drawn and applied to all nodes representative of the same class.

11.4 Appurtenances

11.4.1 Risers, Caissons & J-Tubes

Static In-Place and Fatigue

Risers, caissons and J-tubes are verified either by structural or piping programs for the action of environmental forces, internal pressure and temperature. Particular attention is paid to the bends not always satisfactorily represented by structural programs and the location of the touch-down point now known a-priori.

A fatigue analysis is also performed to assess the fatigue damage to the clamps and the attachments to the jacket.

Pull-In

J-tubes are empty ducts continuously guiding a post-installed riser pulled inside. They are verified by empirical plastic models against the forces generated during pull-in by the friction of the cable and the deformation of the pull head.

11.4.2 Conductors

Conductors are analysed in-place as beam columns on discrete simple supports, these being provided by the horizontal framing of the jacket (typically 20 to 25 m span).

The installation sequence of the different casings must be considered to assess the distribution of stresses in the different tubes forming the overall composite section.

Also the portion of compression force in the conductor caused by the hanging casings is regarded as an internal force (similar to prestressing) which therefore does not induce any buckling tendency.

11.5 Helidecks

The helideck is normally designed to resist an impact load equal to 2.5 times the take-off weight of the heaviest helicopter factored by a DAF of 1.30.

Plastic theories are applicable for designing the plate and stiffeners, while the main framing is analysed elastically.

11.6 Flare Booms

Analyses of flare booms particularly consider:

- variable positions during installation (horizontal pick-up from the barge, lift upright).
- reduced material characteristics due to high temperature in the vicinity of the tip during operation.
- dynamic response under gusty winds.
- local excitation of diagonals by wind vortex-shedding.

12. CONCLUDING SUMMARY

- The analysis of offshore structures is an extensive task.
- The analytical models used in offshore engineering are in some respects similar to those used for other types of steel structures. The same model is used throughout the analysis process.
- The verification of an element consists of comparing its characteristic resistance(s) to a design force or stress. Several methods are available.
- Simple rules are available for preliminary member sizing.
- Static in-plane analysis is always carried out at the early stage of a project to size the main elements of the structure. A dynamic analysis is normally mandatory for every offshore structure.
- With the trend to ever deeper and more slender offshore structures in yet harsher environments, more elaborate theories are necessary to analyse complex situations. There is a risk for the Engineer having increasingly to rely on the sole results of computer analyses at the expense of sound design practice.
- To retain enough control of the process of analysis, the following recommendations are given:
 - Check the interfaces between the different analyses and ensure the consistency of the input/output.
 - Verify the validity of the data resulting from a complex analysis against a simplified model, which can also be used to assess the influence of a particular parameter.
 - Make full use of "good engineering judgement" to criticise the unexpected results of an analysis.

4. A RECENT MINIMUM FACILITY PLATFORM

This chapter presents an overview of a recently installed Minimum Facility Platform. This example is provided to familiarize the reader with the use of minimum structures in the oil and gas industry. This chapter will serve as an introduction to the next chapter, which introduces a hypothetical minimum structure as the case study for this project.

MINIMUM STRUCTURES

Due to their low fabrication and installation costs, Minimum Facility Platforms (MFPs) have become attractive within the last decade, especially for the "fast track" development of marginal oil and gas fields. This would allow marginal fields to start producing typically at about half the cost and in half the time compared to those associated with standard four-pile jackets. Minimum structures have hitherto been used as unmanned platforms in water depths of 40m-60m, mainly for the development of marginal fields.

Compared to traditional jackets, minimum structures are characterised by a slender layout, low stiffness and a low level of redundancy. Figure 4.1 illustrates three minimum structure concepts widely used in the North Sea and Gulf-of-Mexico.

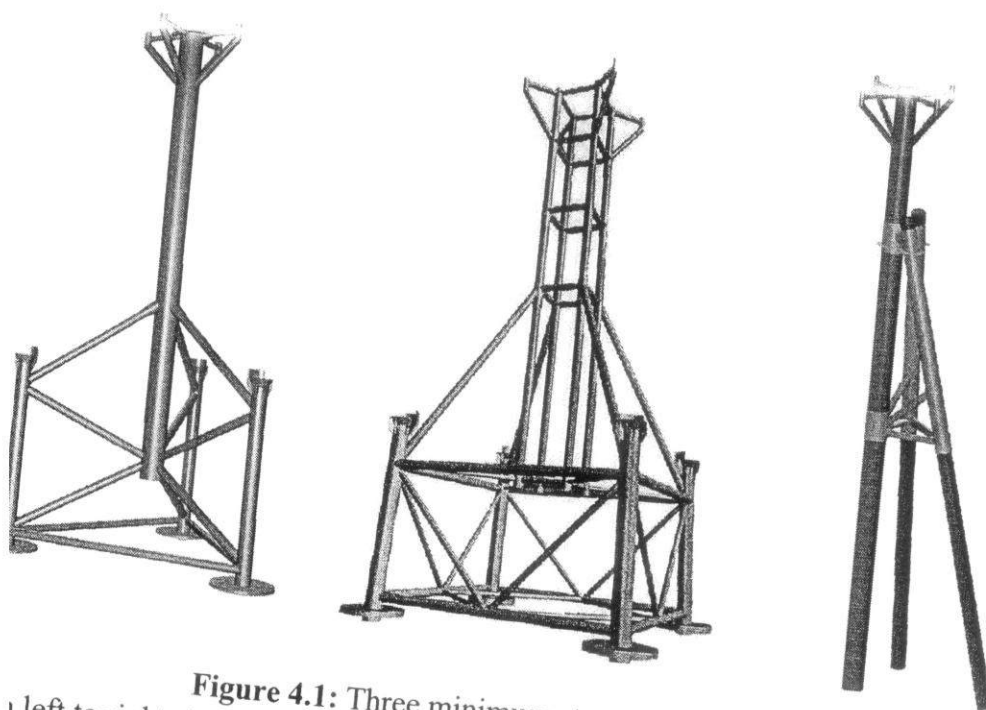


Figure 4.1: Three minimum structure concepts
left to right: 3-Pile Monotower (Monopod), Vierendeel Tower, Braced Caisson

NINI & CECILIE

Nini & Cecilie Platforms

The Nini & Cecilie platforms are two almost identical minimum structure platforms for the development of the Nini and Cecilie Fields in the Danish part of the North Sea. See Figure 4.2.

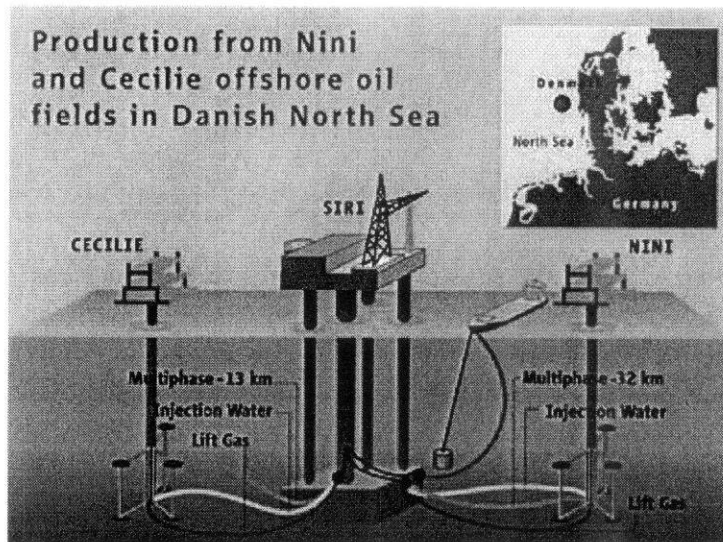


Figure 4.2: Production from Nini and Cecilie offshore oil fields in Danish North Sea

They are robust monopod platforms designed to support large topside loads. Each platform consists of a jacket of 2,200 tonnes and topsides of 650 tonnes. The platforms are located at 60 m of water and are designed for 10 wells. The oil from Nini and Cecilie is exported to the Siri platform, where it is processed and sent onshore. The Nini and Cecilie platforms are both unmanned and are operated from Siri. There are, however, small cabins installed on each platform thus making it possible for operators to stay overnight in case of emergency.

The construction of the two platforms took almost 1 year. Figures 4.3 and 4.4 illustrate the load-out and the transportation of the platforms, respectively. Their installation was completed within only 14 days, and a few days later hook-up of the wells was carried out. Work was completed in June 2003. Figure 4.5 shows the Cecilie platform in its final position.

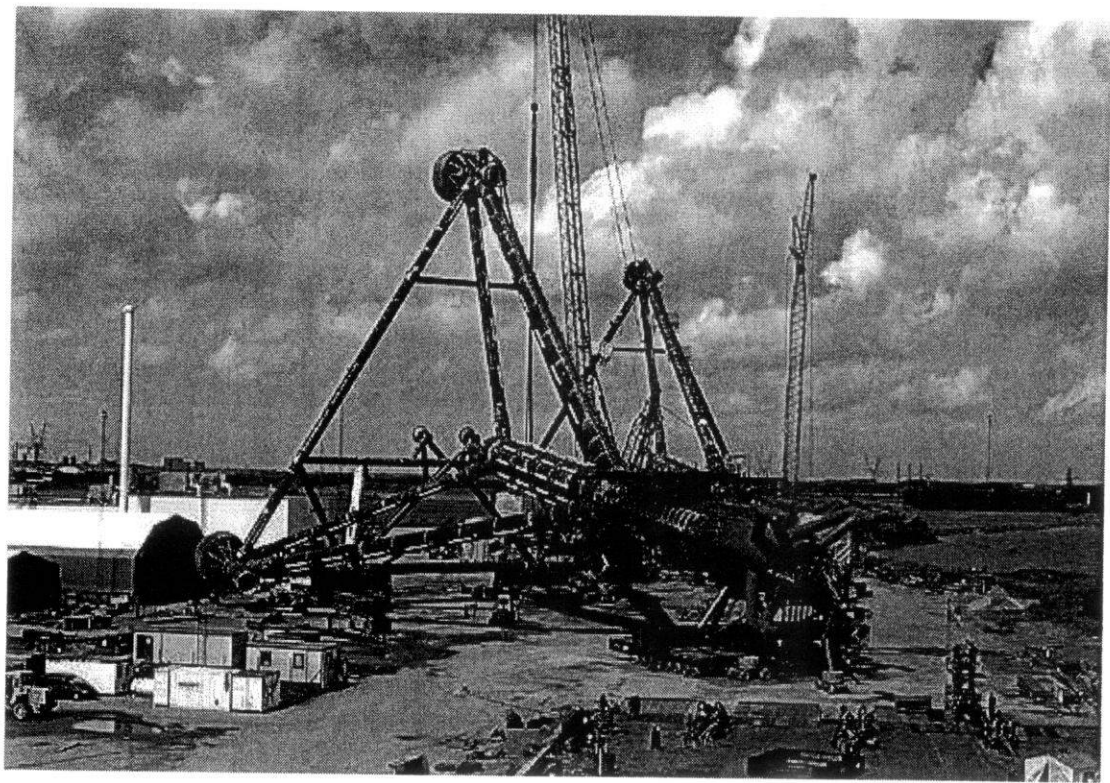


Figure 4.3: Load-out of Nini/Cecilie platforms

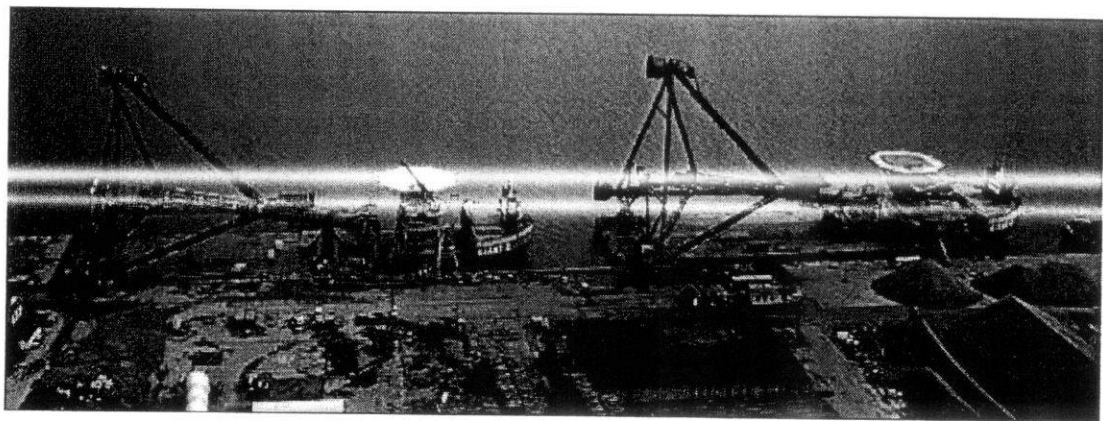


Figure 4.4: Transportation of Nini/Cecilie platforms by barge

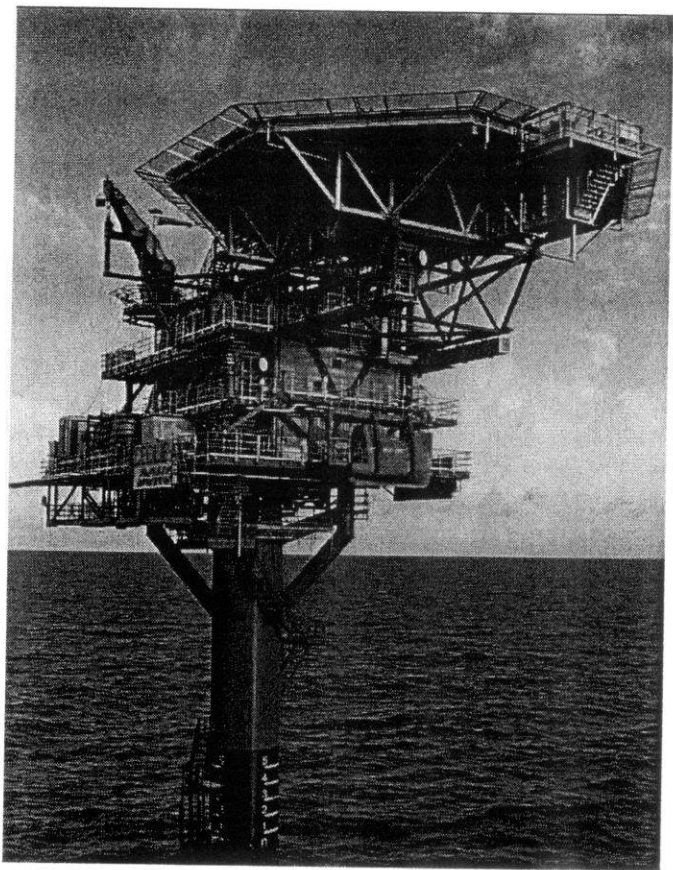


Figure 4.5: The Cecilie platform in operation

Table 4.1 lists the companies that contributed to the Nini/Cecilie project.

Table 4.1: Parties involved in the Nini/Cecilie project

Operator	DONG E&P A/S
Consulting Engineer (Designer)	Rambøll Oil & Gas
Manufacturing Contractor	Bladt Industries A/S

Technical Documents

The writer has been able to obtain design brief documents for the Nini & Cecilie platforms through correspondence with their original designers, Ramboll.

Nini Field Information

Discovered: 2000

Year on stream: 2003

Producing wells: 4

Water-injection wells: 2

Water depth: 60 m

Field delineation: 48.8 km²

Reservoir depth: 1,700 m

Reservoir rock: Sandstone

Reserves at 1 January 2005

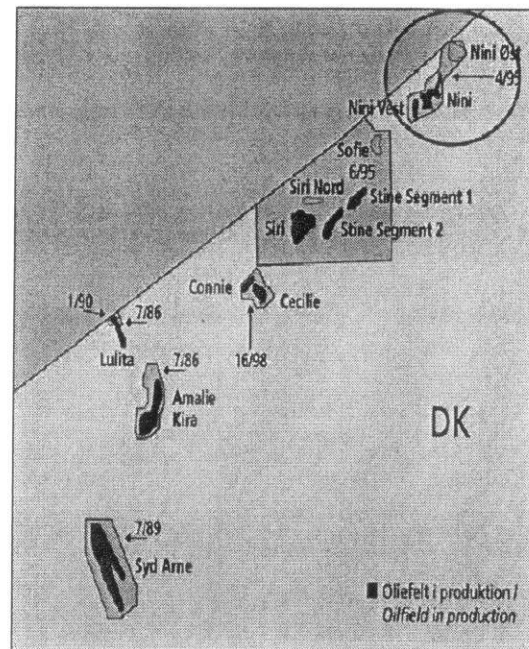
Oil: 2.4 million m³

Gas: 0.0 billion m³

Jan. 2006 production:

7,940 boe/d gross

2,380 boe/d net



Production Facilities

Nini is a satellite development to the Siri Field with one unmanned wellhead platform with a helideck. The unprocessed production is transported to the Siri platform where it is processed and exported to shore via tanker. Injection water and lift gas are conveyed from the Siri platform to the Nini platform.

5. CASE STUDY

This chapter introduces the hypothetical offshore platform selected as the project's case study.

5.1 SELECTED PLATFORM

The Braced Caisson concept, a member of a group of offshore platforms known as “minimum structures”, was selected as the project's case study. A schematic view of the as-designed structure is shown in Figure 5.1. This structure will be subjected to computer simulations (Chapter 6) and scale model experiments (Chapter 7).

Reasons behind Selection

The Braced Caisson concept was chosen for the case study because it has the simplest structure among all possible forms of offshore platforms. It has only 15 main braces compared to about 60 in a conventional 4-pile jacket of similar height. Similarly, the number of tubular joints and circumferential welds is substantially smaller. Therefore, it will be relatively simple to construct the model and analyse it experimentally and theoretically. This will save the writer plenty of time and effort which will be put to better use in developing the project.

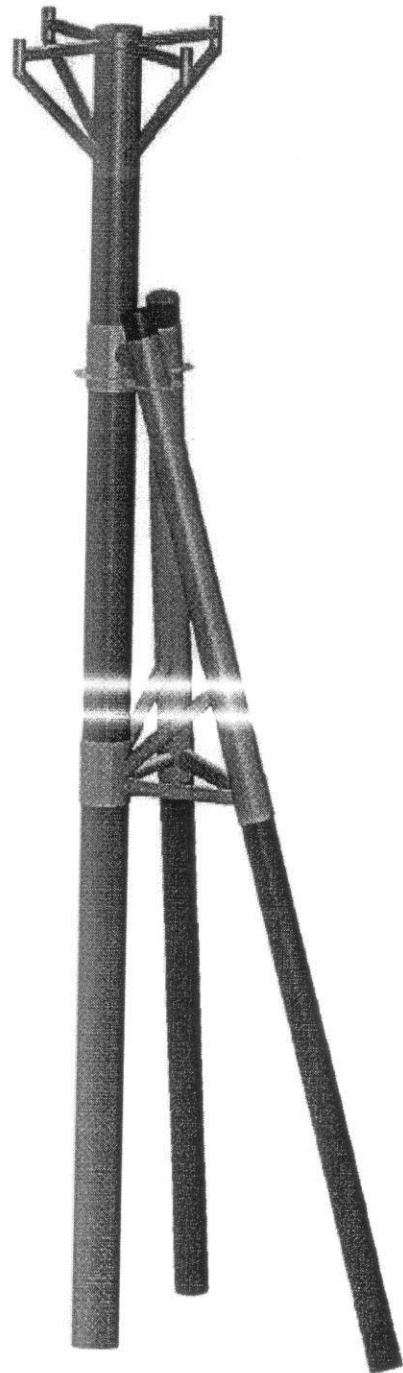


Figure 5.1: Braced Caisson

5.2 JOINT INDUSTRIAL PROJECT (JIP)

The writer found a detailed study of the Braced Caisson concept in the report of the Joint Industry Project (JIP). This project was set up with the overall objective of evaluating and comparing the life-cycle reliability and risk characteristics of minimum structures with those of traditional jacket structures. The report is titled "*Comparative evaluation of minimum structures*", and was prepared by WS Atkins Consultants Ltd for the Health and Safety Executive of the United Kingdom.

The JIP evaluates three minimum structure concepts, namely: (i) 3-Pile Monotower, (ii) Vierendeel Tower, and (iii) Braced Caisson. It introduces each structural concept, designs the structures using common design criteria, and then evaluates the performance/reliability of the designed structures under extreme storm, fatigue and ship collision conditions using various computer analyses.

The writer extracted parts of the above-mentioned report that relate specifically to the Braced Caisson concept, and its reliability under extreme storm conditions. These extracts constitute the remainder of this chapter.

1.1 Background

Due to their low fabrication and installation costs, Minimum Facility Platforms (MFPs) (e.g. monotowers) have become attractive within the last decade, especially for the "fast track" development of marginal oil and gas fields. This would allow marginal fields to start producing typically at about half the cost and in half the time compared to those associated with standard four-pile jackets.

Compared to traditional jackets, minimum structures are characterised by a slender layout, low stiffness and a low level of redundancy. This could make these structures very sensitive to damage and defects that may occur due to design, fabrication or operational errors. There is therefore a need to understand the performance of these structures with regard to reliability, so that informed decisions can be made about their feasibility for a particular field development.

Minimum structures have hitherto been used as unmanned platforms in water depths of 40m-60m, mainly for the development of marginal fields. However, Operators are now considering the use of these structures in deeper water, to support higher topside loads and for providing accommodation facilities as well. Such changes could considerably increase the potential consequences of failure.

The Operators considering using minimum structures are faced with this key question: How do the reliability levels of minimum structures compare with those of standard four-pile jackets?

The choice between a minimum structure and a jacket, and between alternative minimum structure designs, is likely to be influenced by a number of factors such as: lead time, production revenue, service life, initial costs of fabrication and installation, in-service maintenance costs, probabilities of failure, consequences of failure, etc.

1.2 Objectives

The Joint Industry Project was set up with the overall objective of evaluating and comparing the life-cycle reliability and risk characteristics of minimum structures with those of traditional jacket structures. More specifically, the objective was to evaluate and compare system reliability levels of three minimum structures against a standard four-pile jacket under extreme storm, fatigue and ship collision conditions.

The focus of the JIP is on quantifying the inherent reliability of the sub-structure (i.e. the jacket), and for this reason, the failure of the foundation, damage to conductors/risers, wave impingement on the deck, wave breaking, fire and blast effects have specifically been excluded from the study.

1.3 Project Organisation

The JIP was executed by four consultants with the roles defined as below:

WS Atkins	Project Co-ordinator Reliability under extreme storm and fatigue conditions
Ramboll	Dy. Project Manager Conceptual design of selected structures

WS Atkins acted as the main contractor for the project with the sponsors while Ramboll and MSL were sub-contractors to WS Atkins.

1.4 Method of Approach

1.4.1 Framework for Evaluation

The system reliability levels of the selected structure were assessed considering extreme storm conditions.

1.4.2 Work Programme

The Project Work Programme consisted of three Tasks as below. The Consultant responsible for each task is indicated in braces.

Reliability evaluation of structure

Task 1: Conceptual design (Ramboll)

Task 2: Reliability under extreme storm (WS Atkins)

1.5 Organisation of the JIP report

The JIP report summarises the work carried out under the various tasks within the project and presents and discusses the key results obtained. An overview of the remaining sections of this chapter taken from this report is given below.

Section 5.3: Conceptual Design

This Section summarises the work carried out by Ramboll under Task 1. The Design Premise which forms the basis of design of the selected structures is discussed and the key data used in design is summarised. The design and analysis procedures used are discussed, and key design features of the structure are reviewed.

Section 5.4: Reliability under Extreme Storm Conditions

The work carried out by WS Atkins under Task 2 of the Project is summarised in this Section. The methodology used for pushover analysis and system reliability analysis under extreme storm conditions is outlined and the probabilistic modelling of the basic variables is summarised. The key results obtained for the structure are presented.

5.3 CONCEPTUAL DESIGN

Introduction

This section summarises the conceptual design of the three minimum structures and a 4-pile jacket carried out by Ramboll under Task 1 of the Project. Detailed information on the design process and the configuration of the structure can be obtained from References 2 and 3.

The scope of work under Task 1 was to carry out a conceptual design of the structure which will form the basis of a reliability evaluation. The “design premises” were established at the beginning of the project and the structure was designed according to this.

The design premises are discussed next followed by a summary of the design and analysis procedures used. The key design features of the structure are discussed after that.

Design Premises

Design Criteria

With the agreement of the Project Steering Committee (PSC), the Davy field in the Southern North Sea was chosen as the reference site where the structure would be located for the purposes of design. It was also chosen to adopt standard North Sea design criteria and design procedures for conceptual design.

The following conditions were considered for the design of the structure:

- Extreme storm (100-year return)
- Operating storm
- Fatigue
- Vortex shedding
- On-bottom stability

In view of the shallow water depth, it was assumed that fabrication, load-out, transportation and installation conditions do not have a significant influence on design. In view of the conceptual nature of the design, these conditions were not assessed in detail. However, it is considered that the resulting designs are representative of real structures and can actually be fabricated and installed, following detailed engineering.

The designs were carried out largely according to API Recommended Practice 2A-WSD, 20th Edition [Ref. 4].

The key members of the structure were designed for a “utilisation ratio” of close to 0.8. In order to achieve this requirement, wall thickness of members were selected in increments of 1 mm. Hence it is possible that some of the member dimensions may not follow the standard pipe section schedules available in practice.

The focus of the JIP was to study the reliability characteristics of the primary substructure (i.e. the jacket) without being influenced by the chosen soil profile. It was therefore important that the system reliability of the structure was not governed by foundation failure. In the cases where the foundation piles are seen to fail, their failure was suppressed by artificially increasing the yield strength of pile steel and/or increasing the penetration depth. In this way, the pile axial utilisation ratios were kept well below 0.60. It is considered that this has no significant influence on the primary structure dimensions and its failure behaviour.

The service life of the platform was considered to be 20 years. The design for fatigue was based on the UK HSE guidelines [Ref. 5]. In line with the draft ISO standard for design of fixed offshore steel structures (ISO 13819-2, Fixed Steel Offshore Structures, Draft C, 1997), a Fatigue Life Safety Factor of 5.0 was used for the Braced Caisson.

Design Data

The platform was designed to accommodate four O.D. 26 inch conductors and one O.D. 12 inch export riser. The conductors are located inside the caisson and the riser is assumed clamped onto the caisson on the outside.

The topside is assumed to have a total weight of 400 tonnes. A simplified modelling of the topside was adopted. Additional loads due to eccentricity of the C.O.G. of the topside loading, out-of-vertical tolerance for installation, weight of anodes and other appurtenant elements were accounted for.

As mentioned previously, the Davy field in the Southern North Sea was chosen as the reference site. Accordingly, all the environmental data and soil properties were taken from this site. The key environmental parameters are summarised in Table 5.1.

Table 5.1: Environmental parameters used for design

Water Depth including storm surge	36.2 m
100-year return wave height	16.4 m
Period of the 100-year wave	12.6 m
Associated current speed at the surface	0.96 m/sec
Associated wind speed (1 hour mean @ 10 m above LAT)	32.2 m/sec

Design and Analysis Procedures

The environmental loading for the extreme storm and fatigue analysis were generated following API RP 2A-20th edition wave load recipe. Stream function theory was used for the extreme wave loading and Stokes 5th Order wave theory for the fatigue loading. A wave kinematics factor of 0.9 was used and current blockage and Doppler effects were modelled according to API. The environmental criteria given in Table 5.1 were applied omni-directionally.

A marine growth thickness of 50 mm was assumed between LAT and -12.2 m and a thickness of 25 mm from -12.2 m down to the mud line. Values of the hydrodynamic coefficients used were: $C_d = 1.05$ and $C_m = 1.20$ for marine growth fouled members and $C_d = 0.65$ and $C_m = 1.60$ for members not fouled by marine growth. In addition, for large diameter vertical members such as the caissons, the hydrodynamic coefficients were evaluated as a function of the Keulegan-Carpenter number. The above values of the coefficients were increased by 5% to account for the presence of anodes.

A non-linear soil/pile interaction analysis was used for the extreme wave and ship impact analyses, while for fatigue analysis a linear boundary model was used for the foundation support. The soil spring characteristics were calculated according to API.

The dynamic response of the structure for extreme wave and fatigue analysis was modelled through a Dynamic Amplification Factor corresponding to the eigen period of the first bending mode determined based on the analysis of a single degree of freedom system with 2% of the critical damping.

The wind loading on the topside was determined based on a rectangular box of $L = 15$ m, $W = 8$ m, and $H = 16$ m). A wind shape factor of 1.5 was used.

The structure was designed to avoid the risk of vortex shedding induced vibrations and the resulting loads. This was achieved by designing all elements to be outside the locking-on range for cross-flow and in-line excitations. The calculations followed the methods outlined in DNV Classification Note No. 30.5 [Ref. 6]. The particle velocities used for calculation of the reduced velocity parameter, v_r , was the resulting 100 year return period velocities at the relevant depth for the element in question after pertinent combination of wave and current.

Key Design Features

The 3-D view of the as designed Braced Caisson structure is shown in Figure 5.1. The governing conditions for the structure are discussed in the following and its key design features are presented in a table at the end of this section.

Governing Conditions

The design of the Braced Caisson is mainly governed by the in-place extreme storm condition in the case of members and by fatigue in the case of joints.

The upper inclined braces, the upper horizontal braces and their joints (the cow-horn system) are governed by the in-place operational storm condition. The pile sleeves and the horizontal braces at elevation (-)15.0 are governed by element fatigue. The joint fatigue governs for all the joint cans of the pile sleeves and for the caisson sleeves at elevation (-)15.0 and at elevation (+)4.0.

The penetration lengths of the caisson and piles are governed by extreme storm.

The critical velocity for a 1000 t supply boat is found to be 1.78 m/s. The corresponding estimated maximum collision force is 5.3 MN for impact on the caisson, giving an indentation of 369 mm corresponding to an indentation-to-diameter ratio of 0.18.

For impact on the pile sleeve and pile the estimated maximum collision force is 6.8 MN. This gives a maximum indentation of 300 mm for the pile sleeve, corresponding to an indentation-to-diameter ratio of 0.19.

The analysis for the 2.0 m/s impact velocity showed a utilisation ratio of 5.93 in the punching shear check of the caisson at elev. (+)11.6. By increasing the dimensions of the caisson can at this elevation from Ø2134x37 to Ø2134x44, the utilisation ratio in the punching shear check was reduced to 1.13. At elev. (+)17.5 the punching shear check also showed a utilisation ratio of 1.13. By linear interpolation a velocity of 1.78 m/s is expected to give a utilisation ratio of approximately 1.0 for both the joints.

Key Figures

A number of key figures for the four platforms are shown in Table 5.2. The number of nodes and braces gives an indication of the relative effort involved in fabrication and the number of items potentially requiring offshore inspection.

Table 5.2: Key design features

	Braced Caisson
Jacket Weight:	
Primary steel	260 t
Secondary steel	9 t
Pile Weight	190 t
Caisson/Leg Dia.	2.1 m
Pile Diameter	1.5 m
Pile Penetration	41 m
No. of Braces	15
Tubular Joints	26
Cicumf. Welds	82
No. of Piles	2
Critical Velocity (m/s)for 1000 t vessel	1.8 (1.0) ^[5]
Dent Depth/Dia.	0.19

The performance of the Braced Caisson in terms of its system reliability levels under extreme storm conditions will be examined in the following section.

5.4 RELIABILITY UNDER EXTREME STORM

This section presents the work carried out by WS Atkins under Task 2 of the project involving deterministic pushover analysis and system reliability analysis under extreme environmental conditions, see [Ref. 7]. The methodology used is summarised and the key results from the analyses are presented and discussed.

All the analyses were undertaken using the RASOS software package, [Ref. 8], which is a specialised computer code for load generation, progressive collapse analysis and structural system reliability analysis of offshore structures.

Structural and Load Modelling

Data for structural modelling, comprising of material parameters and geometrical dimensions were taken from the Conceptual Design documents for the Braced Caisson [Refs. 2, 3].

The structure was modelled as a space frame with each member represented by an "engineering beam/column" element. For the purpose of collapse analysis joints were modelled as separate elements. Piles inside legs were modelled using beam elements with equivalent properties representing combined stiffness and strength of the two components. A simplified model of the deck was used with members having equivalent stiffness properties to simulate the actual stiffness of the deck structure.

Soil data and geometrical dimensions of plies, used to calculate the foundation response were taken from the Design Premises [Ref. 2] document. The foundation was modelled using pile elements supported on non-linear springs distributed along the piles. The piles themselves were modelled as tubular beam/column elements. Non-linear stiffness of support springs (lateral p-y and axial t-z and q-z springs) were calculated from the soil properties and pile dimensions according to API [Ref. 4].

Data for environmental conditions, in terms of water depth, wave and current characteristics, marine growth and hydrodynamic coefficients were taken from the Design Premises [Ref. 2]. For the extreme environmental loading condition the analyses were based on a static approach. The environmental loading, represented by distributed forces, was calculated using the API RP 2A 20th Edition recipe, [Ref. 4], and the Stoke's 5th order wave theory was used for calculating particle kinematics.

The structural response under 100-year return environmental loading calculated by the three consultants using different software codes, namely Ramboll - ROSA, MSL - USFOS and WS Atkins - RASOS were compared for each structure. After some adjustments of the USFOS and RASOS computer models satisfactory agreement was obtained for all structures.

Deterministic Pushover Analysis

The pushover analysis employed for calculation of the non-linear response of a structure requires an incremental - iterative strategy, as outlined below.

The first step in this strategy was to calculate the deterministic response under the dead load and environmental loading for 100-year return conditions. This analysis

was carried out employing an iterative technique, in order to take into account non-linearity in the soil response.

The global progressive collapse analysis was carried out by factoring-up the wave and current forces from their initial 100-year values until structural collapse occurred. When a member or joint "failed" by yielding or buckling, the surplus forces were redistributed to the remainder of the structure. The plastic deformation and the resulting global non-linear response of the structure were calculated using the Virtual Distortion Method (VDM) developed by Holnicki-Szulc and Gierlinski, [Ref. 9]. The algorithm used in this method introduces virtual distortions into the failed locations to simulate plastic deformations that satisfy the constitutive law and the global equilibrium. This results in a virtual stress-strain state of the structure. Superimposing the virtual state on the original linear-elastic stress-strain state gave the final non-linear stress-strain state of the structure with one or more components failed. The key feature of the above approach is that the governing equations are constructed for the degrees of freedom in damaged locations only. Thus, the number of equations is considerably smaller compared to that for standard FE approach, leading to a substantial reduction in computational effort.

Reliability under Extreme Storm Conditions

For reliability analysis, the Braced Caisson was modelled as a single component with its mean resistance represented by the ultimate base shear capacity obtained from the deterministic pushover analysis.

A number of loading, resistance and model uncertainty parameters were treated as random basic variables described using appropriate probability distributions as summarised in Table 5.3.

Table 5.3: Probability distributions for environmental loading variables

Variable	Distribution	Mean	COV
Wave Height, H [m]	Gumbel	12.6	0.10
Wave Period [sec.]	Lognormal	$0.432 \cdot H + 5.61$	0.10
Current Speed [m/sec.]	Lognormal	$0.028 \cdot H + 0.48$	0.15
Load Model Uncertainty	Normal	Bias = 1.0	0.15
Ultimate Strength Uncertainty	Lognormal	Bias = 1.0	0.15

The random base shear due to the applied loading was evaluated as a function of the basic variables wave height, wave period, current speed and wave load model uncertainty. First and Second- Order Methods (FORM/SORM) were used for calculating the probability of failure.

Results

Deterministic pushover analysis of the structure was carried out by factoring-up the wave and current forces from their initial 100-year values until collapse occurred. Only the most critical wave direction, selected on the basis of design calculations, was considered. Initial analyses showed that the collapse of the Braced Caisson was governed by the failure of the foundation system. In order to focus the comparisons to the jacket part of the structure, the foundation failure was suppressed by either strengthening the piles or by increasing their penetration depth. The results below correspond to the revised design. The collapse modes and sequence of member failures for the structure are shown in Figure 5.2.



Figure 5.2: Pushover collapse mode

The load factor on the 100-year environmental loading versus the horizontal deflection at the deck level for the Braced Caisson is plotted in Figure 5.3.

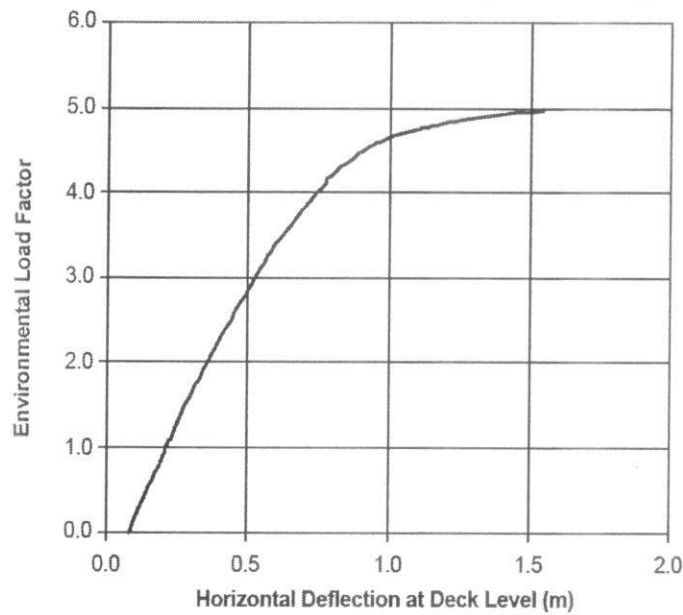


Figure 5.3: Environmental load factor vs. horizontal deck deflection

From the above figure the Braced Caisson shows a stiff behaviour until very close to collapse and a rapid increase in deck displacement as the collapse load is reached.

The key results from the deterministic pushover analyses and system reliability analyses for the extreme storm condition are summarised in Table 5.4.

Table 5.4: Key results for the extreme storm condition

Result	Braced Caisson
100-year design env. base shear [kN]	3,700
Ultimate env. base shear [kN]	18,500
Env. load factor at collapse	5.00
Component reliability index (annual)	5.20
System reliability index (annual)	6.23
Most likely collapse wave [m]	> 27.00
Env. load factor to collapse for the original foundation design	3.12

A high ultimate load factor was obtained for the Braced Caisson and the collapse load factor is relatively high. It also has a reasonably high system reliability index (6.23).

The collapse load factor for the original design of the foundation is given in the last row of Table 3.3. In this case collapse occurred due to failure of the foundation. It can be seen that foundation failure governs the ultimate capacity.

Summary

The performance of the Braced Caisson under extreme storm conditions was studied by carrying out deterministic pushover and system reliability analyses. The results from these analyses are summarised in Table 5.5.

Table 5.5: Performance under extreme storm condition

Item	Braced Caisson
100-yr Wave + Current Base Shear	3.7 MN
Load Factor for Collapse	5.00
Base Shear at Collapse	18.5 MN
Component Reliability Index	5.2
System Reliability Index	6.23
System Failure Probability	2.5E-10

(Note: The Load Factor above is a factor on the 100-year wave + current loading)

The ultimate capacity of the Braced Caisson is derived largely by the axial capacity of one pile and bending capacities of the caisson and the second pile, failure occurring close to the sea bed.

The system reliability of a structure under extreme storm condition is closely related to the Load Factor on environmental loading and not the absolute capacity of the structure. The braced caisson shows comfortably high reliability levels.

The results given in Table 5.5 correspond to the failure of the primary sub-structure with the foundation failure being suppressed by artificially strengthening the piles. When foundation failure was allowed, it is seen that the collapse load factors are in the range of 2.5 to 3.2 with failure occurring in the foundation. Therefore, it should be noted that the high reliability values given in Table 5.5 will not be achieved in practice.

Figure 5.4 shows the relationship between wave height and shear at the base of the Braced Caisson.

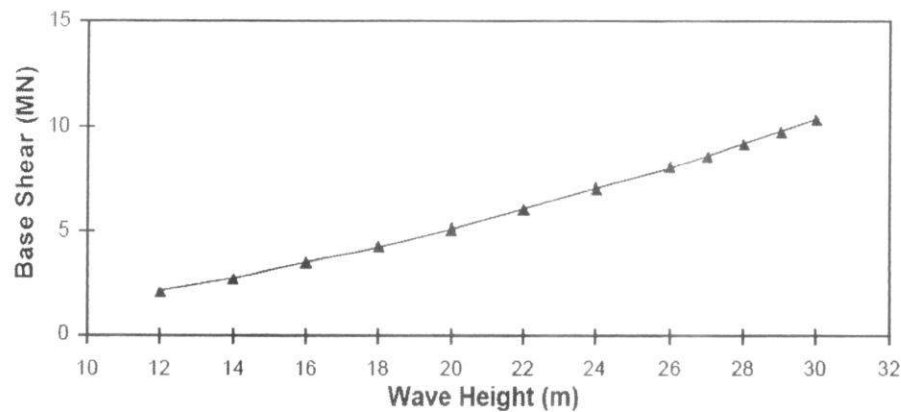


Figure 5.4: Base shear versus wave height

Overall Assessment

The Braced Caisson shows comfortably high levels of system reliability under extreme storm condition when foundation failure is suppressed. In practice, the pushover reliability of the structure will be limited by foundation capacity.

Limitations

The focus of the JIP has been to compare the inherent reliability of the sub-structure, and for this reason, the following considerations were specifically excluded from the study:

- failure of the foundation,
- damage to conductors/risers,
- wave impingement on the deck,
- wave breaking,
- fire and blast effects.

The above factors are very important, and in practice may actually govern the system reliability of the concepts studied. For this reason, the results and conclusions from this study should be used with caution.

Initial studies showed that the reliability under extreme storm condition will be limited by foundation failure.

The various analyses carried out in the project have been based on the North Sea environmental and geotechnical conditions, and standard North Sea design, fabrication, installation, and operation procedures have been assumed. Although some effort has been made to generalise the reliability results to other environmental conditions, care should be exercised in extrapolating the results to other geographical locations with wholly different environmental and geotechnical conditions, and design, fabrication, installation, operation and maintenance practices.

6. COMPUTER SIMULATIONS

This chapter presents the assessment of the structural stability of the case study platform under extreme storm conditions using a software application developed by the author.

6.1 DEVELOPED SOFTWARE (SAOP)

Given the fact that suitable licensed commercial software was unavailable, the writer decided to develop a simple computer program of his own. The developed software was named “Stability Analysis of Offshore Platforms” (SAOP).

SAOP allows for the preliminary stability analysis of offshore platforms by calculating the total shear in the jacket at the sea bed (base shear) under major environmental loads including waves, winds and currents.

Base Shear and Structural Stability

Having obtained the base shear under extreme storm conditions from SAOP and the ultimate capacity of the platform structure from a pushover analysis, we have:
Env. Load Factor at Collapse = Ultimate Env. Base Shear ÷ Design Env. Base Shear
The resulting environmental load factor at collapse is closely related to the system reliability index and probability of failure.

Therefore, the design environmental base shear produced by SAOP provides a good measure of structural reliability and hence, structural stability. Obviously, the higher the base shear, the less stable the platform.

Table 6.1 reiterates the data presented in Table 5.5 as an example of the relationship between the parameters mentioned above.

Table 6.1: Performance of the Braced Caisson structure under extreme storm

Item	Braced Caisson
100-yr Wave + Current Base Shear	3.7 MN
Load Factor for Collapse	5.00
Base Shear at Collapse	18.5 MN
Component Reliability Index	5.2
System Reliability Index	6.23
System Failure Probability	2.5E-10

(Note: The Load Factor above is a factor on the 100-year wave + current loading)

Load Factor for Collapse =

(Base Shear at Collapse) ÷ (100-yr Wave + Current Base Shear) = $\frac{18.5^{MN}}{3.7^{MN}} = 5.00$

6.1.1 Algorithm

SAOP follows the following logical sequence:

1. Input raw data: water level (depth), wave parameters (height and period), wind and current speeds, reference levels and distributions (exponential or logarithmic)
2. Define geometry of structure: dimensions of topsides, dimensions and orientations of jacket members.
3. Select target load combinations.
4. Compute wind drag force on critical side of structure using proper drag coefficient (shape factor); repeat computations for various directions if wind rows are available.
5. Estimate marine growth thickness using a standard suitable for the site. This would affect the diameters and roughness of the respective members.
6. Compute basic wave characteristics, i.e. particle velocities and accelerations using wave mechanics formulae depending on water depth (shallow, transitional or deep water).
7. Estimate empirical parameters to be used in Morison's equation, e.g. drag coefficient, inertia coefficient, modification of parameters for diffraction, etc.
8. Compute total wave forces on all submerged members using Morison's equation incorporating member orientations.
9. Compute current drag force on all submerged members incorporating velocity changes with depth and member orientations.
10. Compute total base shear load using the desired combination of loads.
11. Assess the sensitivity of structural stability to various parameters within their acceptable ranges.

6.1.2 Formulae

SAOP uses the following analytical formulae to find base shear and its constituent environmental forces on an offshore platform. These are well-established relationships taken from fluid mechanics reference texts and standards for offshore platform design. These formulae will be repeatedly referred to in the discussion sections that follow in this chapter.

$$\text{Base shear} = F_{\text{wave}} + F_{\text{wind}} + F_{\text{current}}$$

$$F_{\text{wind}} = \frac{1}{2} \rho_{\text{air}} V_{\text{wind}}^2 C_S A$$

$$F_{\text{current}} = \frac{1}{2} \rho_{\text{water}} V_{\text{current}}^2 C_D A$$

$$F_{\text{wave}} = F_i + F_D \quad (\text{Morison's Equation})$$

$$F_i = C_M \rho_{\text{water}} g \frac{\pi D^2}{4} H K_i$$

$$F_D = C_D \frac{1}{2} \rho_{\text{water}} g D H^2 K_D$$

$$K_i = \frac{1}{2} \tanh\left(\frac{2\pi d}{L}\right) \quad K_D = \frac{1}{4} n$$

$$n = \frac{C_g}{C} = \frac{1}{2} \left(1 + \frac{4\pi d / L}{\sinh[4\pi d / L]}\right)$$

$$L = \frac{gT^2}{2\pi} \sqrt{\tanh\left(\frac{4\pi^2 d}{T^2 g}\right)}$$

6.1.3 Limitations

As indicated in the formula for Base Shear above, SAOP only consider wave, wind and current loads in computing base shear.

In platform design, the effects of current superimposed on waves are taken into account by adding the corresponding fluid velocities. Since drag force varies with the square of the velocity, this addition can greatly increase the forces on a platform. However, as reflected in the formulae for wave forces above, SAOP does not consider these effects because it complicates integration calculations.

6.1.4 Input

The geometry of the Braced Caisson structure defined in the JIP was input into SAOP. Also input were the exact same environmental parameters used in the JIP under extreme storm conditions. See Section 5.3: Conceptual Design and in particular, Figure 5.1 and Tables 5.1 and 5.2. The inputted values are:

Geometry:

Topside Dimensions: 16^m (*height*) \times 15^m (*length*) \times 8^m (*width*)

Caisson Dimensions: 60.6^m length (vertical), 2.1^m diameter

Pile Dimensions: 49.7^m length (14° inclination), 48.2^m to sea floor, 1.5^m diameter

No. of Piles: 2

Wave force coefficients: $C_D = 1.10$, $C_m = 1.26$

Wind force coefficients: $C_{D_{topsides}} = 1.5$, $C_{D_{caisson\&piles}} = 0.5$

Environmental Conditions:

Water Depth = 36.2^m

Wave Height = 16.4^m

Wave Period = 12.6^s

Current speed at surface = $0.96^m/s$

Wind Speed at 10 m above LAT = $32.2^m/s$

6.1.5 Output

Appendix B contains the output of the SAOP software for the input outlined above. The remaining sections of this chapter make use of the output in discussing the breakdown of base shear and its sensitivity to various parameters.

6.2 BREAKDOWN OF BASE SHEAR

By Environmental Loads

Figure 6.2 shows the breakdown of base shear by environmental loads. It is seen that the majority of base shear is caused by wave loads. Therefore, wave loads will play a major role in determining how base shear reacts to changes in different parameters. Thus, wave loads will be the focus of our attempts to justify the results in *Section 6.3: Sensitivity Analysis of Base Shear*.

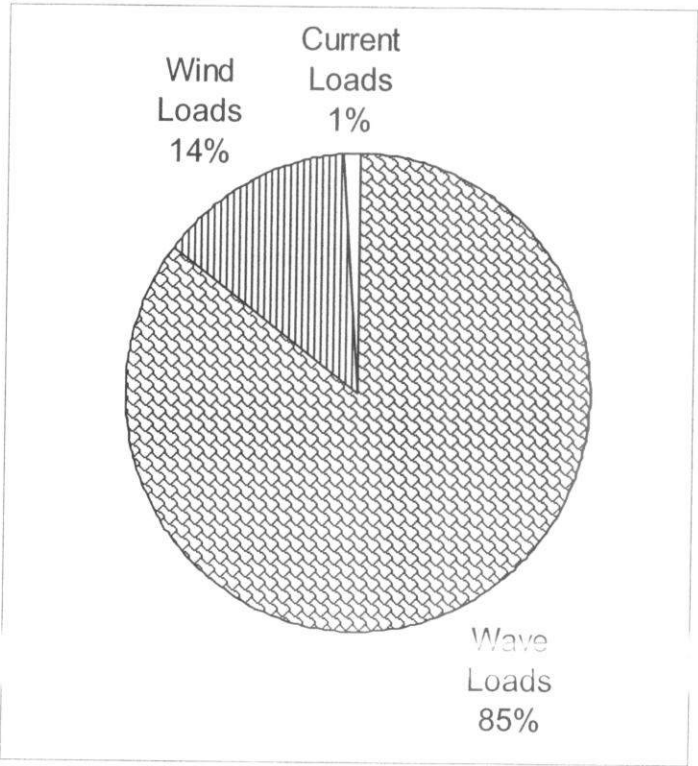


Figure 6.2: Breakdown of base shear by environmental loads

By Environmental Loads and Structural Members

Figure 6.3 breaks base shear down further by indicating the structural members attracting each environmental load. It is evident that the two piles together attract more wave force than the caisson. Also, the topsides attract most of the wind force with the parts of the caisson and piles sticking out of the water playing only a minor role.

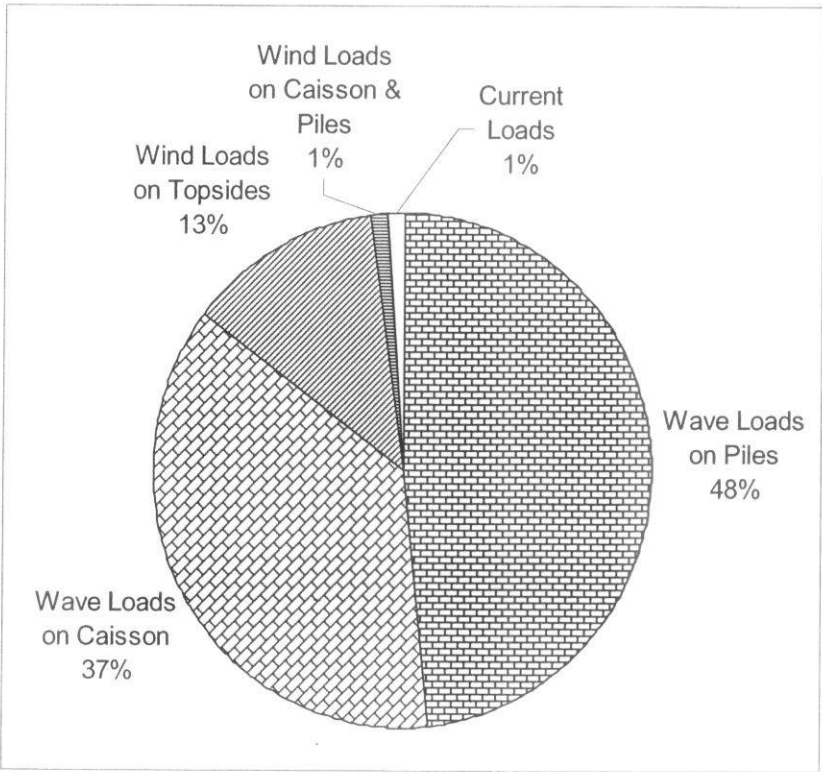


Figure 6.3: Breakdown of base shear by environmental loads and the structural members attracting them

By Structural Members

Figure 6.4 adds the wave, wind and current forces attracted by each of the caisson, piles and topsides in Figure 6.3 to find their shares in the overall base shear. As can be seen, piles attract most of the environmental forces, followed closely by the caisson. Finally, topsides attract a considerable amount of environmental force in the form of wind loads.

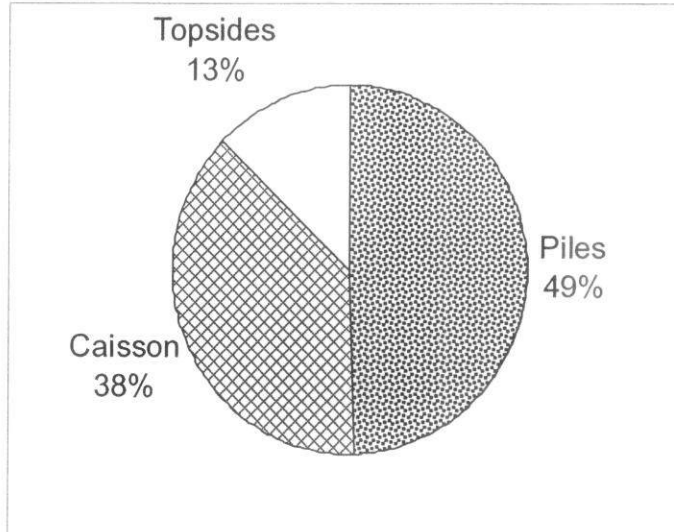


Figure 6.4: Breakdown of base shear by structural members attracting environmental loads

Note that while both piles together give greater base shear than the caisson alone, each pile is responsible for only about $49\% / 2 = 24.5\%$ of the base shear which is less than the caisson's 38% . The ratio of the contributions of a caisson and a pile is greater than the ratio of their diameters.

$$\frac{38\%}{24.5\%} = 1.55 \quad \frac{d_{caisson}}{d_{pile}} = \frac{2.1^m}{1.5^m} = 1.4 \quad 1.55 > 1.4$$

This can be explained by observing that:

1. A pile begins at the seabed but terminates before the caisson connects to the topsides. Therefore, the caisson has a longer length exposed to the wind compared to a pile.
2. F_{wind} and $F_{current}$ are directly proportional to diameter (D) through frontal area (A).

$$F_{wind} = \frac{1}{2} \rho_{air} V_{wind}^2 C_S A \quad F_{current} = \frac{1}{2} \rho_{water} V_{current}^2 C_D A$$

Similarly, F_D in wave forces has a linear relationship with D.

$$F_{wave} = F_i + F_D \quad F_D = C_D \frac{1}{2} \rho_{water} g D H^2 K_D$$

F_i , however, is proportional to diameter squared.

$$F_i = C_M \rho_{water} g \frac{\pi D^2}{4} H K_i$$

Consequently, on the whole, the ratio of base shear produced by the caisson to a pile is slightly greater than the ratio of their diameters.

Breakdown of Wave Loads

Figure 6.5 gives a breakdown of wave force on all submerged members (caisson and piles) by drag and inertial forces as classified in Morison’s equation. $F_{wave} = F_i + F_D$. As will be discussed in Section 6.4, these proportions are related to the Keulegan-Carpenter number and are especially sensitive to member diameters and wave height.

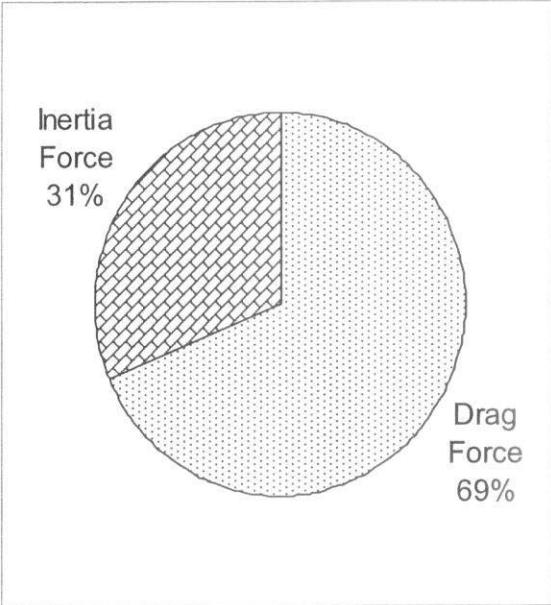


Figure 6.5: Breakdown of wave force by classification in Morison’s equation

Breakdown of Wind Loads

Figure 6.6 gives a breakdown of wind force attracted by the topsides, caisson and piles.

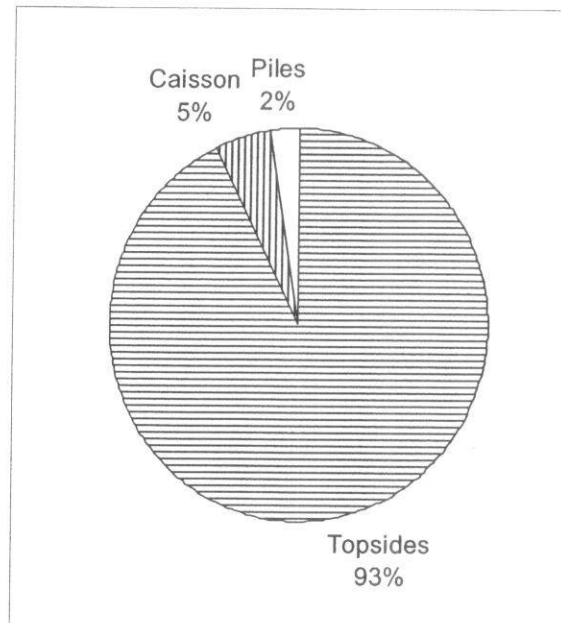


Figure 6.6: Breakdown of wind force by structural members attracting it

The pie chart indicates that most (93%) of the wind loads are exerted on the topsides. This can be attributed to the following factors:

1. The topsides have a much larger frontal area than the caisson or piles.

$$A_{\text{topsidess}} = 16^m \times 15^m = 240^{m^2}$$

$$A_{\text{caisson}} = 2.1^m \times 24.4^m = 51.2^{m^2}$$

2. The topsides have a larger wind drag coefficient.

$$C_{D\text{topsidess}} = 1.5, C_{D\text{caisson/piles}} = 0.5$$

3. The topsides are located at a greater height from the sea water level than the caisson and piles. Thus, they are exposed to greater wind speeds.

The caisson alone draws more wind force than both piles combined ($5\% > 2\%$). The reason for this is that the piles terminate only 12.4 m above the sea water level compared to 24.4 m for the caisson. Therefore, the caisson has a longer length exposed to wind. The distribution of wind speed with height further amplifies the difference.

6.3 SENSITIVITY ANALYSIS OF BASE SHEAR

6.3.1 Introduction

In the analysis of most civil engineering structures, it is helpful to determine how sensitive the structural stability is to the several factors of concern so that proper consideration may be given to them in the design process. Sensitivity, in general, means the relative magnitude of change in the measure of stability (such as base shear or overturning moment) caused by one or more changes in estimated study factor values. Sensitivity analysis is a general non-probabilistic methodology to provide information about the potential impact of uncertainty/change in selected factor estimates.

6.3.2 Individual Sensitivity Analysis

In this Section, we will make explicit the impact of variations in each factor of concern on the overall base shear.

6.3.2.1 Sensitivity to Wave Height

Figure 6.7 shows the sensitivity of base shear to wave height. Both axes are in terms of the percentage changes in these quantities rather than their absolute values. Obviously, base shear and wave height have a direct relationship because a larger wave height means increased wave forces and thus, an increased base shear. The best fit equation to the curve is $y = 0.77x^2 + 1.54x$.

It should be noted that in Figure 6.7 changes in wave height are accompanied by corresponding changes in other storm parameters, i.e. wave period and current speeds, as specified in Table 5.3: $T = 0.432 \times H + 5.61$, $V_{current} = 0.028 \times H + 0.48$. The case where H varies independently of other parameters is discussed in the next section.

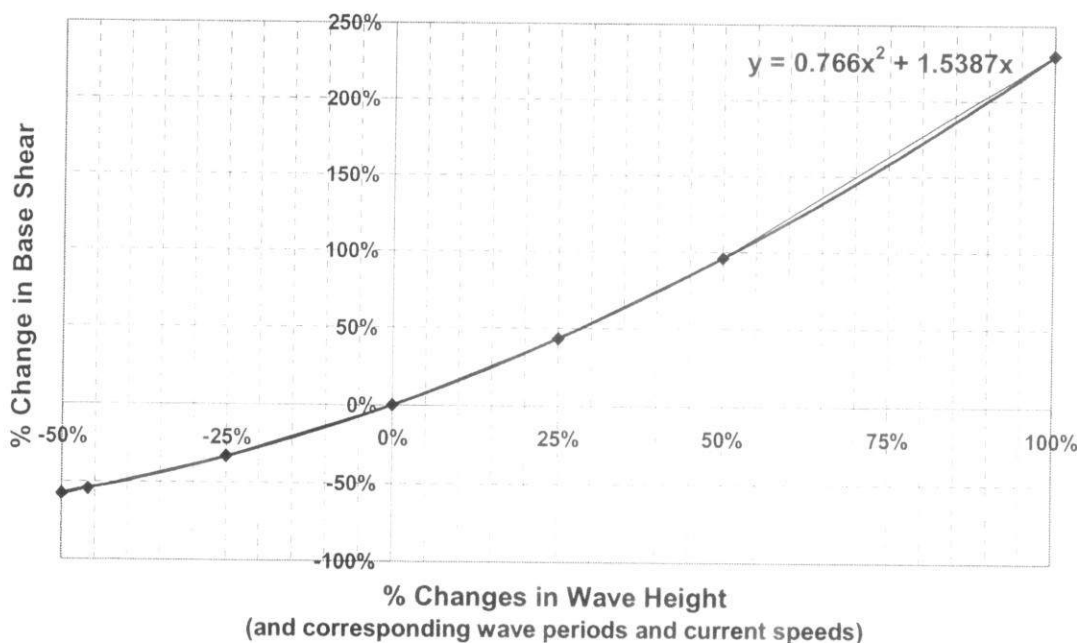


Figure 6.7: Sensitivity of base shear to wave height

Comparison to JIP Results

Figure 6.8 compares base shear versus wave height as calculated by the SAOP program developed by the author and those in Figure 5.4 as in the JIP report. Both axes are in terms of absolute values. It is seen from the graph that the curves show similar trends, with base shear ever increasing with wave height. The ratio of SAOP results to JIP results is in the range of 0.7 to 0.85. As expected, the gap between the curves grows bigger as wave height and base shear increase.

The discrepancy is a result of several factors including:

- Different safety factors: SAOP does not incorporate safety factors in its calculations while the JIP may have. This could be the simple reason why JIP values are constantly higher than SAOP values.
- In platform design, the effects of current superimposed on waves are taken into account by adding the corresponding fluid velocities. Since drag force varies with the square of the velocity, this addition can greatly increase the forces on a platform. SAOP does not consider these effects (because it complicates integration calculations), whereas the JIP probably did.
- Different wave theories: SAOP used the Airy wave theory while the JIP used Stream function theory.
- Different current/wind distributions: SAOP used the logarithmic law model for wind speed and the power law model for current speed. The JIP may have chosen these models differently.

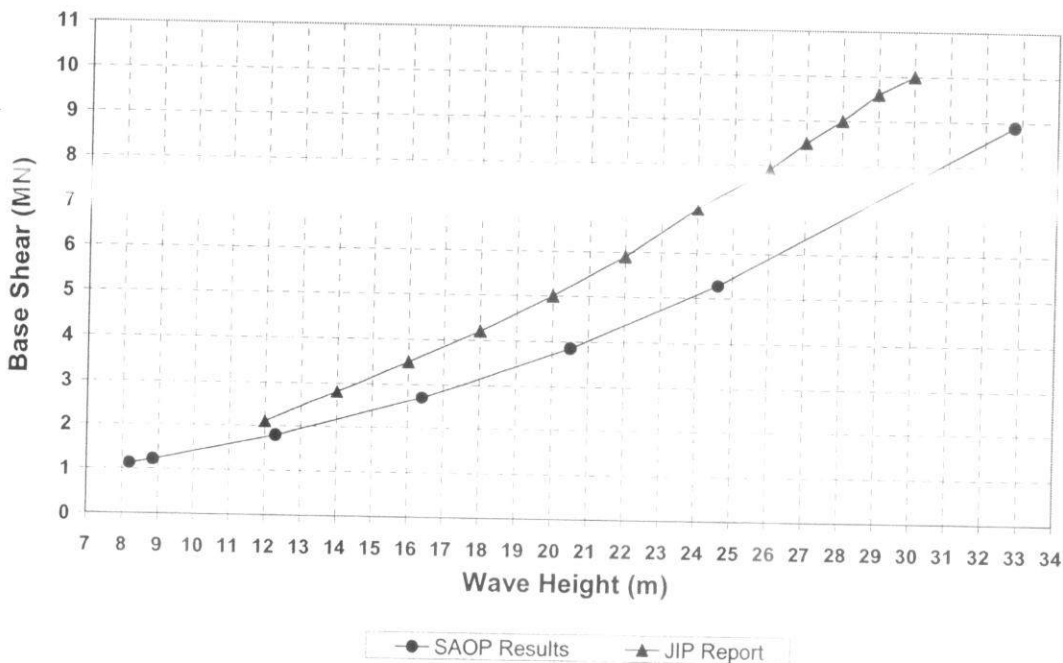


Figure 6.8: Base shear vs. wave height as computed by SAOP and JIP

6.3.2.2 Sensitivity to Wave Height Alone

Figure 6.9 shows the sensitivity of base shear to wave height. Here wave height varies independently of wave period and current speed. Both axes are in terms of the percentage changes in these quantities rather than their absolute values. Obviously, base shear and wave height have a direct relationship because a larger wave height means increased wave forces and thus, an increased base shear. The best fit equation to the curve is $y = 0.59x^2 + 1.44x$.

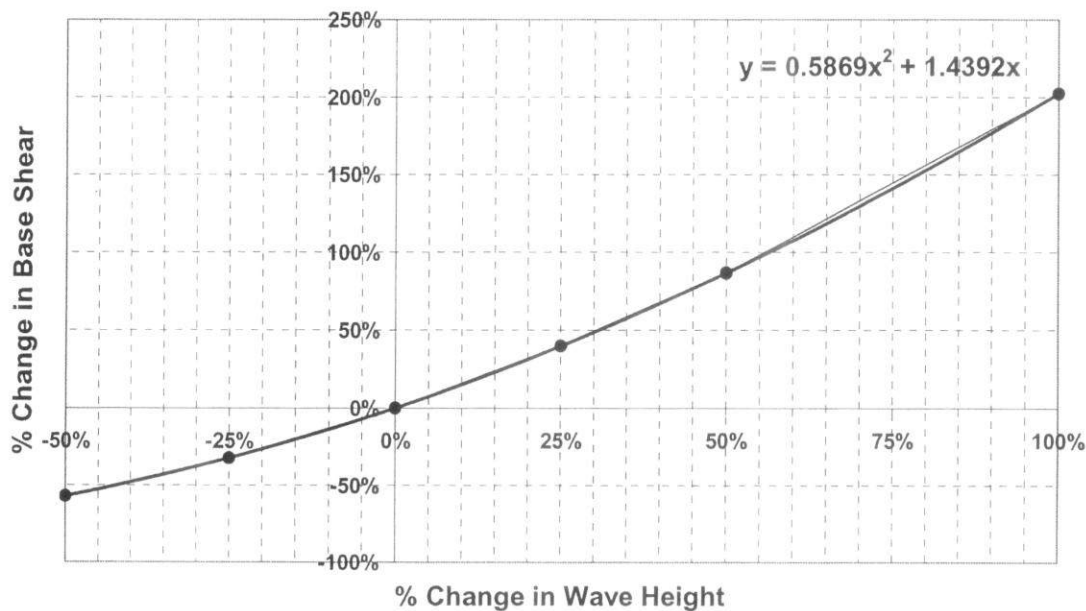


Figure 6.9: Sensitivity of base shear to wave height

As seen in the graph, when wave height is increased by 100%, base shear increases by more than 100%. The justification follows:

Wave forces make up most of the base shear.

$$F_{wave} = F_i + F_D$$

$$F_i = C_M \rho g \frac{\pi D^2}{4} H K_i$$

$$F_D = C_D \frac{1}{2} \rho g D H^2 K_D$$

While F_i is directly proportional to H , F_D is proportional to H^2 . Therefore doubling H would double F_i but quadruple F_D resulting in an F_{wave} which is more than double its original value.

6.3.2.3 Sensitivity to Member Diameters

Figure 6.10 shows the sensitivity of base shear to member diameters. Both axes are in terms of the percentage changes in these quantities rather than their absolute values. Here caisson and pile diameters have been increased simultaneously. Obviously, base shear and member diameters have a positive relationship because larger member diameters mean a larger frontal area for wave, wind and current loads and thus, an increased base shear. The best fit equation to the curve is $y = 0.22x^2 + 1.02x$.

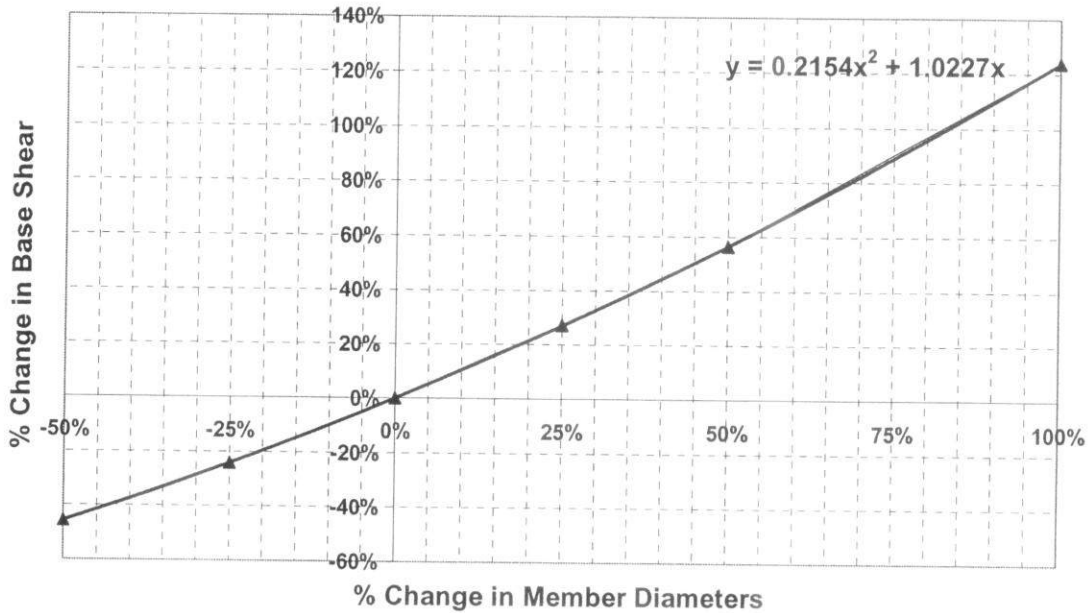


Figure 6.10: Sensitivity of base shear to member diameters

It is observed from the graph that when member diameters are increased by 100%, base shear increases by more than 100%. This can be explained as follows:

Wave forces make up most of the base shear.

$$F_{wave} = F_i + F_D$$

$$F_i = C_M \rho g \frac{\pi D^2}{4} H K_i$$

$$F_D = C_D \frac{1}{2} \rho g D H^2 K_D$$

While F_D is directly proportional to D , F_i is proportional to D^2 . Therefore doubling D would double F_D but quadruple F_i resulting in an F_{wave} which is more than double its original value.

6.3.2.4 Sensitivity to Wind Speed

Figure 6.11 shows the sensitivity of base shear to wind speed. Both axes are in terms of percentage changes in these quantities rather than their absolute values. Obviously, base shear and wind speed have a direct relationship since greater wind speeds result in larger wind forces on topsides and parts of the jacket exposed to wind, and thus, an increased base shear. The best fit equation to the curve is $y = 0.14x^2 + 0.27x$.

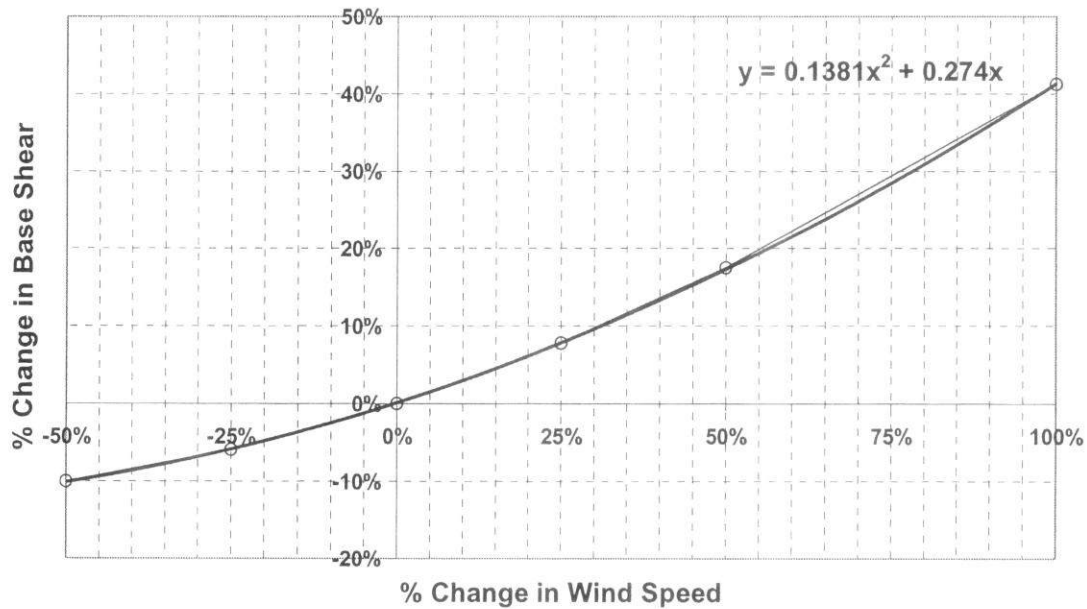


Figure 6.11: Sensitivity of base shear to wind speed

A 100% increase in wind speed leads to a 41.2% increase in base shear. This is justified below:

It is seen in the output file (Appendix B) that at the baseline wind speed (0% change), wind drag constitutes 13.7% of the entire base shear, and the remaining 86.3% are wave and current forces. Doubling wind speed means wind drag will quadruple from 13.7% to $13.7\% \times 4 = 54.8\%$, because F_{wind} is proportional to V_{wind}^2 :

$$F_{\text{wind}} = \frac{1}{2} \rho V_{\text{wind}}^2 C_s A$$

Meanwhile, changing wind speed will not affect the magnitude of wave and current forces. Thus, the new shear is:

$$\begin{aligned} \text{Shear}_2 &= F_{\text{wind } 2} + F_{\text{wave+current } 2} = F_{\text{wind } 2} + F_{\text{wave+current } 1} = \\ &54.8\% \times \text{Shear}_1 + 86.3\% \times \text{Shear}_1 = 141.1\% \times \text{Shear}_1 \end{aligned}$$

This result is very close to the 41.2% increase in shear predicted by the program.

6.3.2.5 Sensitivity to Current Speed

Figure 6.12 shows the sensitivity of base shear to current speed. Here current speed varies independently of wave height and wave period. Both axes are in terms of percentage changes in these quantities rather than their absolute values. Obviously, base shear and current speed have a direct relationship since greater current speeds result in larger current forces on submerged members, and thus, an increased base shear. The best fit equation to the curve is $y = 0.012x^2 + 0.022x$.

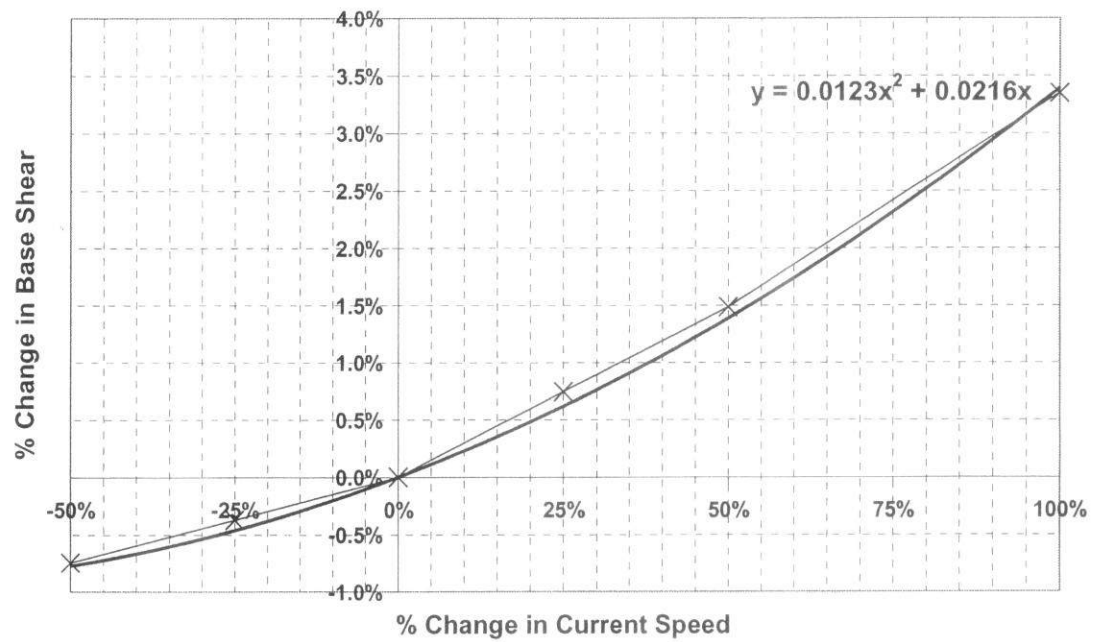


Figure 6.12: Sensitivity of base shear to current speed

As indicated by the small range of variations in base shear (-0.7% to 3.4%) over the range of current speeds in the graph, and as indicated by the relatively small coefficients of the best fit equation (0.012 and 0.022), changing current speed does not cause significant changes in base shear. This is because current loads constitute only a minor portion of the base shear in comparison to wave and wind forces.

However, base shear would have been much more sensitive to current speed if SAOP was programmed to take into account the effects of current superimposed on waves by adding the corresponding fluid velocities. Since drag force varies with the square of the velocity, this addition could have greatly increased the base shear. SAOP does not consider these effects because it would complicate the integration calculations.

6.3.2.6 Sensitivity to Wave Period

Figure 6.13 shows the sensitivity of base shear to wave period. Here wave period varies independently of wave height and current speed. Both axes are in terms of percentage changes in these quantities rather than their absolute values. Base shear and wave period have a positive relationship over most of the graph except at 100% change in wave period where base shear slightly decreases. The best fit equation to the curve is therefore slightly more complex than previous graphs:

$$y = 0.08x^3 + 0.19x^2 + 0.14x$$

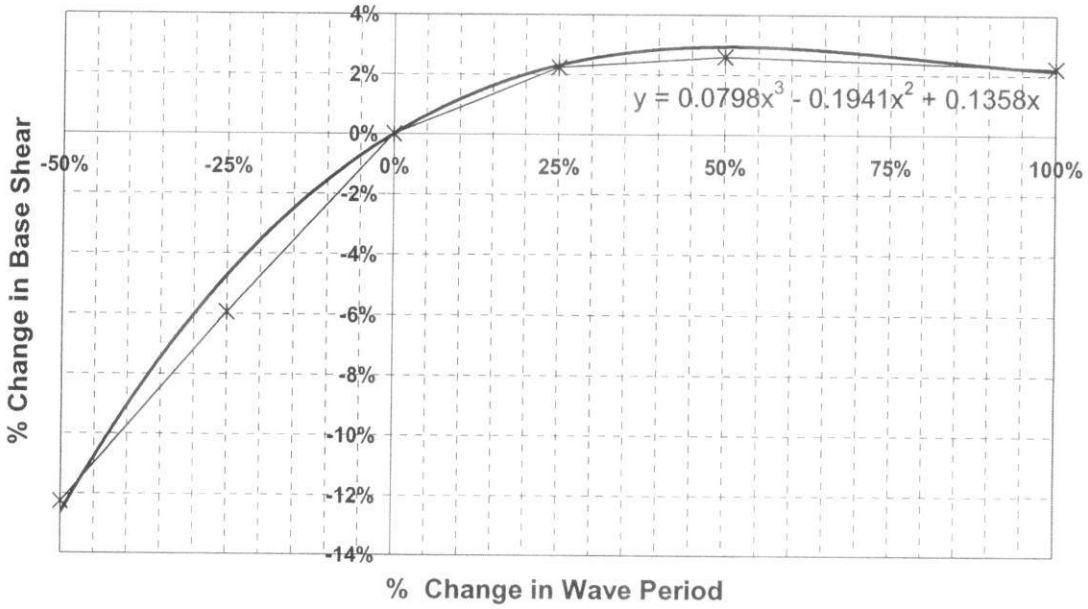


Figure 6.13: Sensitivity of base shear to wave period

Obviously, wave period does not affect wind or current forces, but only wave forces. Wave period does not influence the elements in the F_i and F_D equations except for K_D and K_i .

$$F_{\text{wave}} = F_i + F_D \quad F_i = C_M \rho_{\text{water}} g \frac{\pi D^2}{4} H K_i \quad F_D = C_D \frac{1}{2} \rho_{\text{water}} g D H^2 K_D$$

However, the relationship between wave period and K_D and particularly K_i is complicated and beyond the scope of this study:

$$K_i = \frac{1}{2} \tanh\left(\frac{2\pi d}{L}\right)$$

$$K_D = \frac{1}{4} n \quad n = \frac{C_g}{C} = \frac{1}{2} \left(1 + \frac{4\pi d / L}{\sinh[4\pi d / L]}\right) \quad L = \frac{g T^2}{2\pi} \sqrt{\tanh\left(\frac{4\pi^2 d}{T^2 g}\right)}$$

Therefore we will not attempt to rationalize the relationship between base shear and wave force here.

6.3.2.7 Sensitivity to Water Depth

Figure 6.14 shows the sensitivity of base shear to water depth. Both axes are in terms of percentage changes in these quantities rather than their absolute values. Interestingly, base shear and water depth have an inverse relationship. The best fit equation to the curve is linear with a negative slope: $y = -0.0929x$

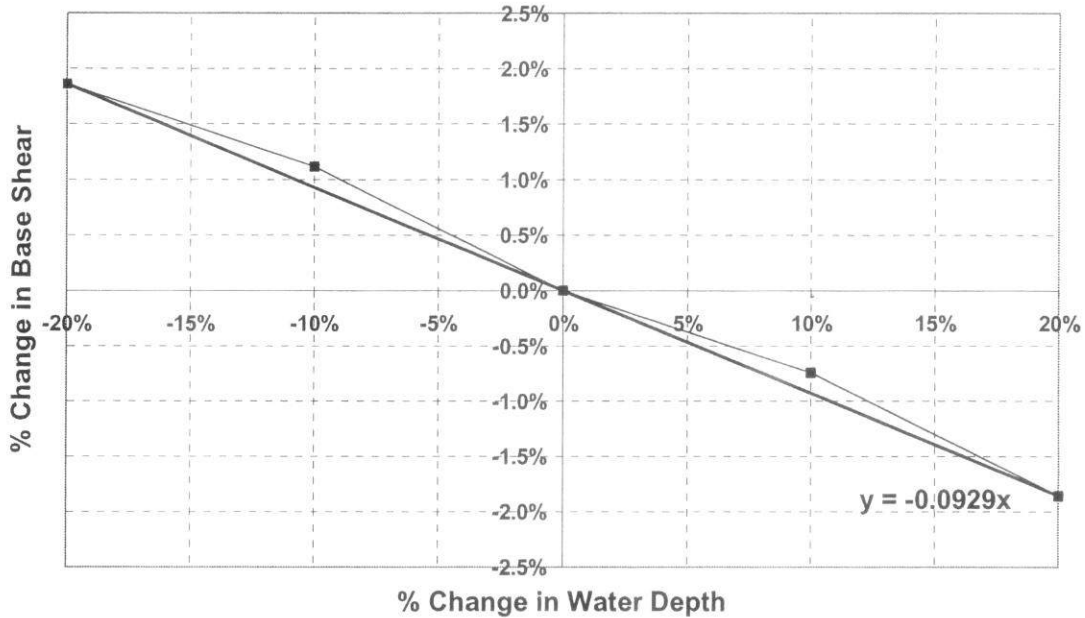


Figure 6.14: Sensitivity of base shear to water depth

Water depth was varied within a $\pm 20\%$ range only because larger variations would:

- be very unlikely at the platform location given the nature of open seas.
- require a redesign of the platform's dimensions. For example, doubling the water depth from 36.2 m to 72.4 m would cause the topsides would mean half of the topsides would be submerged.

The negative relationship between water depth and base shear contradicts one's initial perception. At first, one would predict that when water depth is increased, larger lengths of the caisson and piles will be exposed to the action of waves and hence integrating wave point loads over the larger length will yield a greater overall wave force. However, the graph shows that base shear decreases with increasing water depth. This can be understood by noting that increasing water depth:

- Reduces wind loads by decreasing the frontal area, A , of the caisson and piles exposed to wind.

$$F_{wind} = \frac{1}{2} \rho_{air} V_{wind}^2 C_S A$$

- Reduces wave loads:

Trial and error reveals that increasing d decreases n , which decreases K_D , which in turn decreases F_D :

$$F_D = C_D \frac{1}{2} \rho_{water} g D H^2 K_D \qquad K_D = \frac{1}{4} n$$

$$n = \frac{C_g}{C} = \frac{1}{2} \left(1 + \frac{4 \pi d / L}{\sinh[4 \pi d / L]} \right) \qquad L = \frac{g T^2}{2 \pi} \sqrt{\tanh\left(\frac{4 \pi^2}{T^2} \frac{d}{g}\right)}$$

On the other hand, increasing d increases K_i , which increases F_i :

$$F_i = C_M \rho_{water} g \frac{\pi D^2}{4} H K_i \qquad K_i = \frac{1}{2} \tanh\left(\frac{2 \pi d}{L}\right)$$

However, because F_D is more dominant than F_i at baseline conditions, on the whole, increasing d decreases F_{wave} :

$$F_{wave} = F_i + F_D$$

6.3.3 Comparative Sensitivity Analysis

A sensitivity graph (spider-plot) is an analysis tool that is used when two or more parameters are of concern and an understanding of the sensitivity of structural stability to changes in the value of each parameter is needed.

The sensitivity graph in Figure 6.15 compares the sensitivity of base shear to the different parameters discussed in *Section 6.3.2: Individual Sensitivity Analysis*. Based on this figure the following points can be made:

1. Base shear has a direct relationship with all the plotted parameters except for water depth. This exception was explained in Section 6.3.2.7.
2. Base shear is sensitive to the plotted parameters in this descending order:
 - a. Wave Height
 - b. Wave Height Alone
 - c. Member Diameters
 - d. Wind Speed
 - e. Current Speed
 - f. Wave Period
 - g. Water Depth
3. The above order closely correlates with the pie chart in Figure 6.2. Base shear is most sensitive to those parameters that define loads that have greater share of the base shear. For example, in Figure 6.2, wave loads > wind loads > current loads. Accordingly, wave height, wind speed and current speed appear in the same order in the sensitivity list above.
4. Base shear is more sensitive to wave height when its changes are accompanied by corresponding changes in wave period and current speeds, than when wave height changes alone. This is because wave period and current speed, like wave height, have a direct relationship with base shear (see Sections 6.3.2.6 and 6.3.2.5). Hence they support and magnify the impact of wave height on the base shear.
5. Base shear is more sensitive to wave height than to member diameters. This can be explained as follows:

Wave forces make up most of the base shear, and these are made up of inertial and drag forces. $F_{wave} = F_i + F_D$

F_i is proportional to D^2 and H , so F_i is more sensitive to D : $F_i = C_M \rho g \frac{\pi D^2}{4} H K_i$

F_D is proportional to D and H^2 , so F_D is more sensitive to H :

$$F_D = C_D \frac{1}{2} \rho g D H^2 K_D$$

It is seen in Figure 6.5 that at baseline conditions, drag force (F_D) has a larger contribution to wave force (F_{wave}) than inertial force (F_i). A close look at the output in Appendix B reveals that this is true for both the caisson (65.3% > 34.7%) and the piles (71.2% > 28.8%).

Thus, on the whole F_{wave} is more sensitive to F_D than to F_i , and because F_D is more sensitive to H than to D , F_{wave} is also more sensitive to H than to D .

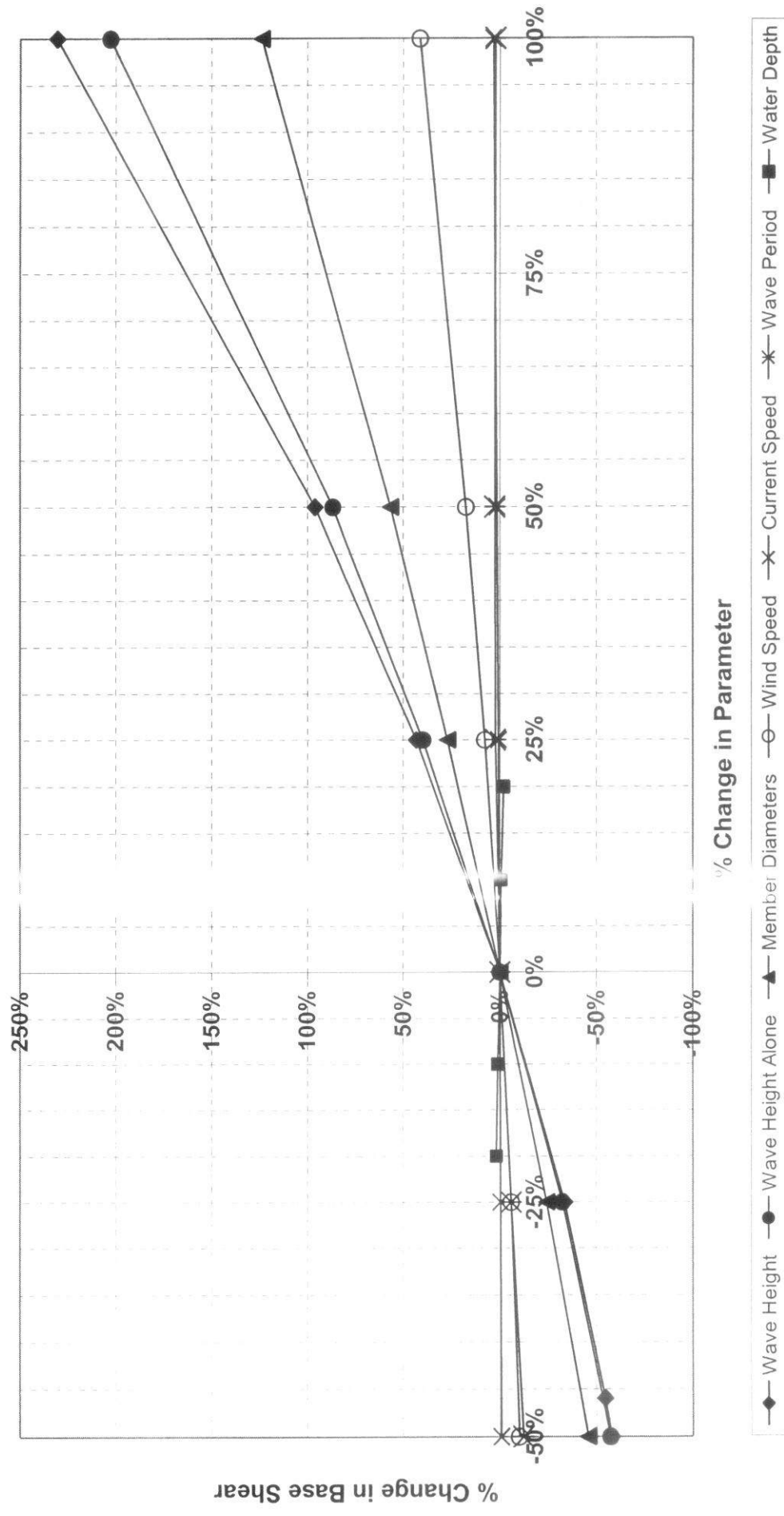


Figure 6.15: Sensitivity of base shear to various parameters

6.4 DRAG / INERTIA RATIO

Keulegan-Carpenter Number

The Keulegan-Carpenter number is a non-dimensional parameter that describes the relation between an oscillatory flow and a cylinder.

$$KC = \frac{U_{\max} T}{D}$$

- U_{\max} : Peak particle velocity
- T : Wave period
- D : Cylinder diameter

- $K > 25$: Particle movement is much greater than D
- $5 < K < 25$
- $K < 5$: Particle movement is smaller than D

- $D/L < 0.2$: Wavelength is much greater than D
- $D/L > 0.2$: Wavelength is not much greater than D

As the Keulegan-Carpenter number grows, drag becomes more dominant and inertia becomes less dominant as elaborated below and in Table 6.2.

$$u = u_m \sin \sigma t; \quad \frac{\partial u}{\partial t} = u_m \sigma \cos \sigma t$$

$$\frac{d(2F_i / \rho u_m^2 D^2)}{d(y/D)} = C_D |\sin \sigma t| \sin \sigma t + C_M \frac{\pi^2 D}{u_m T} \cos \sigma t$$

$$= C_D |\sin \sigma t| \sin \sigma t + C_M \frac{\pi^2}{KC} \cos \sigma t$$

small KC : inertia force > drag force

large KC : inertia force < drag force

Table 6.2: Guide for evaluating wave load calculation procedures.

K	D/L < 0.2	D/L > 0.2
K > 25	Drag dominated. Morison equation with C_m and C_d . $Re > 1.5 \times 10^6$; $C_m = 1.8$, $C_d = 0.62$ $10^5 < Re < 1.5 \times 10^6$; $C_m = 1.8$, C_d varies from 1.0 to 0.6	Morison equation should not be used for computing wave forces. Diffraction theory used.
5 < K < 25	Drag and inertia dominated range Morison equation applicable, but C_m and C_d values show large scatter. Flow behavior and load are complex and uncertain. $Re > 1.5 \times 10^6$; $C_m = 1.8$, $C_d = 0.62$.	
K < 5	Inertia dominated range. Morison equation or Diffraction theory is used. $C_m = 2.0$ Effect of drag is negligible	

Definitions: Keulegan-Carpenter Number, $K = U_m T/D$; Reynolds Number, $Re = U_m D/\nu$; C_m = inertia coefficient; C_d = drag coefficient; U_m = peak velocity; T = wave period; ν = kinematic viscosity; and D = diameter.

Sensitivity to Member Diameters

If we increase member diameters (D), KC will decrease and drag will become less dominant than inertia. See Figure 6.16.

This can also be proven as follows:

$$F_i = C_M \rho g \frac{\pi D^2}{4} H K_i \quad F_D = C_D \frac{1}{2} \rho g D H^2 K_D$$

While F_D is directly proportional to D, F_i is proportional to D^2 . Therefore increasing D will have a greater impact on F_i than on F_D , increasing the relative dominance of inertial forces.

Sensitivity to Wave Height

$$U_{\max} = \frac{H}{2} \frac{gT}{L}$$

By increasing wave height (H), U_{\max} will increase, which in turn increases KC. Thus the ratio of drag to inertial forces increases. See Figure 6.16.

This can also be proven as follows:

$$F_i = C_M \rho g \frac{\pi D^2}{4} H K_i$$

$$F_D = C_D \frac{1}{2} \rho g D H^2 K_D$$

While F_i is directly proportional to H, F_D is proportional to H^2 . Therefore increasing H will have a greater impact on F_D than on F_i , increasing the relative dominance of drag forces.

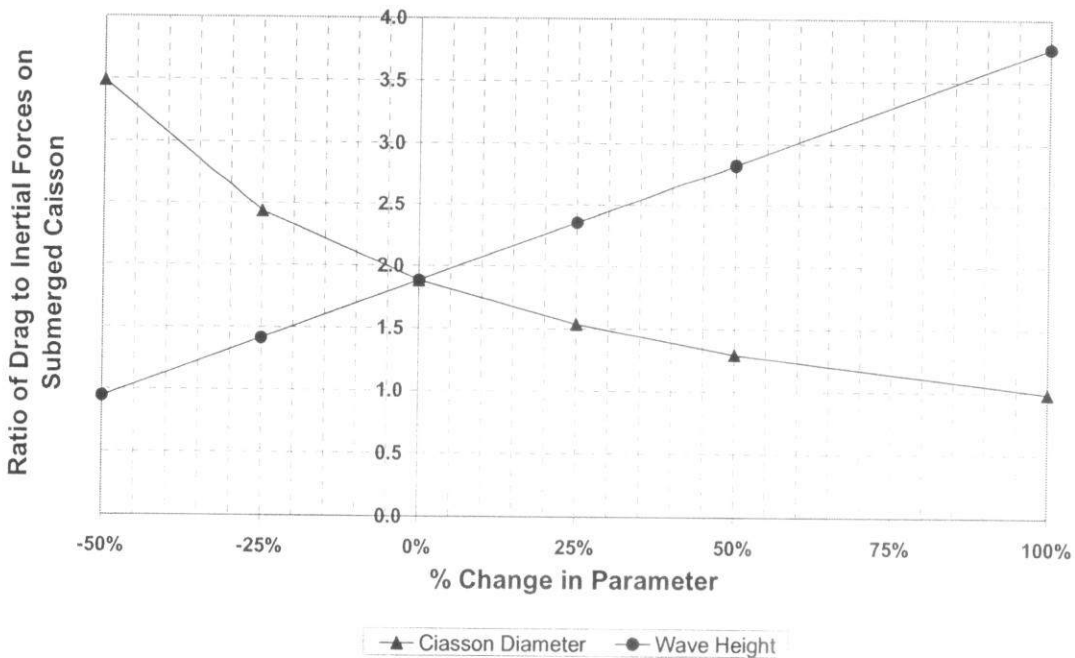


Figure 6.16: Sensitivity of drag/inertia ratio for submerged caisson to caisson diameter and wave height

7. SCALE MODEL EXPERIMENTS

This chapter fully defines the framework for experimental studies on a scaled model of the case study platform in order to assess its structural stability. Conducting the experiments by other researchers would then be feasible.

In this chapter, first an introduction to physical modelling is presented for the unfamiliar reader. Next, the experimental setup is explained including how to replicate the prototype, its environmental conditions and its scales. Then the scaled model built by the author is presented in photographs and compared to the prototype platform. Described next is UTP's Hydraulic Lab Flume that will represent sea conditions at the platform site. After that, experimental procedures are thoroughly outlined. Finally, strain gauge measurements are detailed including installation, calibration and interpretation of results.

7.1 INTRODUCTION

Models are widely used in offshore engineering. Major engineering projects involving structures, aircraft, ships, rivers, harbours, dams, air and water pollution, and so on frequently involve the use of models. Although the term “model” is used in many different contexts, the “engineering model” generally conforms to the following definition. *A **model** is a representation of a physical system that may be used to predict the behaviour of the system in some desired respect.* The physical system for which the predictions are to be made is called the **prototype**. Although *mathematical* or *computer* models may also conform to this definition, our interest will be in physical models, that is, models that resemble the prototype but are generally of a different size, may involve different fluids, and often operate under different conditions (pressures, velocities, etc.). Usually a model is smaller than the prototype. Therefore, it is handled more easily in the laboratory and is less expensive to construct and operate than a large prototype. With the successful development of a valid model, it is possible to predict the behaviour of the prototype under a certain set of conditions.

In the following sections we will develop the procedures for designing models so that the model and prototype will behave in a similar fashion.

Theory of Models

The theory of models can be developed readily by using the principles of dimensional analysis. It has been shown that any given problem can be described in terms of a set of pi terms as

$$\Pi_1 = \phi(\Pi_2, \Pi_3, \dots, \Pi_n) \quad (\text{Eq. 1})$$

In formulating this relationship, only knowledge of the general nature of the physical phenomenon, and the variables involved, is required. Specific values for variables (size of components, fluid properties, and so on) are not needed to perform the dimensional analysis. Thus, Eq. 1 applies to any system that is governed by the same variables. If Eq. 1 describes the behaviour of a particular prototype, a similar relationship can be written for a model of this prototype; that is,

$$\Pi_{1m} = \phi(\Pi_{2m}, \Pi_{3m}, \dots, \Pi_{nm}) \quad (\text{Eq. 2})$$

where the form of the function will be the same as long as the same phenomenon is involved in both the prototype and the model. Variables, or pi terms, without a subscript will refer to the prototype, whereas the subscript m will be used to designate the model variables or pi terms.

The pi terms can be developed so that Π_1 contains the variable that is to be predicted from observations made on the model. Therefore, if the model is designed and operated under the following conditions

$$\begin{aligned} \Pi_{2m} &= \Pi_2 \\ \Pi_{3m} &= \Pi_3 \end{aligned} \quad (\text{Eq. 3})$$

$$\dots$$

$$\Pi_{nm} = \Pi_n$$

Then with the presumption that the form of ϕ is the same for model and prototype, it follows that

$$\Pi_{1m} = \Pi_1 \quad (\text{Eq. 4})$$

Equation 4 is the desired *prediction equation* and indicates that the measured value of Π_{1m} obtained with the model will be equal to the corresponding Π_1 for the prototype as long as the other pi terms are equal. The conditions specified by Eqs. 3 provide the *model design conditions*, also called *similarity requirements* or *modelling laws*.

Generally, to achieve similarity between model and prototype behaviour, *all the corresponding pi terms must be equated between model and prototype*. Usually, one or more of the set pi terms will involve ratios of important lengths; that is, they are purely geometrical. Thus, when we equate the pi terms involving length ratios we are requiring that there be complete *geometric similarity* between the model and the prototype. This means that the model must be a scaled version of the prototype. Geometric scaling may extend to the finest features of the system, such as surface roughness or small protuberances on a structure, since these kinds of geometric features may significantly influence the flow.

Another group of typical pi terms involves force ratios. The equality of these pi terms requires the ratio of like forces in model and prototype to be the same. Thus, for flows in which the Reynolds numbers are equal, the ratio of viscous forces in model and prototype is equal to the ratio of inertial forces. If other pi terms are involved, such as the Froude number or Weber number, a similar conclusion can be drawn; that is, the equality of these pi terms requires the ratio of like forces in model and prototype to be the same. Thus, when these types of pi terms are equal in model and prototype, we have *dynamic similarity* between model and prototype. It follows that with both geometric and dynamic similarity the streamline patterns will be the same and corresponding velocity ratios (V_m/V) and acceleration ratios (a_m/a) are constant throughout the flow field. Thus, *kinematic similarity* exists between model and prototype. To have complete similarity between model and prototype, we must maintain geometric, kinematic, and dynamic similarity between the two systems. This will automatically follow if all the important variables are included in the dimensional analysis and if all the similarity requirements based on the resulting pi terms are satisfied.

Model Scales

It is clear from the preceding section that the ratio of like quantities for the model and prototype naturally arises from the similarity requirements. For example, if in a given problem there are two length variables l_1 and l_2 , the resulting similarity requirement based on a pi term obtained from these variables is

$$\frac{l_1}{l_2} = \frac{l_{1m}}{l_{2m}} \quad \text{so that} \quad \frac{l_{1m}}{l_1} = \frac{l_{2m}}{l_2}$$

We define the ratio l_{1m}/l_1 or l_{2m}/l_2 as the **length scale**. For true models there will be only one length scale, and all lengths are fixed in accordance with this scale. There are, however, other scales, such as the velocity scale V_m/V , density scale ρ_m/ρ , viscosity scale μ_m/μ and so on. In fact, we can define a scale for each of the variables in the problem. Thus, it is actually meaningless to talk about a “scale” of a model without specifying which scale.

We will designate the length scale as λ_l , and other scales as λ_v , λ_ρ , λ_μ , and so on, where the subscript indicates the particular scale. Also, we will take the ratio of the model value to the prototype value as the scale (rather than the inverse). Length scales are often specified, for example, as 1:10 or as a $\frac{1}{10}$ scale model. The meaning of this specification is that the model is one-tenth the size of the prototype, and the tacit assumption is that all relevant lengths are scaled accordingly so the model is geometrically similar to the prototype.

Distorted Models

Although the general idea behind establishing similarity requirements for models is straightforward (we simply equate pi terms), it is not always possible to satisfy all the known requirements. If one or more of the similarity requirements are not met, for example, if $\Pi_{2m} \neq \Pi_2$, then it follows that the prediction equation $\Pi_{1m} = \Pi_1$ is not true; that is, $\Pi_{1m} \neq \Pi_1$. Models for which one or more of the similarity requirements are not satisfied are called **distorted models**.

Distorted models are rather commonplace and can arise for a variety of reasons. For instance, perhaps a suitable fluid cannot be found for the model. The classic example of a distorted model occurs in the study of open channel or free-surface flows. Typically in these problems both the Reynolds number, $\rho V l / \mu$, and the Froude number, $V / \sqrt{g l}$, are involved. Generally, hydraulic models of this type are distorted and are designed on the basis of the Froude number, with the Reynolds number different in model and prototype.

Distorted models can be used successfully, but the interpretation of results obtained with this type of model is obviously more difficult than the interpretation of results obtained with **true models** for which all similarity requirements are met.

Flow with a Free Surface

Flows in canals, rivers, spillways, and stilling basins, as well as flow around ships, are all examples of flow phenomena involving a free surface. For this class of problems, both gravitational and inertial forces are important and, therefore, the Froude number becomes an important similarity parameter. Also, because there is a free surface with a liquid-air interface, forces due to surface tension may be significant, and the Weber number becomes another similarity parameter that needs to be considered along with the Reynolds number. Geometric variables will obviously still be important. Thus a general formulation for problems involving flow with a free surface can be expressed as

$$\text{Dependent pi term} = \phi\left(\frac{l_i}{l}, \frac{\varepsilon}{l}, \frac{\rho V l}{\mu}, \frac{V}{\sqrt{g l}}, \frac{\rho V l^2}{\sigma}\right)$$

As discussed previously, l is some characteristic length of the system, l_i represents other pertinent lengths, and ε/l is the relative roughness of the various surfaces. Because gravity is the driving force in these problems, Froude number similarity is definitely required so that

$$\frac{V_m}{\sqrt{g_m l_m}} = \frac{V}{\sqrt{g l}}$$

The model and prototype are expected to operate in the same gravitational field ($g_m = g$), and therefore it follows that

$$\frac{V_m}{V} = \sqrt{\frac{l_m}{l}} = \sqrt{\lambda_l}$$

Thus, when models are designed on the basis of Froude number similarity, the velocity scale is determined by the square root of the length scale. As is discussed in the “Distorted Models” section, to simultaneously have Reynolds and Froude number similarity it is necessary that the kinematic viscosity scale be related to the length

scale as

$$\frac{\nu_m}{\nu} = (\lambda_l)^{3/2}$$

The working fluid for the prototype is normally either freshwater or seawater and the length scale is small. Under these circumstances it is virtually impossible to satisfy the above equation, so models involving free-surface flows are usually distorted. The problem is further complicated if an attempt is made to model surface tension effects, as this requires equality of Weber numbers. Fortunately, in many problems involving free-surface flows, both surface tension and viscous forces are small and consequently strict adherence to Weber and Reynolds number similarity is not required.

For large hydraulic structures, such as dam spillways, the Reynolds numbers are large so that viscous forces are small in comparison to the forces due to gravity and inertia. In this case Reynolds number similarity is not maintained and models are designed on the basis of Froude number similarity. Care must be taken to ensure that the model Reynolds numbers are also large, but they are not required to be equal to those of the prototype. This type of hydraulic model is usually made as large as possible so that the Reynolds number will be large.

7.2 SETUP

Model

A scaled model of the Braced Caisson introduced as the case study in Chapter 5 was constructed by the writer. See *Section 7.3: Built Model* and Figures 7.2 and 7.3.

Care was taken to ensure the model resembles the actual structure as much as possible, i.e. dimensions, thicknesses, strengths, etc.

The platform model is designed to be placed in the flume in UTP's Hydraulic Lab. See *Section 7.4: Hydraulic Lab Flume* for details. This flume is a one-dimensional representation of the Davy Field in the Southern North Sea complete with adjustable waves, wind and currents. Most of the caisson and piles will be submerged in flume water while the topsides will stand above water.

Foundation

If soil is placed at the bottom of the flume to represent the seabed and those parts of the platform's caisson and piles that lie beneath the seabed are included in the tests, the limited height of the lab flume would have to be divided between soil and water. This would force the model to be scaled down a great deal, and too small a model is undesirable. To solve this problem, the model's caisson and pile sleeves will be fixed directly and firmly to the flume bed. Thus, soil and the platform's piles will be absent in the model.

Hence, the focus of the project is quantifying the inherent reliability of the sub-structure (i.e. the jacket) only. The failure of the foundation will be excluded from the experimental study. It is considered that this has no significant influence on the primary platform dimensions and its failure behaviour.

In real life, however, foundation failure governs the ultimate capacity of most offshore platforms. Studies indicate that when foundation failure is allowed, failure usually occurs in the foundation first. Therefore, the high reliability values obtained in this experimental study will not be achieved in practice for this platform.

Scales

Geometric Scale

As indicated in Table 5.1, at the location of the Braced Caisson, the water depth including storm surge is 36.2^m and the 100-year return wave height is 12.6^m. Thus, the top of the splash zone is 36.2 + 12.6 = 48.8^m above the seabed. Given that the height of hydraulic flume is 450^{mm}, in order for the water not to spill out of the flume, the adopted scale should be smaller than

$$\frac{0.45^{(m)}}{48.8^{(m)}} \cong \frac{1}{109}$$

Therefore, we will choose a scale of $\frac{1}{110}$ or 1:110.

The horizontal distance between the outer surfaces of the two piles or caisson in the Braced Caisson is approximately 13 m. This, when scaled down at 1:110, measures 118 mm, comfortably within the width of the flume, 300 mm. Thus, a model scaled at 1:110 will fit in the flume in any direction.

Other Scales

As with most models involving free-surface flows and high-speed flows around immersed bodies, our model will be distorted. Dynamic similitude is especially difficult to attain for an offshore platform that is partially submerged: it is affected by wind forces in the air above it, by hydrodynamic forces within the water under it, and especially by wave motions at the interface between the water and the air. The scaling requirements for each of these phenomena differ, so models cannot replicate what happens to a full sized platform nearly as well as can be done for an aircraft or submarine - each of which operates entirely within one medium. Moreover, one must consider the limitations of experimental facilities, materials and measurement equipment in scaling down the various variables involved.

Therefore, determining the ratios of variables between model and prototype is not an easy task. It will require detailed study and investigation.

7.3 BUILT MODEL

Dimensions

Figure 7.1 illustrates the dimensions calculated for the model. The scale is 1:110.

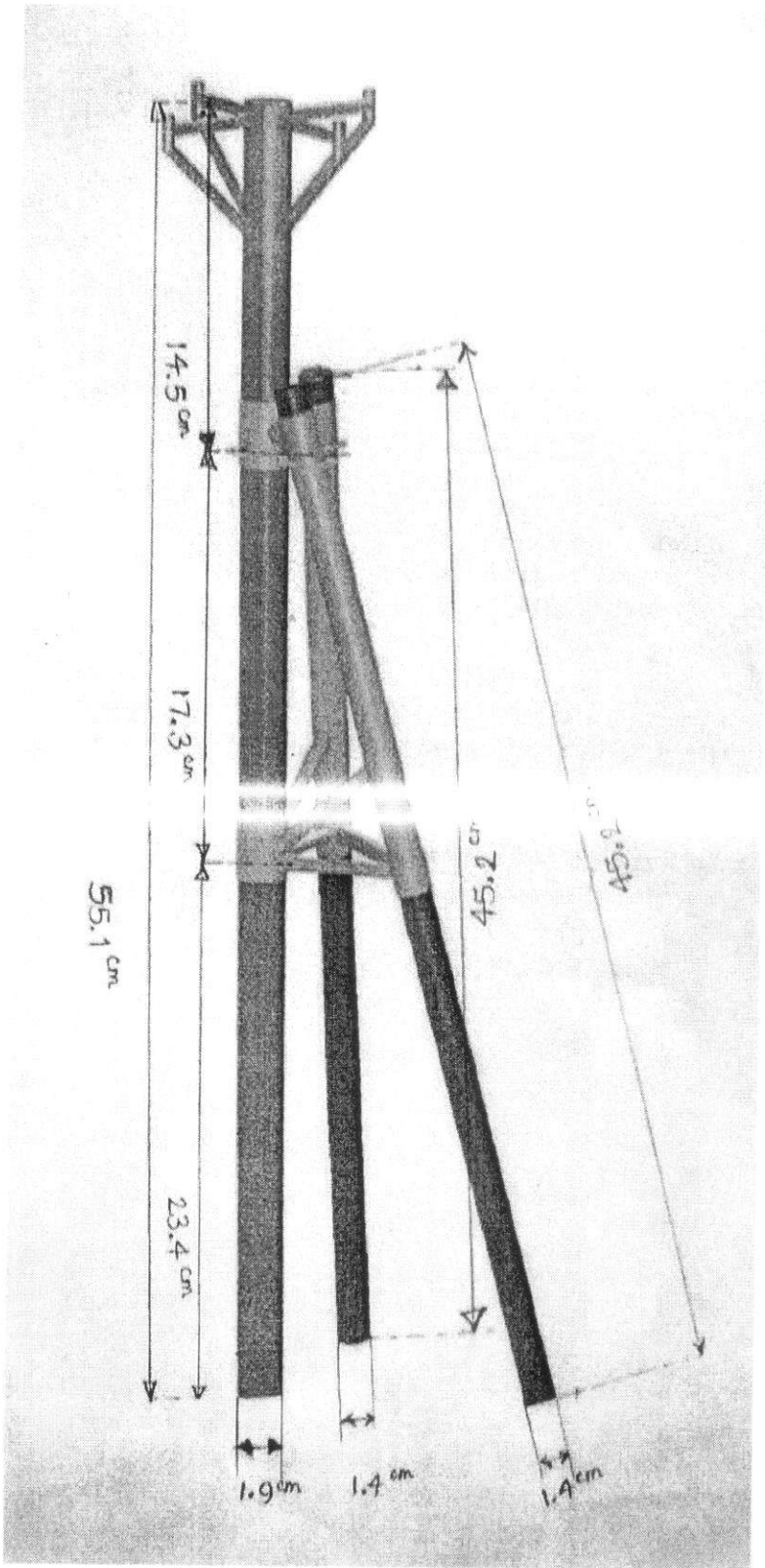


Figure 7.1: Model dimensions

Materials

The model jacket's materials were chosen carefully. PVC was chosen for the caisson while wood was selected for the piles. The resulting elasticity of the platform is such that its deflections under extreme loads will be:

- a) large enough to be visually identified.
- b) small enough for the model to maintain its stability.

Final Product

Figures 7.2 and 7.3 demonstrate the completed scale model from the side and from the front, respectively. The marker on the base plate gives a rough indication of its size.

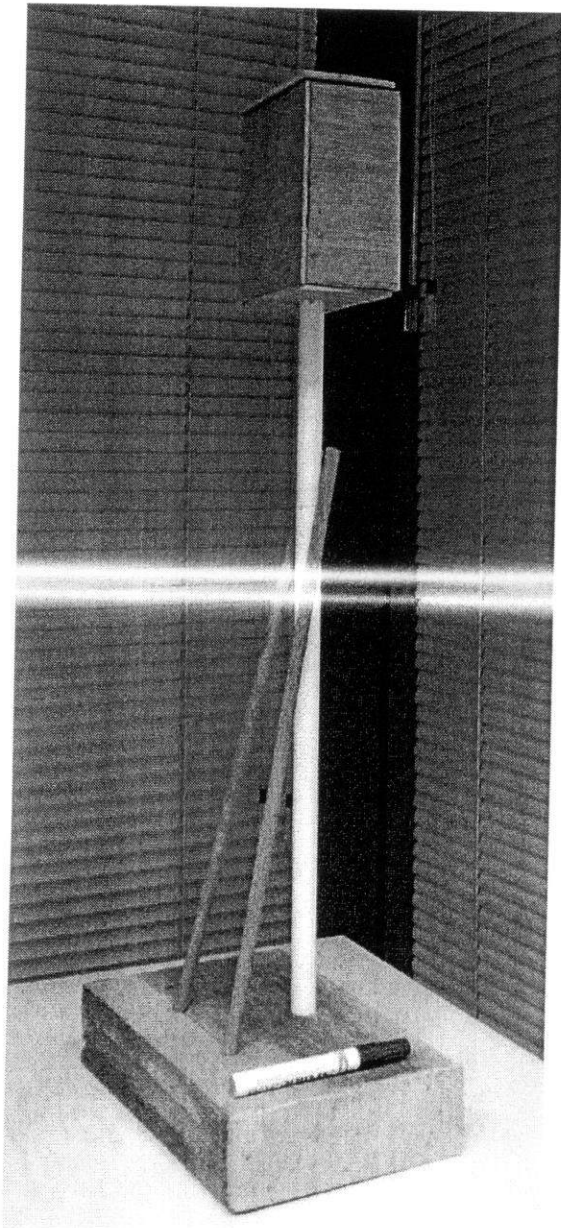


Figure 7.2: Completed model
(side view)

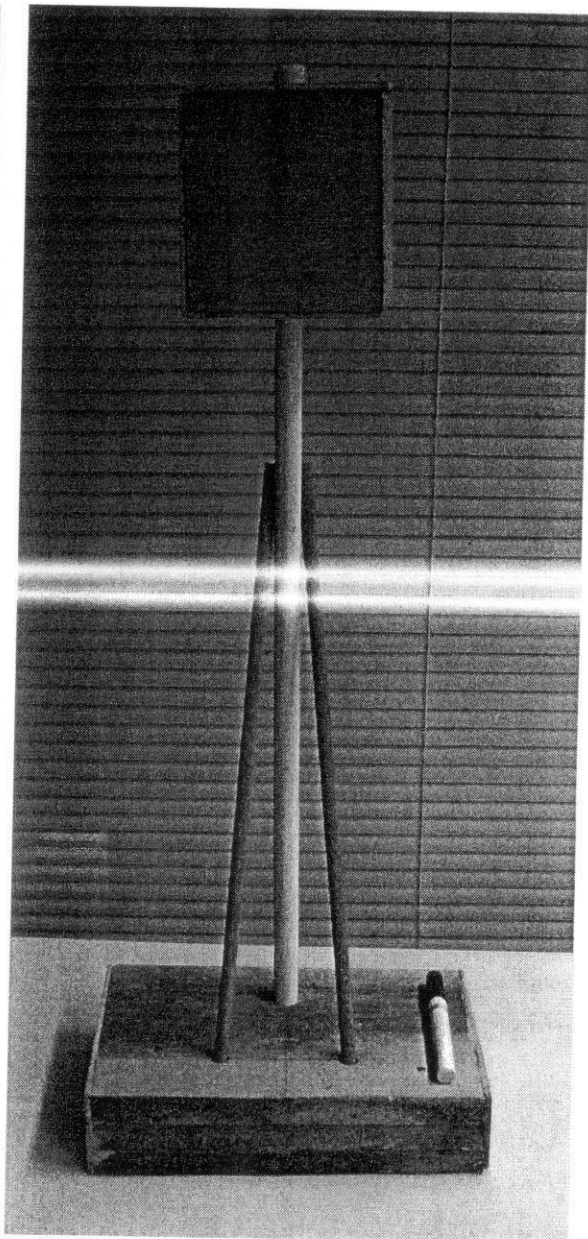


Figure 7.3: Completed model
(front view)

Figure 7.4 shows the author and the model that he built of the Braced Caisson platform chosen as the project’s case study.

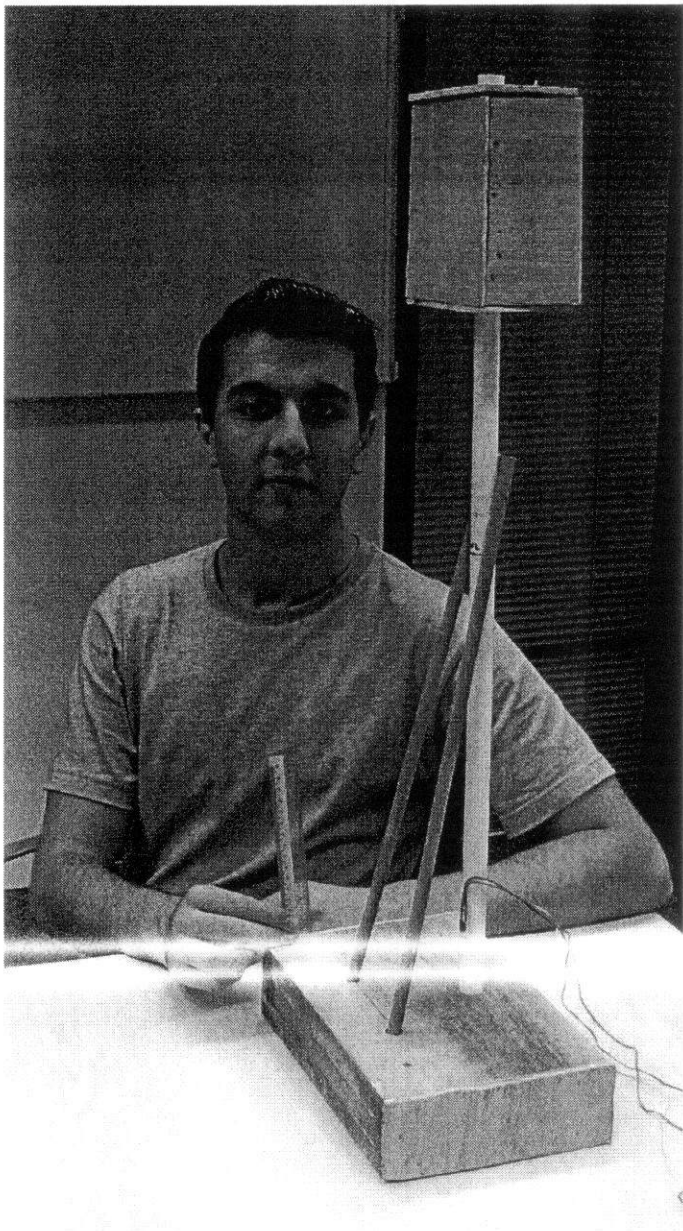


Figure 7.4: The author and the scaled model he built

Resemblance to Prototype

Figure 7.5 shows the close resemblance between the prototype Braced Caisson platform and the scaled model constructed by the author.

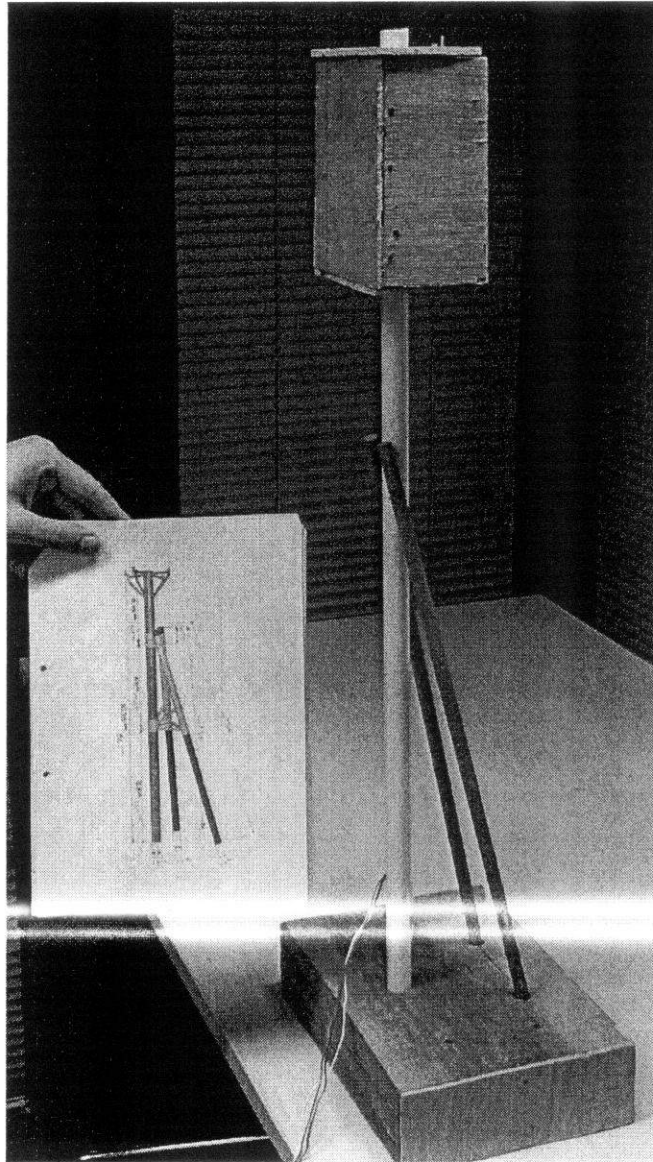


Figure 7.5: Comparison of the prototype and model platforms

In comparing these structures, note that:

- 1) The caisson in the prototype is the PVC pipe in the model.
 - 2) The piles in the prototype are the two inclined round wooden rods in the model.
 - 3) The prototype drawing does not show the topsides represented by the wooden box in the scale model.
 - 4) The scaled model excludes the following features of the prototype jacket:
 - i) The upper inclined braces, the upper horizontal braces and their joints (the cow-horn system) supporting the topsides
 - ii) The braces connecting the piles and the caisson at (-)15.0 m
- It is assumed that these small members do not play a significant role in the stability of the structure.

7.4 HYDRAULIC LAB FLUME

This section describes the features of the hydraulic lab flume to be used in conducting the scale model experiments.

Modular Flow Channel

Modular Flow Channel HM 162 (Figure 7.6) is an open flume providing experimentation possibilities for weirs, overflows, sluices, oceanography, and offshore engineering, etc.

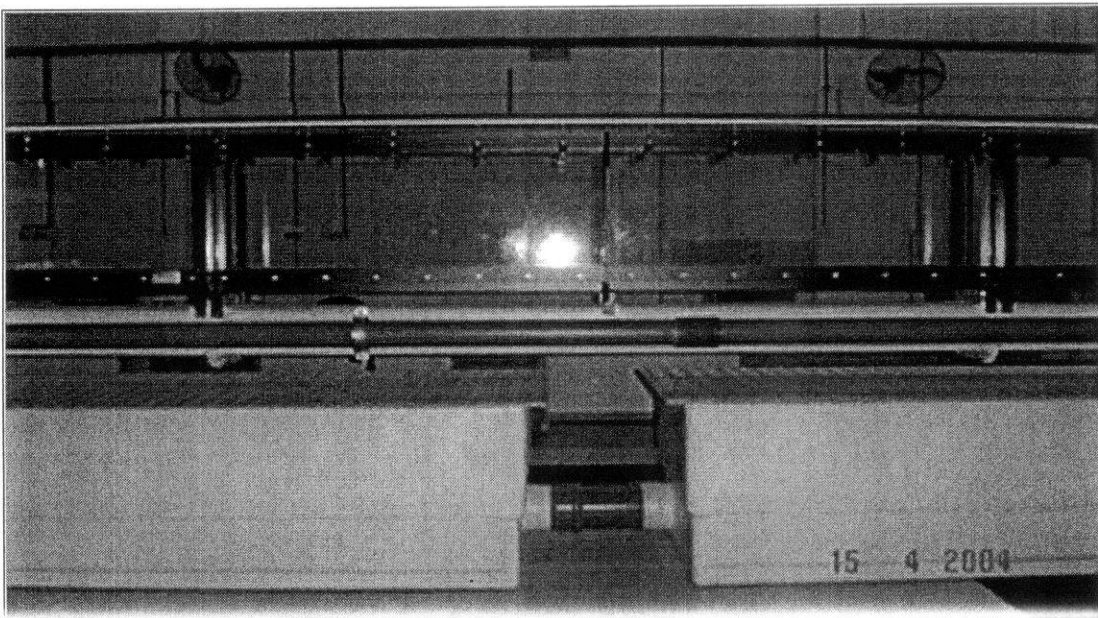


Figure 7.6: Modular Flow Channel

The flume is 12 m long, 300 mm wide and 450 mm deep (Figure 7.7). The transparent sides of the flume are made of hardened glass which is particularly resistant to scratching and abrasion, do not discolour and are easy to clean.

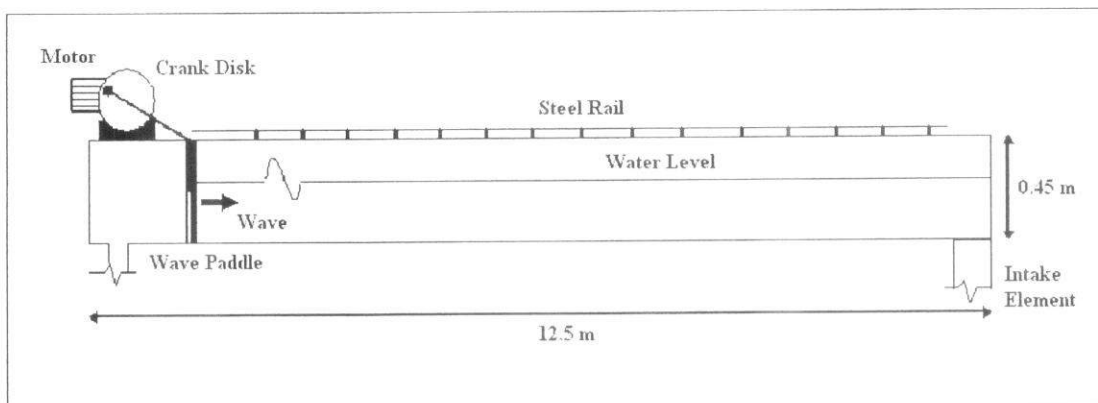


Figure 7.7: Schematic drawing of the wave flume

Wave Generator Flap

The Wave Generator HM 162.41 (Figure 7.8) is used to create waves of various types in the flume. This accessory unit helps obtain information on the behaviour of waves in offshore areas and in coastal protection. The following wave properties are adjustable:

- Height (amplitude)
- Length (frequency)
- Velocity
- Shape

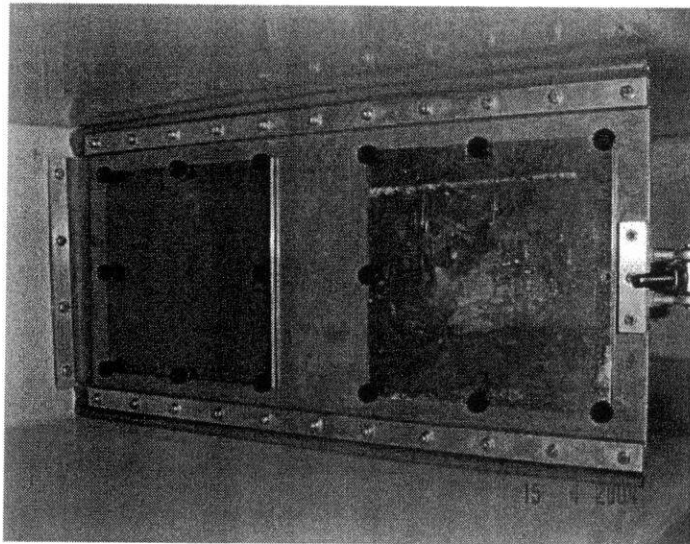


Figure 7.8: Wave Generator Flap

The wave generator is bolted onto the surrounding edge of the flume outlet. The wave generator is driven by a worm gear motor. The rotary movement of the motor is converted into harmonic stroke motion of the movable over-flow weir via a crank disk and a push rod connected to the overflow weir. See Figure 7.9. Rotational speed can be varied by a frequency converter and a potentiometer.

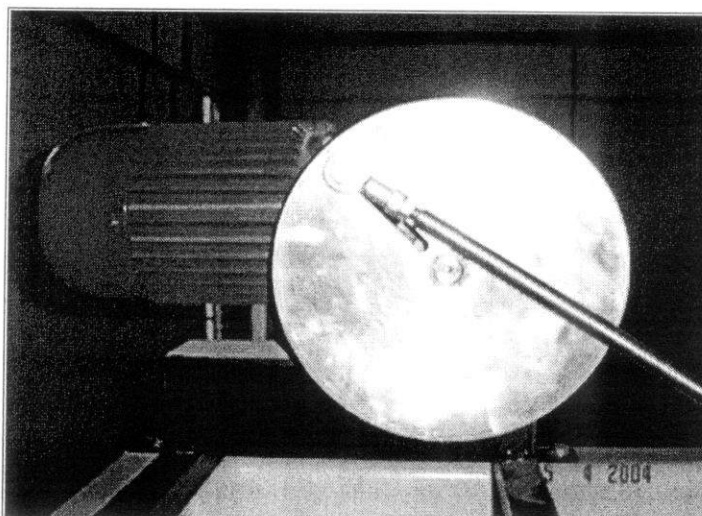


Figure 7.9: Motor, crank disk and push rod

Switch Box

All electrical switching units required for operations are located in the cover of a switch box (Figure 7.10). The rotational speed gives the stroke frequency of the wave generator and can be adjusted via a 10-gear helical potentiometer. The potentiometer has a scale disk for guaranteeing assignment of the rotational speed. At 100%, the rotational speed is 114 rpm, i.e. 1.9 Hz. The rotational speed varies linearly down to 0 rpm at 0%.

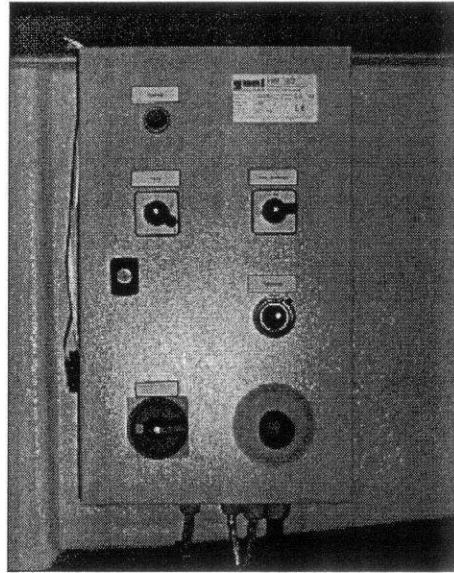


Figure 7.10: Switch Box

Hook and Point Gauge

The hook and point gauge (Figure 7.11) is used to measure levels/water levels in the flume. It is possible to carry out measurements over the entire working range of the flow channel, since the measuring point can be traced in the longitudinal direction, across the width and in the depth of the flow cross section.

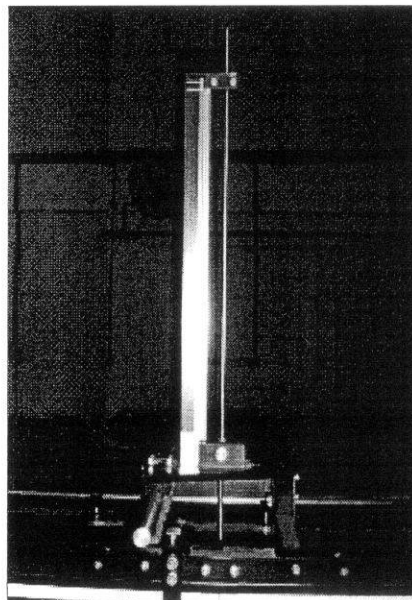


Figure 7.11: Hook and Point Gauge

Pump

The pump (Figure 7.12) consists of a base plate, a centrifugal pump and a flanged-on three-phase motor. On the motor there is a shut-off valve with a lever on the suction side and a shut-off valve with gears and a hand-wheel on the pressure side. The flow rate is adjusted via the pressure-side shut-off valve during operation.

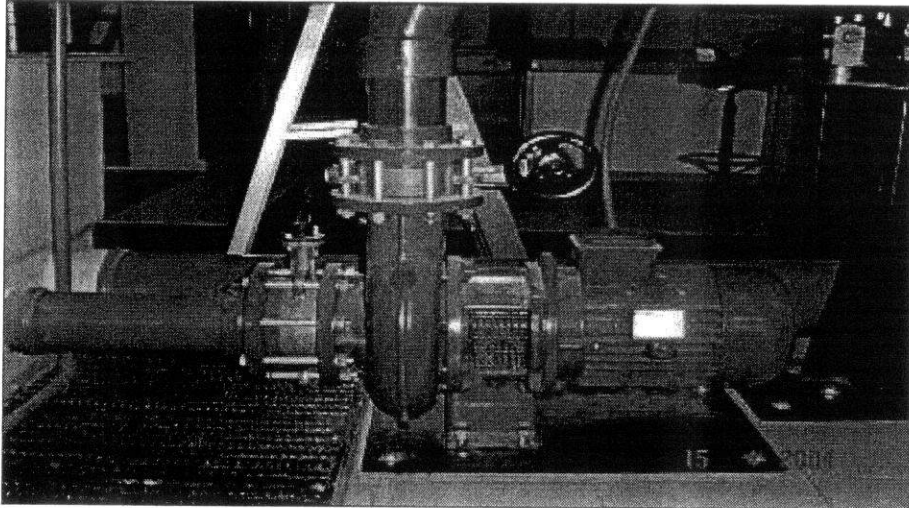


Figure 7.12: Pump

7.5 PROCEDURES

Loads

Dead and live loads will be imposed on the model using weights. External loads will be simulated for the model platform as follows:

Extreme Storm

Waves are generated by the flume's wave generator flap. Wind is simulated using a conventional fan fixed over the flume near the model blowing air horizontally over the topsides in the direction of wave propagation. Current is provided by the flume's pump. The wave properties, wind and current velocities are of course set to their appropriate scaled values.

Fatigue

Welded joints in minimum structures are normally designed to have minimum fatigue lives of 5 times the service life (assumed = 20 years). Simple calculations involving time scale between prototype and model show that in order to properly simulate fatigue, one would have to keep the flume running for 7 years. This is obviously not practical. For that reason, we will not consider fatigue in our scale model experiments.

Number of Experiments

The number of tests to be conducted in the study is as presented in Table 7.1.

Table 7.1: Number of tests

Variables	No. of situations	Description
Wave, Wind, Current	8 directions	Extreme Storm(100-year return)

Total number of tests = 8

Wave, Wind, Current

A total of 8 directions should be analysed to ensure that the worst load scenario is covered, i.e. maximum tension/compression in a pile. An example is presented in Table 7.2.

Table 7.2: 50-year directional waves for the Cecilie platform

	N	NE	E	SE	S	SW	W	NW
H_{\max}	18.9	17.6	17.9	18.9	20.6	21.9	25.2	25.2
$T_{H\max}$	12.6	12.2	12.3	12.6	13.2	13.6	14.5	14.5

Measurements

Water Velocity

Water velocity can be measured in two ways:

- a) A pipe flow meter that connects to the flume's main pipe will measure the discharge in the flow channel. Dividing the discharge by the width of the flume and the height of the water will give average current velocity in the flume.
- b) A current meter consisting of a standard velocity probe with a needle point will measure velocities at different points in the flume.

Wave Properties

The height and period of waves created in a flume are normally measured using wave probes. However, due to the absence of wave probes in our Hydraulic Lab we may resort to visual observation. Transparent graph paper can be attached to the glass walls of the flume. A video camera can record the passing of waves. Reviewing the film will allow for measurement of the wave profiles over time. See Figure 7.13.

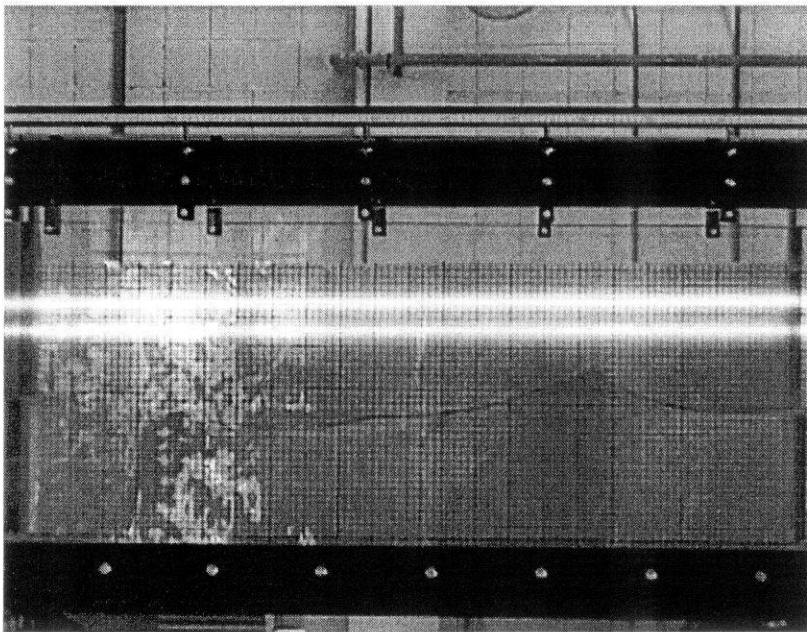


Figure 7.13: Visual measurement via transparent graph paper glued to the flume walls

Deflections

Deflections can be measured visually as in wave measurements.

Stresses

Strain gauges will measure strain in critical members which can later be translated into shear forces and bending moments. See *Section 7.6: Strain Gauge Measurements* for details.

Execution

Execution of the experiments is outside the scope of this project. The objective was only to define and present the framework for the laboratory experiments in detail. The implementation of the procedures outlined here can be pursued by others in the future.

7.6 STRAIN GAUGE MEASUREMENTS

In this section, procedures are outlined to determine the loads that are equivalent to the influence of waves, winds and currents on the scaled model in the hydraulic flume. A strain gauge is installed on the scaled model. The strain gauge is calibrated outside of the flume for varying loads in different locations. The resulting relationships are then used to equate the strain readings obtained during experiments to loads at selected locations. The results may be helpful in designing the platform to resist extreme storms.

Basics

This section presents an overview of the workings of the strain gauge and its associated equipment used in this experimental study.

Strain Gauge

In the experiments measurement of strain from the various loads on the structure are made with the aid of an electric strain gauge as shown in Figure 7.14.

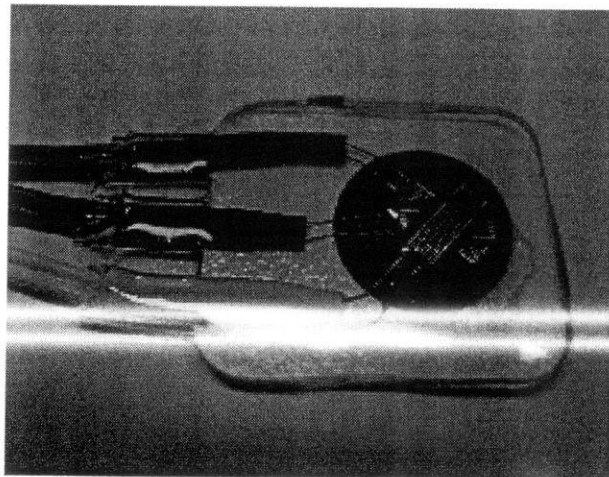


Figure 7.14: Triaxial strain gauge

Principles

Strain gauges are designed to electrically detect the “strain”, minute mechanical change occurring in response to applied force. They enable detection of imperceptible elongation or shrinkage occurring in structures. Measurement of such elongation or shrinkage reveals the stress applied to structures.

Dynamic strain is strain whose magnitude changes quickly and sharply as when structures are subjected to vibration and impact. Such strain is usually measured with a strain amplifier.

In the present study, KFW waterproof strain gauge, which is manufactured in Japan, was selected for the measurement of dynamic strain mainly because it can be conveniently applied to structures of varied materials and shapes. The strain sensor is 10 mm in diameter and approximately 0.2 mm in thickness. This foil strain sensor is protected with special plastic coatings on the surfaces to ensure outstanding

waterproofing. It is usable for 100 hours or more under 10 MPa in water. Some other specifications of the gauge are stated in Table 7.3.

Table 7.3: Specifications of KFW waterproof strain gauge

Gauge pattern	Triaxial
Applicable linear expansion coefficient	$23 \times 10^{-6} / ^\circ\text{C}$
Resistance	350 Ω
Operational temperature range	-10 – 80 $^\circ\text{C}$
Leadwire cable	Polyester-coated cooper wire

If the direction of the principal stress is known in advance, a uniaxial gauge aligning the sensitivity axis with the direction is needed. Then, the strain gauge output expresses the principal strain.

Data Acquisition Units

KFW gauge is connected to KYOWA sensor interfaces PCD-30A series, which makes the existing PC a versatile measuring instrument. The PCD-30A enables the PC to perform force measurement through the use of strain gauges. The 265.2 x 215 x 24.7-mm sensor interface has 4 measuring channels with maximum sampling frequency of 5 kHz. Once sensors are connected, interactive operation on the PC enables measurement of strain data at a desired sampling rate. The control software PCD-30A enables the PC to control the sensor interfaces PCD-30A. Using the software, the PC sets measuring conditions and performs data acquisition, graph display and file conversion to CVS format on MS-Windows 98/2000/XP (Figure 7.15).

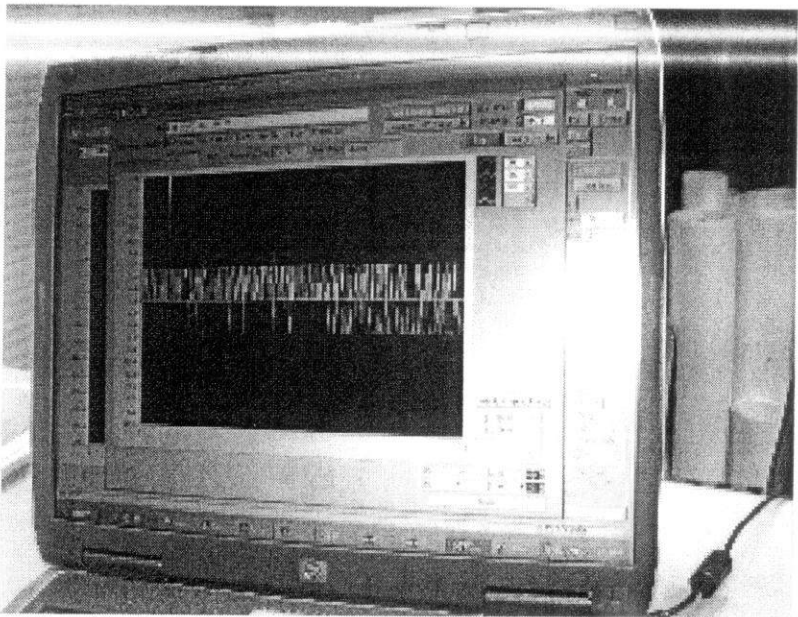


Figure 7.15: PCD-30A software

Installation

Because the piles are long and slender, we assume they are designed mainly to act in tension rather than in compression when supporting the caisson under extreme storm conditions. That is, we assume the platform is positioned on the site such that the dominant waves, winds and currents approach the Braced Caisson on the plane which includes the imaginary line in between the two piles and the caisson, reaching the piles before the caisson.

Consequently, when the caisson bends under extreme storm loads, that side of the caisson which is facing the piles is under tension, while the other side is under compression. We shall fix the strain gauge to that side of the caisson which is under tension, i.e. the side facing the piles. Figure 7.16 shows where the strain gauge is connected to the model.

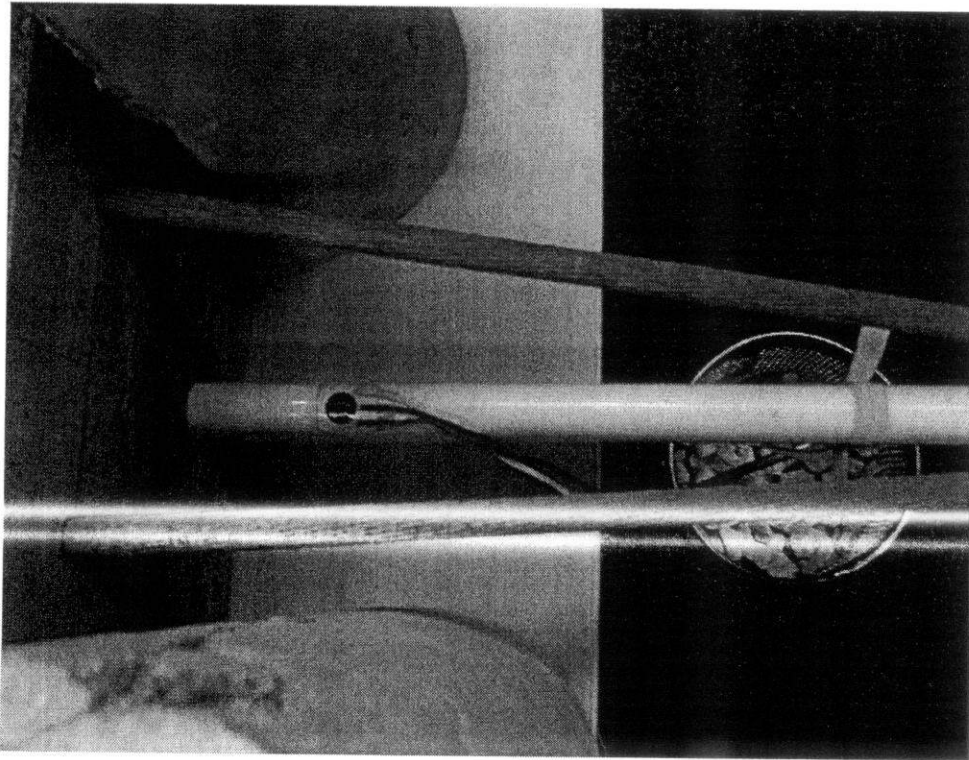


Figure 7.16: Location of the strain gauge on the physical model

As seen in Figure 7.16, the strain gauge was installed on the bottom of the caisson. This is because:

- a. That is where the maximum base shear and bending moment occur.
- b. That part of the caisson experiences the largest bending. Therefore, the strain gauge would give the largest readings there with the least error.

The strain gauge must be firmly glued to the caisson over its entire area, so that it can bend together with the surface of the pipe and pick up the smallest of strains.

Collection of Strain Data

Wires from the strain gauge are connected to the data logger, which is connected to a computer through a USB port for data collection. Figure 7.17 shows the connections of the strain gauge to the data logger and the computer software that processes the input. The graph on the screen shows the variations of the signals received from the strain gauge with time.

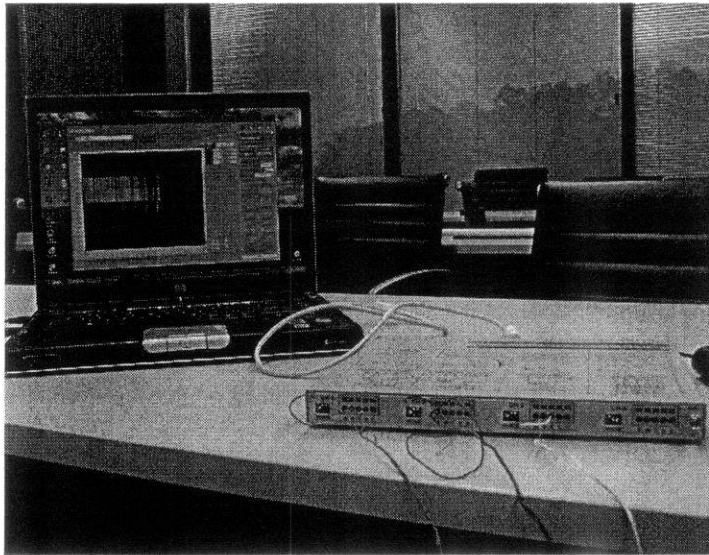


Figure 7.17: The data logger receives signals through 3 wires from the strain gauge and sends data to the computer software for processing.

The sequence of data transfer is: Strain Gauge → Data Logger → Computer Software

Calibration

Calibration of the strain gauge in this study is the process of determining the relationship between its output signal in the form of strain ($\mu\text{m}/\text{m}$) and the magnitude and location of the applied loads.

Strain outputs corresponding to forces in a certain range can be recorded by KYOWA sensor interface PCD-30A. A calibration graph can be plotted, using which the load corresponding to a measured strain can be estimated.

Setup

The simplest method of applying a specific load to a structure is by hanging objects from it whose weights we accurately know. The gravitational forces applied in this manner are vertical. However, in our lab experiments, waves, winds and currents will exert entirely horizontal forces on the structure.

In order to solve this problem, we will rotate the model by 90 degrees (so the base stands vertically and the caisson is horizontal) and we will hang weights from it. See Figure 7.18. The result is vertical weight forces that are normal to the horizontal caisson, just as horizontal environmental loads are normal to the vertical caisson in an upright platform.

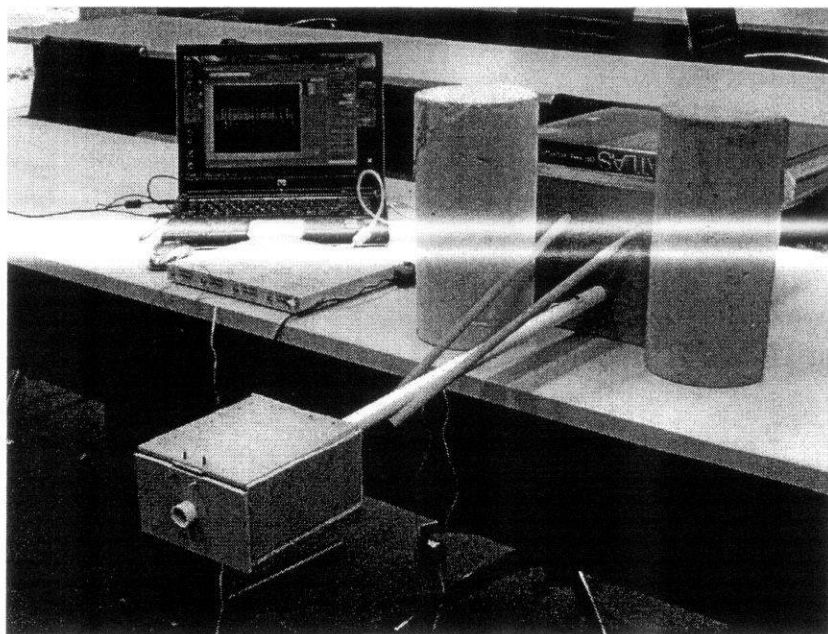


Figure 7.18: The model was rotated by 90 degrees so we could apply known weights to it instead of horizontal forces which are difficult to measure.

As seen in the figure, heavy objects such as books and concrete blocks were used to prevent the base from slipping from its vertical position during loading.

Procedures

We shall calibrate the strain gauge by recording the strain readings resulting from placing different weights at different locations.

Load Locations

Three representative weight locations were chosen based on the distribution of wind, wave and current forces (power/logarithmic law distributions, etc):

1. Location of resultant wind forces on topsides: Middle of topsides (Figure 7.19)
2. Location of resultant wind forces on caisson and piles: Somewhere between the sea water level mark and the bottom of the topsides (Figure 7.20)
3. Location of resultant wave and current forces: Somewhere between the base and the sea water level mark (Figure 7.21)

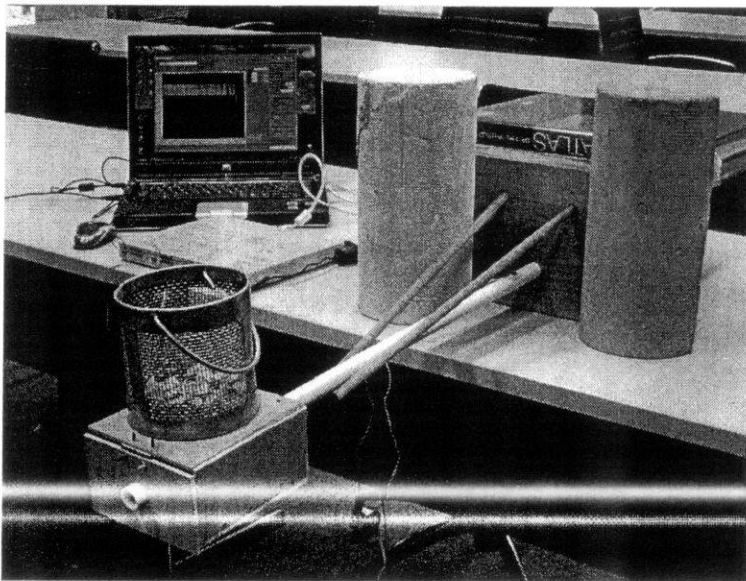


Figure 7.19: Weight applied at location of resultant wind forces on topsides

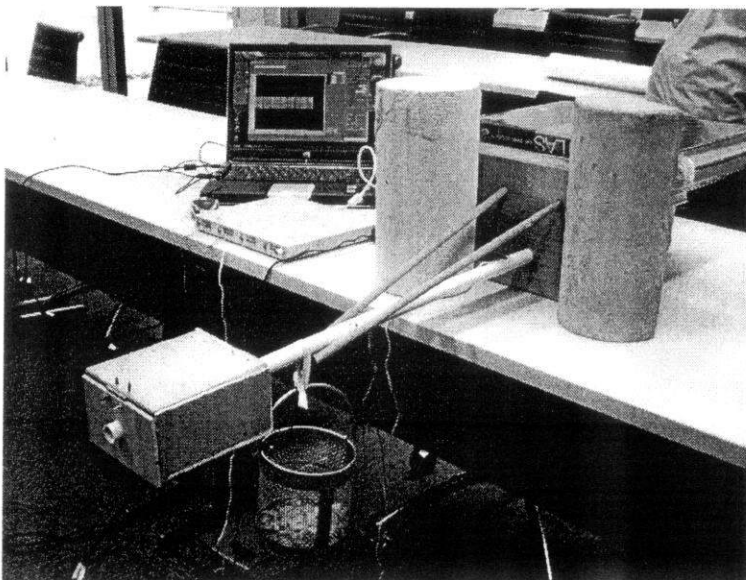


Figure 7.20: Weight applied at location of resultant wind forces on piles and caisson

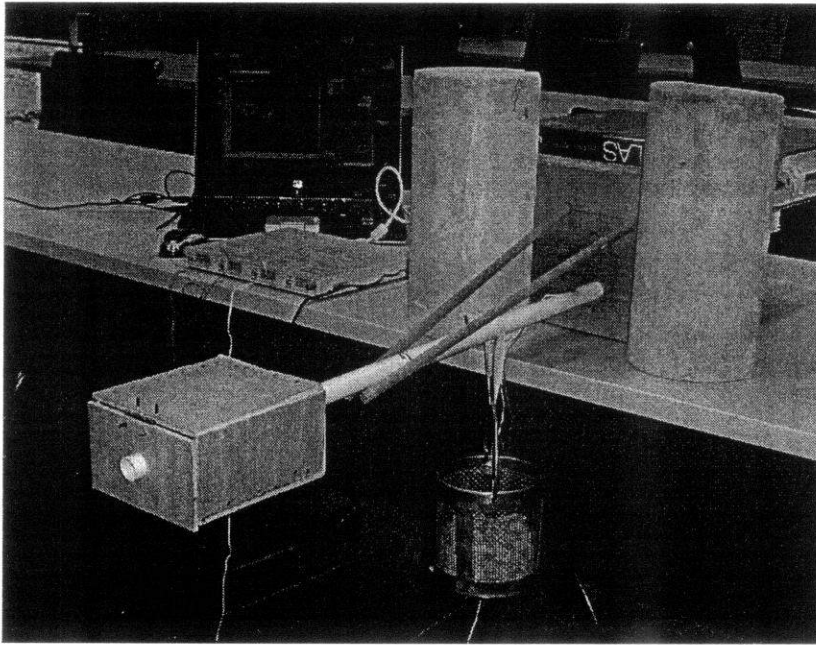


Figure 7.21: Weight applied at location of resultant wave and current forces

Load Variations

Loads are varied at each location. In Figure 7.22, first an empty metal basket was placed on the topsides (left). Later, small stones were placed inside it to increase the weight (right). Several increments of weight are tested.

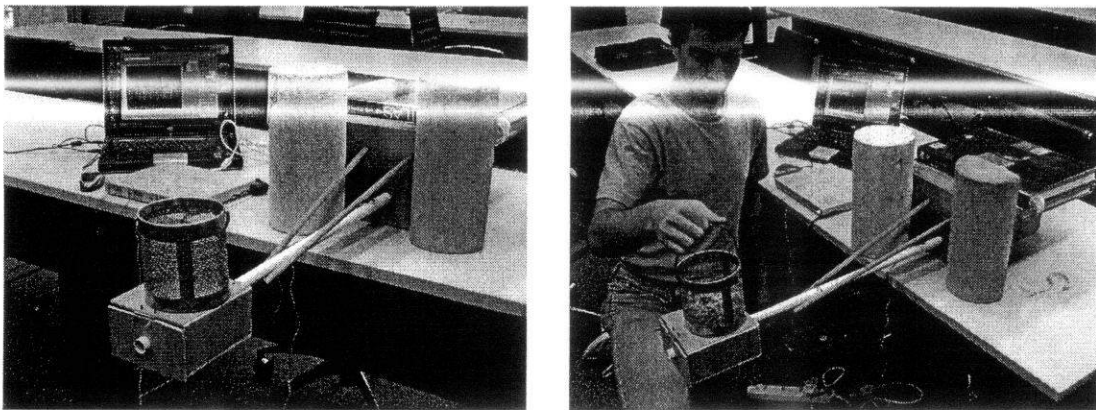


Figure 7.22: Several weights are applied at each location.

In this figure, weights are varied at the middle of the topsides.

Left: Self-weight of empty metal basket, Right: Stones added to increase weight

Calibration Graphs

For each load location, strain readings for different loads are recorded and the results are plotted on a strain vs. load graph. These calibration graphs will be referred to in the next step.

Interpretation of Experimental Results

Once the strain gauge calibration has been done and all the graphs have been produced, the scale model is placed in the hydraulic lab flume and the experiments are run. With each set of environmental parameters, we shall record the strain reading. Then we will refer to our calibration graphs to find the load that produces that same strain reading at selected locations.

For example, if the strain reading acquired from the lab test is $10^{\mu\text{m/m}}$, and during calibration placing a 10^{N} weight on the topsides gave a strain reading of $10^{\mu\text{m/m}}$, we may conclude that the combined effect of the waves, winds and currents acting on the model is equivalent to the effect of a 10^{N} horizontal load applied to the topsides.

Usefulness of Results

The equivalent loads at selected locations obtained from the calibration graphs can be analytically correlated with base shear and bending moment in the caisson and piles. This will be of use in designing these members to resist environmental loads. However, these correlations are considered outside the scope of this study and can be studied in future researches.

REFERENCES

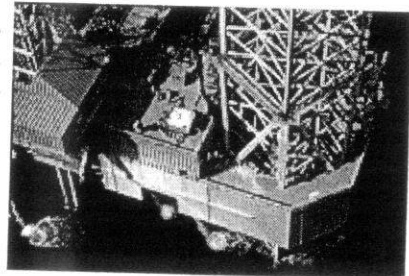
1. WS Atkins Consultants Ltd, *Comparative Evaluation of Minimum Structures and Jackets: Offshore Technology Report*, Health & Safety Executive, UK, 2001
2. RAMBØLL, "Conceptual Design - Summary Report", Job No. 978503, doc. No. 340_005, rev. 1, 1999-01-05, JIP on Comparative Evaluation of Minimum Structures and Jackets.
3. RAMBØLL, "Conceptual Design Report, Braced Caisson", Job No. 978503, doc. No. 340_004, rev. 0, 1998-10-30, JIP on Comparative Evaluation of Minimum Structures and Jackets.
4. American Petroleum Institute, "Recommended Practice for Planning, Designing and Construction Fixed Offshore Structures - Working Stress Design", RP 2A - WSD, Twentieth Edition, July 1, 1993.
5. UK Health and Safety Executive, "Guidance on Design, Construction and Certification. Offshore Installations" Third Amendment to Fourth Edition, 1995.
6. Det Norske Veritas, "Environmental Conditions and Environmental Loads", Classification Notes, Note No. 30.5, March 1991.
7. Gierlinski, JT and Rozmarynowski, B. "Task I.2 and II.3: System Reliability of Intact and Damaged Structures under Extreme Environment and Fatigue Conditions", Report No. WSA/AM3681/TaskI.2/Dec.99. JIP on Comparative Evaluation of Minimum Structures and Jackets.
8. "RASOS User's Manual - Version 4", WS Atkins, Doc. Ref. WSA/AM1703, July 1996.
9. Holnicki-Szulc, J. and Gierlinski, J.T.: "*Structural Analysis, Design and Control by the Virtual Distortion Method*", John Wiley and Sons, 1995.
10. USFOS: Ultimate Strength for Offshore Structures, Computer Software, SINTEF, Norway, 1998.
11. Gerwick B. C. (2000), *Construction of Marine and Offshore Structures*, 2nd Edition, CRC Press LLC, USA
12. Young D. F., Munson B. R., Okiishi T. H. (2004), *A brief introduction to Fluid Mechanics*, 3rd Edition, John Wiley & Sons, Inc., USA
13. C081-DONG-N-FC-002, Rev. 1.3: *Design Brief – Nini/Cecilie Jackets In-Place Analysis*, Bladt/Ramboll, 2002.

14. http://www.naturalgas.org/naturalgas/extraction_offshore.asp
15. <http://www.ukooa.co.uk/issues/decommissioning/background.htm#overview>
16. http://www.worldoil.com/INFOCENTER/STATISTICS_DETAIL.asp?Statfile=int-offshore-rigs
17. <http://www.ale-heavylift.com/marketsectors/index.asp?cid=%C5y>
18. Coastal Engineering Manual, Coastal and Hydraulics Laboratory, US Army Corps of Engineers, 2006

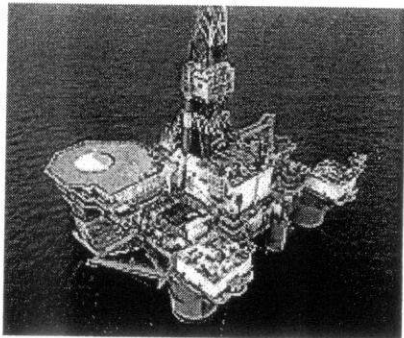
APPENDICES

A. OFFSHORE PLATFORMS GLOSSARY

- Caisson:** Length of pipe extending vertically downwards from an installation into the sea as a means of disposing of waste waters, or for the location of a sea water pump.
- Conventional Waters:** Depth of up to 500 metres.
- Crane Barge:** A large barge, capable of lifting heavy equipment onto offshore platforms. Also known as a "derrick barge".
- Deep waters:** Depths of over 500 metres.
- Deck:** Area of a vessel or platform where work equipment is located: process plant and equipment, accommodation modules and drilling units.
- Decommissioning:** Preferred term (rather than Abandonment) for the re-use, recycling and disposal of redundant oil and gas facilities
- Installation:** May be fixed or mobile and used directly or indirectly for the exploration or production of mineral resources.
- Installation, Fixed:** A fixed offshore structure involved in the production of oil or gas which may be constructed of steel or concrete. Term used frequently in the UK to describe an offshore installation.
- Installation, Mobile:** One which can be moved from place to place without major dismantling or modification.
- Jacket:** Steel support framework used to support platform topsides fixed to the seabed.
- Jackup Drill Rig:** A mobile, bottom-supported, offshore drilling structure. Legs or columns rest on the seafloor and the platform is raised or adjusted by moving up or down the legs.



- Module:** Self-contained liftable package forming part of the topside facilities of an offshore installation. e.g. accommodation module, compressor module, drilling module, etc.
- Offshore/Onshore:** The term offshore indicates a portion of open sea and, by induction, the activities carried out in such area, while onshore refers to land operations.
- Pile:** Long and heavy steel pylon driven into the seabed; a system of piles is used as foundation for anchoring a fixed platform or other offshore structures.

Platform, Offshore:	A fixed offshore structure involved in the production of oil or gas which may be constructed of steel or concrete. Term used frequently by Americans to describe an offshore installation.
Rig:	A term normally associated with drilling equipment, that is to say a drilling rig. Also a slang term used extensively to describe any of the structures and vessels associated with oil and gas exploration and production.
Rig, Drilling:	A drilling unit that is not permanently fixed to the seabed, e.g. a drillship, a semi-submersible or a jack-up unit. Also means the derrick and its associated machinery.
Riser:	The vertical portion of a subsea pipeline (including the bottom bend) arriving on or departing from a platform.
Semi-Submersible Rig:	<div><div>A mobile offshore drilling unit that floats on the water's surface above the subsea wellhead and is anchored in place. The semi-submersible rig gets its name from pontoons at its base which are empty while being towed to the drilling location and are partially filled with water to steady the rig over the well.</div><div></div></div>
Spar:	Floating production system, anchored to the seabed through a semi-rigid mooring system, comprising a vertical cylindrical hull supporting the platform structure.
Tendons:	Pulling cables used on tension leg platforms used to ensure platform stability during operations.
Tension Leg Platform (TLP):	Fixed-type floating platform held in position by a system of tendons and anchored to ballast caissons located on the seabed. These platforms are used in ultra-deep waters.
Topsides:	Upper part of a fixed installation which sits on top of the jacket and consists of the decks, accommodation and process equipment.
Ultra Deepwater:	Generally defined as operation in water depths of 5000 ft or greater.

B. SAOP OUTPUT

What follows is the output produced by SAOP for the Braced Caisson structure defined in the JIP under the exact same environmental parameters used in the JIP under extreme storm conditions. See Section 6.1.4 for details.

05-10-2007 12:12:33

SAOP

Stability Analysis of Offshore Platforms

To compute the total base shear on jacket/piles of an offshore platform under wave + wind + current loads only.

By Mohammad Reza Saiedi
May 2007

BASIC PARAMETERS

Water depth (m)	Wave Height (m)	Wave Period (s)	Wave Length (m)	Wave Celerity (m/s)	Group Number, n	
36.20	16.40	12.60	210.96	16.74	0.75	

Max. Water Particle Velocity at SWL (m/s)	Max. Water Particle Acceleration at SWL (m/s ²)	Cm for Waves on Submerged Members	Cd for Waves on Submerged Members	K _i (-)	K _d (-)
4.80	2.39	1.26	1.10	0.40	0.19

Wind Speed at 10 m above LAT (m/s)	Wind Frontal Area (m2)	Air Gap (m)	Height of Topsides (m)	C _d for Wind on Topsides	Current Speed at Surface (m/s)
32.20	240.00	24.40	16.00	1.50	0.96

RESULTS

$F_{\text{wind on topsides (MN)}} = 0.343$ acting at 32.40 meters from SWL

Member Type No. 1: Caisson above SWL

Dry member, then:

$F_{\text{wave (MN)}} = 0.$

$F_{\text{current (MN)}} = 0$

For one member only:

$F_{\text{wind (MN)}} = 0.018$

Total for all members of this type:

$F_{\text{wind (MN)}} = 0.018$

Member Type No. 2: Caisson below SWL

Wet member, then:

$F_{\text{wind (MN)}} = 0.$

For one member only:

$F_{\text{current (MN)}} = 0.012$

$F_{\text{wave (MN)}} =$	$F_D(\text{MN})$	+	$F_i(\text{MN})$
0.991	0.647		0.344
100.0%	65.3%		34.7%

$F_{\text{total (MN)}} =$	$F_{\text{current (MN)}}$	+	$F_{\text{wave (MN)}}$
1.003	0.012		0.991
100.0%	1.2%		98.8%

Total for all members of this type:

$F_{\text{current (MN)}} = 0.012$

$F_{\text{wave (MN)}} = 0.991$

$F_{\text{total (MN)}} = 1.003$

Member Type No. 3: Piles above SWL

Dry member, then:

$F_{Wave} \text{ (MN)} = 0.$

$F_{Current} \text{ (MN)} = 0$

For one member only:

$F_{Wind} \text{ (MN)} = 0.005$

Total for all members of this type:

$F_{Wind} \text{ (MN)} = 0.009$

Member Type No. 4: Piles below SWL

Wet member, then:

$F_{Wind} \text{ (MN)} = 0.$

For one member only:

$F_{current} \text{ (MN)} = 0.009$

$F_{wave} \text{ (MN)} =$	$F_D \text{ (MN)}$	+	$F_i \text{ (MN)}$
0.652	0.464		0.188
100.0%	71.2%		28.8%
$F_{total} \text{ (MN)} =$	$F_{current} \text{ (MN)}$	+	$F_{wave} \text{ (MN)}$
0.660	0.009		0.652
100.0%	1.3%		98.7%

Total for all members of this type:

$F_{current} \text{ (MN)} = 0.018$

$F_{wave} \text{ (MN)} = 1.304$

$F_{total} \text{ (MN)} = 1.320$

Total Base Shear

Base Shear (MN) =	$F_{wind \text{ on topsides}}$	+	$F_{wind \text{ on others}}$	+	$F_{current}$	+	F_{wave}
2.693	0.343		0.027		0.030		2.294
100.0%	12.7%		1.0%		1.1%		85.2%